STATIC AND DYNAMIC FINITE ELEMENT ANALYSIS OF LAMINATED COMPOSITE PLATES

BY

Dhrudat M. Patel

11MCLC08

NIRMA UNIVERSITY
INSTITUTE OF TECHNOLOGY

DEPARTMENT OF CIVIL ENGINEERING

AHMEDABAD-382481

May 2013

STATIC AND DYNAMIC FINITE ELEMENT ANALYSIS OF LAMINATED COMPOSITE PLATES

Major Project

Submitted in partial fulfillment of the requirements

For the degree of

Master of Technology in Civil Engineering

(Computer Aided Structural Analysis and Design)

By

Dhrudat M. Patel

11MCLC08

DEPARTMENT OF CIVIL ENGINEERING

AHMEDABAD-382481

May 2013

Declaration

This is to certify that

a. The major project comprises my original work towards the Degree of Master of Technology in Civil Engineering (Computer Aided Structural Analysis and Design) at Nirma University and has not been submitted elsewhere for a degree.

b. Due acknowledgement has been made in the text to all other material used.

Dhrudat M. Patel

Certificate

This is to certify that the Major Project entitled "Static and Dynamic Finite Element Analysis of Laminated Composite Plates" submitted by Mr. Dhrudat M. Patel (11MCLC08), towards the partial fulfillment of the requirement for the degree of Master of Technology in Civil Engineering (Computer Aided Structural Analysis and Design) of Nirma University, Ahmedabad, is the record of work carried out by his under my supervision and guidance. In my opinion, the submitted work has reached a level required for being accepted for examination. The results embodied in this major project, to the best of my knowledge, haven't been submitted to any other university or institution for award of any degree or diploma.

Dr. P. V. Patel and Dr. S. P. Purohit
Guide and Professor,
Department of Civil Engineering,
Institute of Technology,
Nirma University, Ahmedabad.

Dr. P. H. Shah
Professor and Head,
Department of Civil Engineering,
Institute of Technology,
Nirma University, Ahmedabad.

Dr K Kotecha
Director,
Institute of Technology,
Nirma University,
Ahmedabad.

____

Examiner

____

Date of Examination

Abstract

Fibre Reinforced Laminated composites are widely used in Aerospace and Civil Engineering Structures due to its higher strength to weight and stiffness to weight ratio.

The present study is concerned with the analysis of plates made of continuous fibre reinforced laminated composite materials, using finite element method. Specifically the study concerns the behaviour of laminated plates including transverse shear deformations, and transverse normal stresses and strains.

Two Displacement models with six and eleven degrees of freedom per node based on Higher Order Shear Deformation Theory (HOSDT) are considered to derive finite element formulation. First displacement model considers transverse displacement, rotations and their higher order terms. While second displacement model is based on inplane and transverse displacements, rotations and their higher order terms. Stiffness matrix, load vector and mass matrix of eight - node Quadrilateral isoparametric finite element are derived considering two displacement models. The objective is to study the performance of above derived finite elements in static and dynamic analysis of laminated composite plate. Finite element analysis is carried out to evaluate displacements and stresses under static load with varying width-to-thickness ratio, material anisotropy, and number of layers of the fibers with different angle of orientation and support conditions. Further free vibration analysis is carried out using finite element method to obtain natural frequencies and corresponding mode shapes.

Results for plate deformations, internal stresses and natural frequencies for several examples are compared with the results available in literatures for evaluating accuracy of displacement models. Computer programs are developed for automatic meshing of laminated composite plate, for static analysis to obtain deflection and interlaminar stresses under uniform and sinusoidal loading, for dynamic analysis to obtain natural frequencies and mode shapes. The programs are capable to handle any number of elements, geometry, support conditions and loading.

Further to explore the concept of intelligent structure and to enhance its application in the field of structural engineering, study on a composite laminate embedded with smart patches of piezoelectric material is presented. A displacement model with two mechanical degrees of freedom and one electrical degree of freedom (i.e. voltage) is considered. Finite element formulation is derived using 8-node isoparametric element based on considered displacement fields. Electromechanical coupling behaviour is studied from direct piezoelectric effect (Sensing action) and converse piezoelectric effect (actuation action). Analysis of piezoelectric laminated composite is illustrated through an example of bimorph beam constructed by two PVDF beam using developed computer program.

Acknowledgement

I would like to express my immense gratitude to my guide **Dr. Paresh V. Patel** and **Dr. Sharadkumar P. Purohit** for their never ending ardent concern and knowledge base guidance during my major project work. Their perennial encouragement and support during my project work fortified me with a thorough understanding of different aspects of the project work. Their esteemed supervision and direction right from beginning afforded me the perseverance and dedication to complete this work.

My sincere thanks to **Prof. N. C. Vyas**, Professor, Department of Civil Engineering, **Shri Himmat Solanki**, Visiting Faculty, Department of Civil Engineering, **Dr. U. V. Dave**, Professor, Department of Civil Engineering for their valuable suggestions and kind words of motivation throughout the major project work.

My heartfelt thanks to **Dr. P. H. Shah**, Head, Department of Civil Engineering and **Dr K Kotecha**, Director, Institute of Technology, Nirma University, Ahmedabad for providing all kind of required resources during my study.

I would like to thank my all friends for their everlasting support and encouragement in all possible ways throughout the major project work.

Most importantly deepest appreciation and thanks to Almighty and my family for their unending love, affection and personal sacrifices during the whole tenure of my study at Nirma University.

- Dhrudat M. Patel

11MCLC08

Abbreviation, Notation and Nomenclature

x,y,z .... Global coordinate system

1,2,3 .... Lamina reference coordinate system

E_L, E_T .... Longitudinal modulus of elasticity of lamina in the direction of fibre

E_1, E_2, E_3 . Transverse modulus of elasticity of lamina in the cross direction of fibre

$\sigma_1, \sigma_2, \sigma_3$ Normal stresses at any point on the laminate with reference to the lamina axes

$\sigma_x, \sigma_y, \sigma_z$. Normal stresses at any point on the laminate with reference to the global axes

$\varepsilon_1, \varepsilon_2, \varepsilon_3$ .. Normal strains at any point on the laminate with reference to the lamina axes

$\varepsilon_x, \varepsilon_y, \varepsilon_z$ .. Normal strains at any point on the laminate with reference to the global axes

ν_{ij} ... Poissons ratio giving the strain in the j^{th} direction caused by strain in the i^{th} direction

G_{12}, G_{23}, G_{13} .... Shear modulus of lamina

$\tau_{12}, \tau_{23}, \tau_{13}$ Shear stresses at any point on the laminate with references to the lamina axes

$\tau_{xy}, \tau_{yz}, \tau_{xz}$ Shear stresses at any point on the laminate with references to the global axes

$\gamma_{12}, \gamma_{23}, \gamma_{13}$ Shear strains at any point on the laminate with references to the lamina axes

$\gamma_{xy}, \gamma_{yz}, \gamma_{xz}$ Shear strains at any point on the laminate with references to the global axes

S_{ij}, Qij ... Component of the matrix represents the relationship between strain and stress

$[T]$ .... Transformation matrix for coordinate system

$[R]$ .... Represent the relationship between engineering and tensor strain vector

u, v, w_0 .... Displacements of a point along x, y and z directions

u^*, v^*, w_0^* ....Higher order terms displacements of a point along x, y and z direction respectively

θ_x, θ_y Rotations of the normal to the mid-plane in the x-z and y-z plane respectively

θ_x^*, θ_y^* Higher order terms rotations of the normal to the mid-plane in the x-z and y-z plane respectively

a,b ....Plan dimensions of laminate in x and y direction respectively

z_L ....Dimension of the lamina in z-direction

h_k ....Thickness of k^{th} layer in laminate

K_x, K_y, K_{xy}, K_z .... Components of bending-curvature vector

$K_x^*, K_y^*, K_{xy}^*, K_z^*$ .... Higher order terms of components of bending-curvature vector

$\phi_x, \phi_y, \psi_x, \psi_y$ .... Components of shear-rotation vector

ϕ_x^*, ϕ_y^* Higher order terms of components of shear-rotation vector

M_x, M_y, M_z .....Bending moments per unit length perpendicular to x, y and z axes respectively

M_{xy} ....Twisting moments per unit length perpendicular to x axes respectively

M_x^*, M_y^*, M_z^* .Higher order terms of bending moments per unit length perpendicular to x, y and z axes respectively

M_{xy}^* ....Higher order terms of twisting moments per unit length perpendicular to x axes respectively

Q_x, Q_y ....Shearing forces parallel to z-axis per unit length

Q_x^*, Q_y^*, S_x, S_y Higher order terms of shearing forces parallel to z-axis per unit length

N_x, N_y, N_z ....Normal forces per unit length

N_x^*, N_y^*, N_z^* .... Higher order terms of normal forces per unit length

N_{xy} ....Shearing force in direction of y axis per unit length

N_{xy}^* ......Higher order terms of shearing force in direction of y axis per unit length

N_i ....Shape function at i node

NN .... Number of nodes

NG ....Number of Gauss points

NL ....Number of layers in laminate

ξ, η ....Natural coordinate system

δ_i .... Displacement vector at i node

$[B_b]$ .... Bending curvature displacement relation

$[B_s]$ .... Shear rotation displacement relation

$[d_i]$ .... Nodal displacement vector

$[D_b]$ .... Flexure stiffness matrix

$[D_s]$ .... Shear stiffness matrix

$[K^e]$ .... Element stiffness matrix

$[J]$ .... Jacobian matrix

W_a, W_b .... Weighting factors corresponding to Gauss sampling points

g .... Acceleration due to gravity in z-direction

ρ .... Density of material

$[P_g^e]$ .... Load vector due to gravity load

$[P_0]$ .... Surface pressure

$[P_{pi}]$ .... Load vector due to surface pressure

f_z .... Uniformly distributed load

$[P_{ui}]$ .... Load vector due to uniformly distributed load

$[P_{pti}]$ .... Point load along transverse direction

$[q]$ .... Calculated displacement vector from governing equation

$[K]$ .... Overall stiffness matrix in governing equation

$[P]$ .... Overall load vector in governing equation

$\overline{W}$ .... Nondimensional deflection

$\overline{\sigma}_x, \overline{\sigma}_y$ .... Nondimensional stresses

$[I_i]$ .... Inertia terms

$[m]$ .... Inertia matrix

$[M]$ .... Mass matrix

ω .... Circular frequency

λ .... Eigen value

f .... Natural frequency

$\overline{\omega}$ .... Nondimensional natural frequency

$[C]$ .... Constitutive law model for a mechanical stress-strain

$[e]$ .... Piezoelectric constant matrix

$[\mu]$ .... Dielectric constant matrix

d_{ij} .... Electromechanical coupling coefficient

L, W, t .... Width, Length and thickness of bimorph plate respectively

V .... Voltage developed across thickness

Ez_i .... Electrical field at i node in z direction

$[K_{uu}]$ .... Stiffness matrix corresponding to the mechanical degrees of freedom

$[K_{uE}]$ .... Stiffness matrix due to electromechanical coupling

$[K_{EE}]$ .... Stiffness matrix due to electrical degrees of freedom

F_e .... Element load vector

q_e .... Element charge vector

Contents

List of Tables

List of Figures

Chapter 1

Introduction

1.1 General

The word 'composite' in composite material signifies that a material system which consists of a combination of two or more material with significantly different physical and chemical properties on a microscopic scale to achieve more useful material.[1]

The first high performance composite material is as old as man as himself, for it is the human body: the bones, muscle tissues that are multidirectional fibrous laminate. Current developments are pointed towards combination of unusually strong, high modulus fibers and organic, ceramic, or metal matrices. Such materials promise to be far more efficient than any structural materials known previously.

1.2 History

Composite materials have very long history of usage. Their beginnings are unknown, but all recorded history contains references to some form of composite material. The concept of fiber reinforced materials can be traced back to 2000 b. c. or earlier from the Biblical references that the use of straw as reinforcement in mud bricks and composite bows found in Egypt and Mongolia. The Japanese Samurai warriors used laminated metals in their swords. In nineteenth century in the late 1930s the use of short glass fiber reinforcement in cement in the United States was started. After World War II, US manufacturers began producing fiberglass and polyester resin composite boat hulls and radomes (radar cover). The automotive industry first introduced composites into vehicle bodies in the early 1950s. Because of the highly desirable lightweight, corrosion resistance, and high strength characteristics in composites; research emphasis went into improving the material science and manufacturing process. That effort led to the development of two new manufacturing techniques known as filament winding and pultrusion, which helped advance the composite technology into new markets. There was a great demand by the recreation industry for composite fishing rods, tennis rackets, ski equipment and golf clubs. The Aerospace industry began to use composites in pressure vessels, containers, and non-structural aircraft components. The US Navy applied composites in mine sweeping vessels, crew boats and submarine parts. The domestic consumers began installing composite bathtubs, covers, railings, ladders and electrical equipment. The first civil application in composites was a dome structure built in Benghazi in 1968, and other structures followed slowly.[1]

1.3 Classification of Composite Materials

Composite materials are commonly classified at following two distinct levels:

- The first level of classification is usually made with respect to the matrix constituent. The major composite classes include Organic Matrix Composites ($OMCs$), Metal Matrix Composites ($MMCs$) and Ceramic Matrix Composites ($CMCs$). The term organic matrix composite is generally assumed to include two classes of composites, namely Polymer Matrix Composites ($PMCs$) and carbon matrix composites commonly referred to as carbon-carbon composites.
- The second level of classification refers to the reinforcement form - fibre reinforced composites, laminar composites and particulate composites, describe as

follows:

1. Fibrous composites, which consists of fibers in matrix.
2. Particulate composites, which is composed of particles in a matrix.
3. Laminated composites, which consists of layers of various materials.

1.3.1 Fibrous Composites

Long fibers in various forms are inherently much stiffer and stronger than the same material in the bulk form because of the more perfect structure of a fiber. The crystals are aligned in the fiber along the fiber axis. Few selected common fiber materials are Aluminium, Titanium, Steel, E-glass, S-glass, Carbon, Beryllium, Boron, and Graphite etc.

The binder material is generally called a matrix. The purpose of matrix is to manifold, support, protection, stress transfer etc. Typically, the matrix is of considerably lower density, stiffness and strength than the fibers. A typical organic epoxy matrix material such as Narmco 2387 has a density of 11.9 kN/m^3, compressive strength of 0.158 GN/m^2, compressive modulus of 3.86 GN/m^2, tensile strength of 0.029 GN/m^2 and tensile modulus of 3.38 GN/m^2. Metals are also used as matrices.

1.3.2 Particulate Composites

Particulate composites consist of particles of one or more materials suspended in a matrix of another material. The particles can be either metallic or nonmetallic as can the matrix. Common combinations are:

Nonmetallic in Nonmetallic Composites

The most common example of a nonmetallic particle system in a nonmetallic matrix is concrete. Concrete is particles of sand and rock that are bound together by a mixture of cement and water that has chemically reacted and hardened.

Metallic in Nonmetallic Composites

Metal flakes in a suspension are common. For example, aluminium paint is actually aluminium flakes suspended in paint. Upon application, the flakes orient themselves parallel to the surface giving very good coverage.

Metallic in Metallic Composites

Unlike any alloy, a metallic particle in a metallic matrix does not dissolve. Lead particles are commonly used in copper alloys and steel to improve the machine ability (metal comes off in shaving rather than chip form).

Nonmetallic in Metallic Composites

Nonmetallic particles such as ceramics can be suspended in a metal matrix. The resulting composite is called a cermet. Two common classes of cermets are oxide based and carbide-based composites. Oxide-based cermets can be either oxide particles in a metal matrix or metal particles in an oxide-matrix.

1.3.3 Laminated Composites

What is Lamina?

A lamina is a flat (sometimes curved in a shell) arrangement of unidirectional fibers as shown in Fig.1.1 in matrix. The fibers are the principal reinforcing or load-carrying agent. They are typically strong and stiff. The matrix can be organic, ceramic, or metallic. The function of matrix is to support and protect the fibers and to provide a means of distributing load among and transmitting load between the fibers.

Fibers generally exhibit linear elastic behaviour, although reinforcing steel bars in concrete are more nearly elastic-perfectly plastic as shown in Fig.1.2. Aluminium and some composites exhibit elastic-plastic behaviour, which is really nonlinear elastic behavior if there is no unloading. Resinous matrix materials are exhibit viscoelastic behaviour in the absence of viscoplastic behaviour Fig.1.3. Fiber-reinforced composites such as boron-epoxy and graphite-epoxy are usually treated as linear elastic materials since the fibers provide the majority of the strength and stiffness.

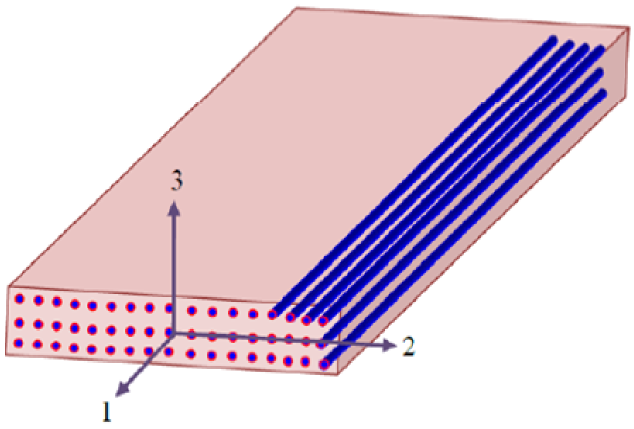

Figure 1.1: Lamina with unidirectional fibers

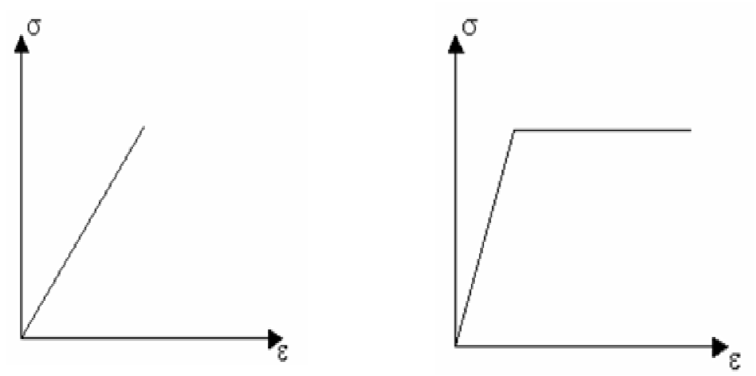

Figure 1.2: Various stress-strain behavior: (a) Linear elastic and (b) Elastic-perfectly Plastic

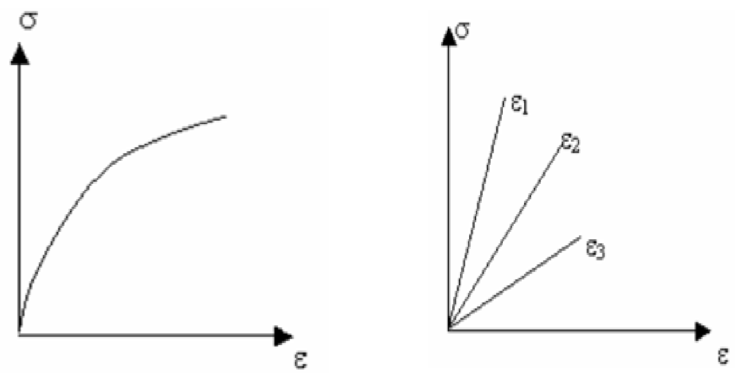

Figure 1.3: Various stress-strain behavior: (a) Elastic-Plastic and (b) Viscoelastic (e1 > e2 > e3)

What is Laminate?

A laminate is a stack of laminae with various orientations of principal material directions in the laminae as in Fig.1.4. The layers of a laminate are usually bound together by the same matrix material that is used in the laminae. Laminate can be composed of plates of different materials or, in the present context, layers of fiber reinforced laminae. A laminated circular cylindrical shell can be constructed by winding resin-coated fibers on a mandrel first with one orientation to the shell axis, then another, and so on until the desired thickness is built up.

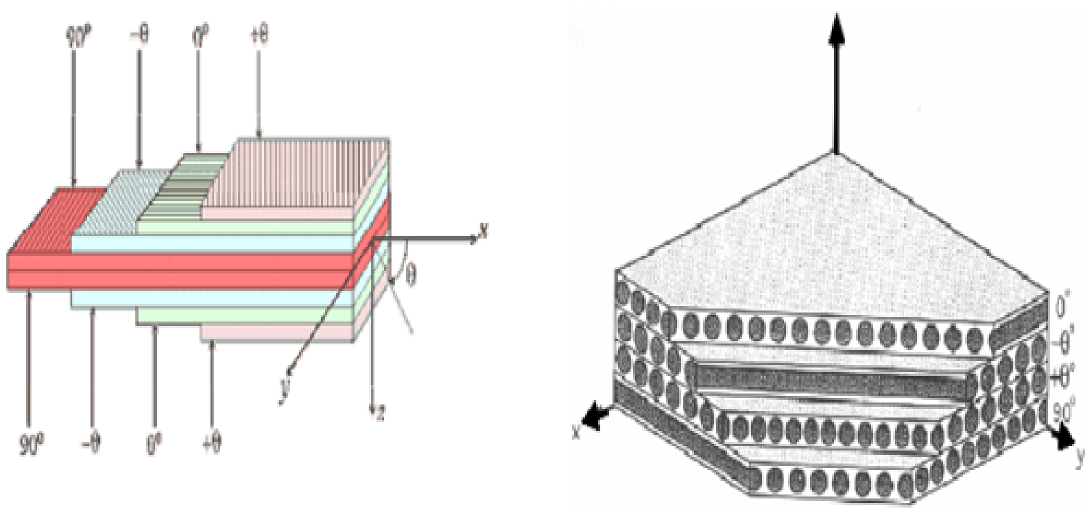

Figure 1.4: A multi-ply laminate construction [4]

A major purpose of lamination is to tailor the directional dependence of strength and stiffness of a material to match the loading environment of the structural element. Laminates are uniquely suited to this objective since the principal material directions of each layer can be oriented according to need.

A potential problem in the construction of laminates is the introduction of shearing stresses between layers. The shearing stresses arise due to the tendency of each layer to deform independently of its neighbours because all may have different properties (at least from standpoint of orientation of principal material directions). Such shearing stresses are largest at the edges of a laminate and may cause delaminations there.

The properties that can be emphasized by lamination are strength, stiffness, low weight, and corrosion resistance, wear resistance, beauty or attractiveness, thermal insulation, acoustical insulation etc.Examples of laminated composites are Bimetals, Clad metals, laminated glass, plastic-based laminates, and laminated fibrous composites as described below:

Bimetals

Bimetals are laminates of two different metals with significantly different coefficients of thermal expansion. Under change in temperature, bimetals warp or deflect a predictable amount and are therefore well suited for use in temperature measuring device such as thermostat.

Clad Metals

The cladding or sheathing of one metal with another is done to obtain the best property of both. For example, high-strength aluminium alloys do not resist corrosion; however, pure aluminium and some aluminium alloys are very corrosion resistant. Thus, a high-strength aluminium alloy covered with a corrosion-resistant aluminium alloy is a composite material with unique and attractive advantages over its constituents.

Laminated Glass

The concept of protection of one layer of material by another as described under "clad metals" can be extended in a rather unique way to safety glass. Ordinary glass is durable enough to retain its transparency under the extremes of weather. However, glass is quite brittle and is dangerous because it can break into many sharp-edged pieces. On the other hand, a plastic called polyvinyl butyral is very tough (deforms to high strains without fracture), but is very flexible and susceptible to scratching. Safety glass is a layer of polyvinyl butyral sandwiched between two layers of glass. The glass in the composite protects the plastic from scratching and gives it stiffness. The plastic provides the toughness of the composite.

Plastic-based laminates

Many materials can be saturated with various plastics and subsequently treated for many purposes. The common product Formica is a merely layer of heavy Kraft paper impregnated with a phenolic resin overlaid by a plastic-saturated decorative sheet which, in turn, is overlaid by a plastic-saturated cellulose mat. Heat and pressures are used to bind the layers together.

Laminated Fibrous Composites

They are a hybrid class of composites involving both fibrous composites and lamination techniques. A more common name is laminated fiber-reinforced composites. Here, layers of fiber-reinforced material are built up with the fiber directions of each layer typically oriented in different directions to give different stiffness and strengths in the various directions. Thus, the strengths and stiffness of the laminated fiber-reinforced composite can be tailored to the specific design requirements of the structural element being built.

1.4 Characteristics of Composites

The mechanical properties of composites depend on many variables such as fiber types, orientations, and architecture. The fiber architecture refers to the preformed textile configurations by braiding, knitting, or weaving. Composites are anisotropic materials with their strength being different in any direction. Their stress-strain curves are linearly elastic to the point of failure by rupture. The polymeric resin in a composite material, which consists of viscous fluid and elastic solids, responds viscoelastically to applied loads. Although the Viscoelastic material will creep and relax under a sustained load, it can be designed to perform satisfactorily. Composites have many excellent structural qualities and some examples are high strength, material toughness, fatigue endurance, and lightweight. Other highly desirable qualities are high resistance to elevated temperature, abrasion, corrosion, and chemical attack.

1.5 Manufacturing Processes

There are many manufacturing techniques in producing composite structural products, with many variations and patented processes but basically three techniques are generally followed:

1. The pultrusion process involves a continuous pulling of the fiber roving and mats through a resin bath and then into a heated die. The elevated temperature inside the die cures the composite matrix into a constant cross-section structural shape.

2. The filament winding process can be automated to wrap resin-wetted fibers around a mandrel to produce circular or polygonal shapes.

3. The lay-up process engages a hand or machine build up of mats of fibers that are held together permanently by a resin system. This method enables numerous layers of different fiber orientations to be built up to a desired sheet thickness and product shape.

1.6 Civil Structural Application

Fibre-Reinforced composites are being used in civil engineering, Aircraft, Automotive, Marine and in other industries where the structural engineering comes in a way since of their low densities, high strength and stiffness to weight ratio with many advantages. Composite materials have more environmental resistance than traditional civil engineering materials such as steel, concrete, masonry, and plaster. Degradation in strength and stiffness for steel structures due to the corrosion problem requires frequent inspection, maintenance, and repair. Similarly, stress cracking due to the warm/cold weathering limits the service life of concrete structures. Timber is susceptible to moisture-swelling problems and paste attack.

Most important of all, these traditional construction materials are relatively inefficient in earthquake and fatigue resistance. Composite materials are as stiff as steel, but weigh approximately 80 times less and have stiffness-to-weight ratio higher (approx. 5 times) than that of steel and so less susceptible to be in resonance with the ground motion of an earthquake. For this reason alone, composite materials structures are safer and can minimize property and life loss induced by earthquake.

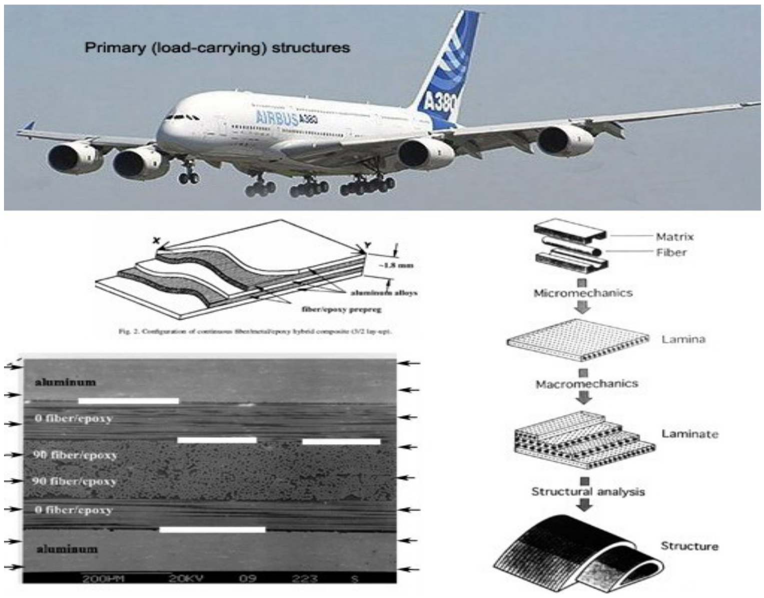

Figure 1.5: Application of composite material in Aircraft [40]

Major applications in the field of civil engineering with example of important constructed structures are as follow:

- Currently, composite materials are being used to retrofit and/or reinforce existing Infrastructures.
- Flat composite laminates have been bonded to the exterior surface of reinforced concrete deck to increase its bending stiffness.
- Several pedestrian bridges have been built successfully.

- Composite materials are suitable for construction of Tall Buildings, Highway Bridges, Power Transmission towers, Silos, Office/Residential Buildings, etc.

- Some of the important structures constructed earlier using Glass-fiber reinforced Polyester ($GFRP$) are given below [37]:

  1. Dome structure in Benghazi in 1968.
  2. Roof structures to the Dubai Airport built in 1972.
  3. Covert Garden Flower Market at Nine Elms, London.
  4. 37m high Chimney at Hendon, London.
  5. Prestigious American Express Building in Brighton, England.
  6. Radome structure - 30.5 m high $GFRP$ towers inserted into steel tower at the Chicago McCook Illinois.
  7. Sulpher factory using singly curved small roof of span 10 meter.
  8. Swimming pool building near Abezdeen, Scotland.
  9. Mondial International telephone service, Central London.
  10. Air roof survilence rader.

- The first USA advanced composite vehicular bridge superstructure was dedicated into service on December 4, 1996 in Russell, Kansas.

- Demonstration bridge projects are being developed in other states such as Delaware, West Virginia and California of USA.

- Continued research projects using composite reinforcing bars in concrete slabs are being studied in New Hampshire, Washington, D.C. and Michigan.

Advantages

- Some of the advantages in the use of composite structural members include the ease of manufacturing, fabrication, handling, and erection. Project delivery time can be short.

- It took the Russell county engineer one day to install the deck panels in the first vehicular composite bridge. Composites can be formulated and designed for high performance, durability and extended service life.

- They have excellent strength to weight ratios. If durability can be proven to last 75 years, composites can be economically justified using the life - cycle cost method.

- Due to greater reliability, there are fewer inspections and structural repairs.

- Directional tailoring capabilities to meet the design requirements. The fibre pattern can be laid in a manner that will tailor the structure to efficiently sustain the applied loads.

- Composites offer improved torsional stiffness.

- Thermoplastics have rapid process cycles, making them attractive for high volume commercial applications that traditionally have been the domain of sheet metals. Moreover, thermoplastics can also be reformed.

- Composites are dimensionally stable i.e. they have low thermal conductivity and low coefficient of thermal expansion. Composite materials can be tailored to comply with a broad range of thermal expansion design requirements and to minimise thermal stresses.

Disadvantages

- Some of the disadvantages in the use of composites in bridges are high first cost, creep, and shrinkage.

- The design and construction require highly trained specialists from many engineering and material science disciplines.

- The composites have a potential for environmental degradation, for examples, alkalis' attack and ultraviolet radiation exposure.

- There are very little or nonexistent design guidance and/or standards. There is a lack of joining and/or fastening technology.
- Because of the use of thin sections, there are concerns in global and local buckling. Although the lightweight feature may be an advantage in the response to earthquake loading, it could render the structure aerodynamically unstable. In manufacturing with the hand lay-up process, there is a concern about the consistency of the material properties.
- Composites are more brittle than wrought metals and thus are more easily damaged.
- Transverse properties may be weak.

1.7 Laminated Composite with Piezoelectric Material

1.7.1 Introduction

"Piezo" is the Greek word for Pressure. When any electric voltage is applied to certain materials they experience a dimensional change", such materials are known as "Piezoelectric Material". Because of converse effect, they generate electricity when pressure is applied. The Piezoelectric effect was discovered in 1880 by Curie brothers Pierre Curie and Jacques Curie.
The nature of piezoelectric material is closely linked to the significant quantity of electrical dipoles within these materials.

Dipole : An dipole is a separation of positive and negative charges. The simplest example of this is a pair of electric charges of equal magnitude but opposite sign.

The centers of the negative and positive charges of the each molecule co-inside. The external effects of the charges are reciprocally canceled. As a result, an electrically neutral molecule appears as shown in Fig.1.6. After exerting some pressure on the material, the internal structure is deformed, that causes the separation of the positive and negative centers of the molecules. As a result, little dipoles are generated as shown in Fig.1.6.

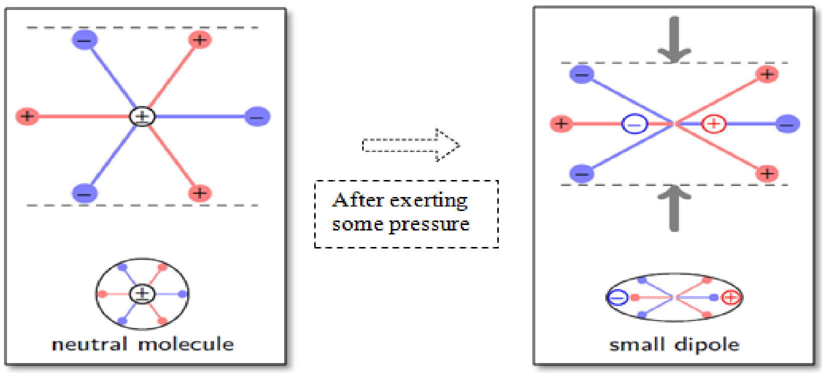

Figure 1.6: Dipole effect

A dipole is a vector with direction and value in accordance to electric charge around. These dipoles are generally randomly oriented, and they altogether form regions called Weiss domains as shown in Fig.1.7.

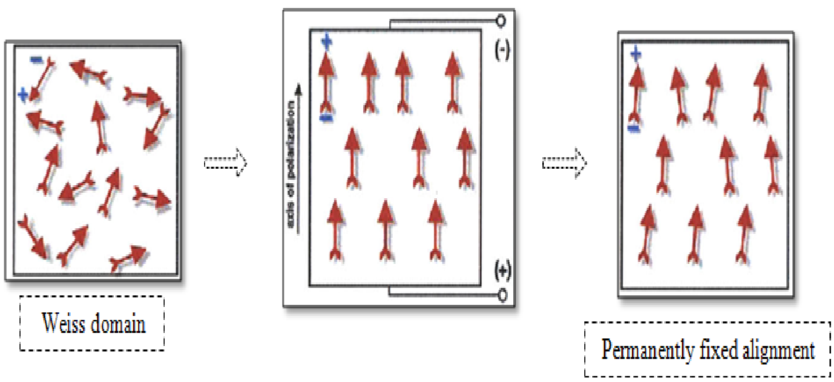

Figure 1.7: Response of molecules under electric field

A piezoelecric material has a characteristic Curie temperature. When it is heated above this temperature, the dipoles can change their orientation in the solid phase material. Then applying strong electric field the dipoles shift into alignment with the direction of this field. Now the alignment of dipoles is permanently fixed as shown in Fig.1.7. During this process the dipoles respond collectively to produce a macroscopic

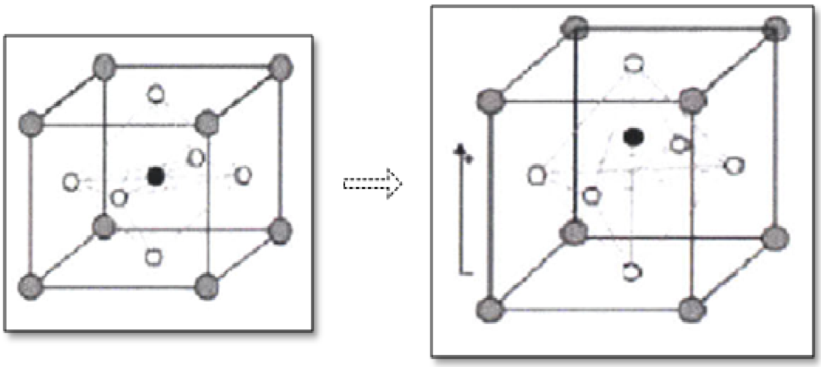

Figure 1.8: Microscopic Expansion of solid along the poling axis

expansion along the poling axis and contraction perpendicular to it as shown in fig Fig.1.8.

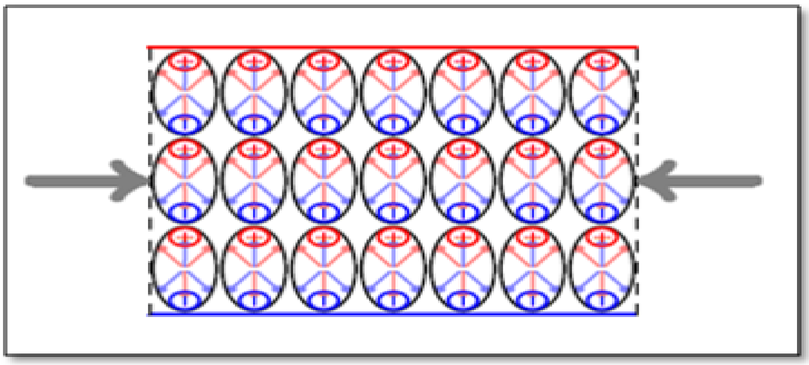

Figure 1.9: Converse effect

Converse effect: By applying external pressure the polarization generates an electric field and can be used to transform the mechanical energy of the material's deformation into electrical energy.

1.7.2 Materials used as a Piezoelectric Material

The most known material is Quartz (SiO_2), but there are other piezoelectric materials such as,

- Lead Zirconate Titanate (PZT)
- Berlinite ($AlPO_4$)

- Gallium orthophosphate ($GaPO_4$)
- Tourmaline
- Barium Titanate ($BaTiO_3$)
- Zinc Oxide (ZnO)
- Aluminum Nitride (AlN)
- Polyvinylidene Fluoride ($PVDF$)

1.7.3 Need of Piezoelectric Material

To enhance the response control and measurement of structural element laminated with composite plates under applied mechanical and electrical field by embedding actuator and sensor.

1.8 Laminated Composite with Functionally Graded Material

The concept of functionally graded material (FGM) was proposed in 1984 by the material scientists during space plane project in Japan . The FGM is a composite material whose composition varies from one side of the material to the other side either gradually or stepwise according to the required performance. It is an anisotropic composite material where a material gradient has been deliberately introduced over two different materials. By applying this concept, materials like ceramics, metals and plastics can be brought together with a gradual change of property from one material to another with no joint for specific application. FGMs allow the achievement of varied properties unlike uniform composites.

In particulate composites a graded structure can be obtained by either changing the particle volume fraction (Vp), or (b) the particle size along the thickness of the composite.

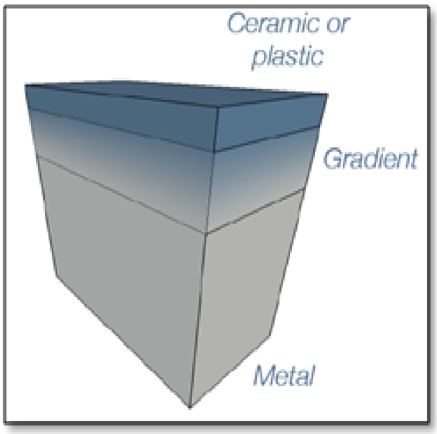

Figure 1.10: Gradual variation of material properties

1.8.1 Need of Functionally Graded Material

In conventional laminated composite structures, homogeneous elastic lamina are bonded together to obtain enhanced mechanical and thermal properties. The main inconvenience of such an assembly is to create stress concentrations along the interfaces and more specifically when high temperatures are involved. Because of sudden change of the mechanical properties at the interface between the layers it can lead to delaminations, matrix cracks, and other damage mechanisms.

One way to overcome this problem is to use functionally graded materials within which material properties vary continuously. So that an optimum distribution of properties can be obtained depending on the functional requirements and are therefore, free from interface weaknesses typically consists in laminated composites and sandwiches.

1.9 Objective of Study

Following are the main objectives of present work:

- To study different higher order shear deformation theories for analysis of laminated composite plates.

- To derive the formulation of 8-node Isoparametric Quadrilateral finite element for Static and Dynamic analysis of Laminated Composite Plates.
- To develop computer program for static and dynamic analysis of laminated composite plates.
- To study effect of various parameters on static and dynamic response of laminated composite plates.
- To study the behaviour and response of Laminated Composite Plates with piezoelectric material under Static Load.

1.10 Scope of Work

Scope of present work is as follows:

- Formulation of 8-node Isoparametric Quadrilateral finite element for Static Dynamic analysis of Laminated Composite Plates.
- Formulation of 8-node Isoparametric Quadrilateral finite element for Dynamic analysis of Laminated Composite Plates.
- Static analysis of Laminated Composite Plates with Piezoelectric Material.

1.11 Organization of Report

The content of Major Project report is divided in to various chapters as follows:

An Introduction of Laminated Composite is discussed in **Chapter 1**. Various applications in the field of Civil Engineering, classification and characteristics of Laminated Composite are also discussed. An overview of manufacturing process of composite lamina is discussed. Introduction to Laminated Composite with Piezoelectric material and Functionally Graded Material (FGM) with their advantages are discussed.

Literature review is presented in **Chapter 2**. It includes review of literature related to static and dynamic analysis of laminated composite plate as well as analysis of laminated composite plate with piezoelectric material and functionally graded material.

Static Analysis of Laminated Composite Plate is discussed in **Chapter 3**. Basic Mechanics of laminated plate is discussed in this chapter. Based on two displacement models with different degrees of freedom, using Higher Order Shear Deformation Theory(HOSDT) Finite Element Element Formulation has been derived. 8-Node Isoparametric Element has been considered to derive the finite element formulation for static and dynamic(Free vibration analysis) analysis of laminated Composite plates.

Computer Program with illustrative examples of static and dynamic is developed in **Chapter 4**. Computer Program is developed to carry out static and dynamic analysis of laminated composite plates with varying width-to-thickness ratio, material anisotropy, number of layers, support conditions and orientation of fibres.

Static Analysis of Laminated composite plates and results are discussed in **Chapter 5**.To validate the finite element formulation, a comparison study of obtained numerical results is carried out.

Dynamic Analysis of Laminated composite plates and results are discussed in **Chapter 6**. To validate the finite element formulation, a comparison study of obtained numerical results is carried out.

Static Analysis of bimorph composite laminate made up of piezoelectric material is discussed by solving one illustrative example in **Chapter 7**.

Summary of major project, conclusion and future scope of work are presented in **Chapter 8**.

Chapter 2

Literature Review

2.1 General

Literature review related to static and dynamic Finite Element Analysis of Laminated Composite Plates is presented in this chapter. Various research papers have been refereed to understand theoretical formulation for analysis of laminated composite plates. A literature review is categorised based on the type of analysis and composite materials used in Plates. The available literature has been classified in four groups as follows:

1. Static Analysis of Laminated Composite Plates.
2. Dynamic (eigen value problem) Analysis of Laminated Composite Plates.
3. Analysis of Laminated Composite Plates with Piezoelectric material.
4. Analysis of Laminated Composite Plates with Functionally Graded Material.

2.2 Literature Review

2.2.1 Static Analysis of Laminated Composite Plates

Sivkumaran et al.[7] presented the studies on finite element analysis of laminated composite plates including transverse shear deformations, and transverse normal stresses and strains. They have considered three displacement model based on finite elements considering different higher-order theories. The three different displacement functions expanded, resulting in three, five and six degrees of freedom per node. Based on displacement model they derived nine-node lagrangian isoparametric element stiffness matrices and the corresponding load vectors. The performance and accuracy of derived finite element formulation had been studied by comparing the results with other solutions like three-dimensional elasticity solutions, closed-form solutions, and other finite element models.

Reddy and Chao[11] studied the effects of reduced integration, mesh size, and element type on the accuracy of deflection, stresses and natural frequencies based on penalty finite element theory. They developed exact closed from solutions to assess the accuracy of the present finite element for cross-ply and antisymmetric angle-ply rectangular plates simply supported and subjected to sinusoidally distributed mechanical and/or thermal loadings, and free vibration. Based on this study by calculating various examples with different a/h ratios, they concluded that the reduced integration is essential for the analysis of thin plates, but is not crucial for thick plates.

Pandya and Kant[9] presented the studies on a finite element formulation for flexure of a symmetrically laminated plate based on a higher-order displacement model and a three-dimensional state of stress and strain. These studies incorporated linear variation of transverse normal strains and parabolic variation of transverse shear strains through the plate thickness. Nine-noded Lagrangian parabolic isoparametric plate bending element described and, discussed with applications to bending of laminated plates with various loading, boundary conditions, and lamination types. The numerical evaluations also included the convergence study of the element used. In addition, theory included the effect of direct normal stress in the thickness direction which is, though negligible, very important to study the delamination mode of failure in laminated composites. Based on higher order theory they compared solutions for deflections and stresses with those obtained using the three-dimensional elasticity theory, closed-form solutions with another high-order shear deformation theory, and the Mindlin's theory.

Pandya and Kant[8] presented the studies on a C^0 continuous displacement isoparametric finite element formulation of a higher-order theory for flexure of thick arbitrary laminated composite plates under transverse loads. They introduced the displacement model to accounts the non-linear and constant variation of in-plane and transverse displacement respectively through the plate thickness. The assumed displacement model eliminating the use of shear correction coefficients. Nine-noded quadrilateral element with nine degrees-of-freedom per node developed. They compared the results for plate deformations, internal stress-resultants and stresses for selected examples with the closed-form, the theory of elasticity and the finite element solutions with another higher-order displacement model by the same authors. A computer program developed which incorporated the realistic prediction of interlaminar stresses from equilibrium equations. The difference in the results of transverse shear stresses obtained using equilibrium equations and plate constitutive relations were found to be a maximum for the sandwich plate rather than the laminated plates.

Kant and Swaminathan[10] presented the studies on the theoretical model considering laminate deformations which account for the effects of transverse shear deformation, transverse normal strain/stress and a nonlinear variation of in-plane displacements with respect to the thickness coordinate. The comparison of the results obtained from presented theory with the available elasticity solutions and the results computed independently using the first order and the other higher order theories available in the literature showed that this refined theory predicted the transverse displacement and the stresses more accurately than all other theories considered in this paper. Further new results for the stretching-bending coupling behaviour of antisymmetric sandwich laminates using all the theories considered in this paper were presented which will serve as a benchmark for future investigations.

Xiao et al.[12] presented the studies to analyze static infinitesimal deformations of thick laminated composite elastic plates under different boundary conditions, using the meshless local Petrov-Galerkin (MLPG) method with radial basis functions (RBFs), and the higher order shear and normal deformable plate theory (HOSNDPT). Two types of RBFs, namely, multiquadrics (MQ) and thin plate splines (TPS), had been employed for constructing trial functions while a fourth order spline function have been used as the test function. Computed results for different lamination schemes found to match well with those obtained by other researchers. A benefit of using RBFs over those generated was that no special treatment was needed to impose essential boundary conditions, which substantially reduced the computational cost. Furthermore, they also concluded that MLPG method did not require nodal connectivity which reduced the time required to prepare the input data.

Shimpi and Patel[15] presented the studies on analysis of orthotropic plates. For analysis they developed a new theory, which involved only two unknown functions and yet took into account shear deformations. So the presented theory gave rise to only two governing equations. Number of unknown functions involved were only two, as against three in case of simple shear deformation theories of Mindlin and Reissner. The theory presented was variationally consistent, had strong similarity with classical plate theory in many aspects. Well studied examples, available in literature, had been solved to validate the theory. The results obtained for plate with various thickness ratios using the theory were not only substantially more accurate than those obtained using the classical plate theory, but were almost comparable to those obtained using higher order theories having more number of unknown functions.

Pagano[13] presented the studies on three-dimensional elasticity solutions, for rectangular laminates with pinned edges. The lamination geometry with arbitrary numbers of layers which could be isotropic or orthotropic with material symmetry axes parallel to the plate axes. They also presented further evidence regarding the range of validity and limitations of CPT. Several specific example problems solved, including a sandwich plate, and compared to the analogous results in classical laminated plate theory. They concluded that the accuracy of the CPT solution of a particular problem depend upon material properties, lamination geometry, and span-to-depth ratios. They observed the slower convergence of the exact solution to the CPT result and, also a convergence of the elasticity solution to CPT, which was more rapid for the stress components than plate deflection. This observation proved an importance of selecting the form of a plate theory required in the solution of a specific boundary value problem.

Park et al.[17] presented the studies on static and dynamic analysis of laminated composite plates and shells using 4-node Quasi-conforming shell element. The element formulations use interrelated displacement-rotation interpolations making it applicable for moderately thick and thin composite shells. The stiffness matrices for the elements were explicitly expressed and the stresses were taken accurately at the nodal points. A lot of numerical tests were carried out for the validation of presented 4-node composite shell element and the results were in good agreement with the references. The presented quasi-conforming formulation based on first order transverse shear deformation overcame the limit in the thin plates and shells. Also the presented solutions in the linear displacement and natural frequency showed very good agreement with the referenced solutions.

Iyengar and Pandya[14] presented the studies on analysis of orthotropic rectangular thick plates, using a method of initial functions. The formulation was capable to obtain a theory of any order and refinement. A sixth-order governing equation used to analyse uniformly loaded simply supported square plates for various thickness and material properties. The variation across the thickness of maximum stresses and displacements compared with those obtained by the application of Ambartsumyan's theory and Reissner's theory.

Ghugal and Sayyad[16] presented the studies on analysis of isotropic plate using

Trigonometric Shear Deformation Theory (TSDT). The presented theory was formulated based on classical plate theory using right handed cartesian coordinate system. In presented theory the displacement model was able to consider the shear deformation effect and effect of transverse normal strain. Governing equations and boundary conditions of the theory were obtained using the principle of virtual work. The theory obviates the need of shear correction factor. Results obtained for static flexural analysis of simply supported thick isotropic plates for various loading cases were compared with those of other refined theories and exact solution from theory of elasticity, which showed good agreement.

2.2.2 Dynamic Analysis of Laminated Composite Plates

Kant and Mallikarjuna[18] presented the studies on non linear dynamics of laminated plates with a higher order theory and C^0 finite elements. A nine node isoparametric quadrilateral element based on higher-order theory developed. An experimentally established contact law which accounts for the permanent indentation incorporated into the finite element program to evaluate the impact force. In the time integration, the explicit central difference technique had been used in conjunction with the special mass matrix diagonalization scheme. Numerical results, including contact force histories, deflections and strains in the plate, were presented.

Khante et al.[19]investigated the studies on damped transient dynamic elasto-plastic analysis of plate. A finite element model based on a C^0 higher order shear deformation theory was developed. Nine noded Lagrangian element with five degrees of freedom per node was used. Selective Gauss integration was used to evaluate energy terms so as to avoid shear locking and spurious mechanisms. Explicit central difference time stepping scheme was employed to integrate temporal equations. The mass matrix was diagonalized by using the efficient proportional mass lumping scheme. A program was developed for damped transient dynamic finite element analysis of elasto-plastic plate. Several numerical examples were studied to unfold different facets of damping of elasto-plastic plates.

They also studied the response of the plate under different degrees of damping measured by α (defined previously). The sensitivity of response of the plate to absolute damping i.e. mass proportional damping was seen to be dependent on non-dimensional parameter (NDP). For the larger NDP values the plate was observed to be insensitive to damping considered. For the sensitive plates, it was found that with increase in damping coefficient α the central displacement decreases without affecting effective period of vibration of plate as is true in case of elastic plates.

Jameel and Abed[20]presented the studies on free vibration analysis of composite laminated plates using HOST 12 FE model. The theory of a Higher Order Shear Deformation Theory (HOST 12) used to solve the problem of free vibration of simply supported symmetric and antisymmetric angle-ply composite laminated plates. The presented HOST12 FE model incorporated laminate deformations which account for the effects of transverse shear deformation, transverse normal strain/stress and a non-linear variation of in-plane displacements with respect to the thickness coordinate - thus modeling the warping of transverse cross-sections more accurately and eliminating the need for shear correction coefficients. Solutions were obtained in closed-form using Navier's technique by solving the Eigne value equation. The results compared with those from exact analysis and various theories from references. It was concluded for all the parameters considered based on Reddy's theory that natural frequencies were over predicted for the composite and sandwich plates.

Kant and Swaminathan[21]presented the studies on Free Vibration of Laminated Composite and Sandwich plates based on a higher-order refined theory. Here presented theoretical model incorporated laminate deformation which account for the effects of transverse shear deformation, transverse normal strain/stress and a non-linear variation of in-plane displacements with respect to thickness coordinate. The equations of motion were obtained using Hamilton's principle. Solutions were obtained in close form using Navier's technique. The comparison of the present results with available elasticity solutions and the other higher order theories showed that presented refined theory predict more accurate frequencies.

Kant and Mallikarjuna[22] presented the studies on vibrations of unsymmetrically laminated plates analyzed by using a higher order theory with a C^0 finite element formulation. Vibration analysis of laminated composite and sandwich plates in conjunction with a C^0 isoparametric finite element formulation was carried out with consideration of higher order displacement model. A special mass lumping procedure was used in the equilibrium equations. The numerical examples presented were compared with 3-D elasticity/analytical and Mindlin's plate solutions, and presented model predict frequencies more accurately.

Kant and Mallikarjuna[24] presented the studies on a refined higher-order theory for free vibration analysis of unsymmetrically laminated multilayered plates. A simple C^0 finite element formulation was presented and the nine-noded lagrangian element was chosen with seven degrees of freedom per node. Numerical results were compared with first-order and classical plate theories, which showed that presented theory predict frequencies more accurately.

Kulkarni and Khandagale[25] presented the studies on finite element analysis of thick isotropic rectangular and skew plates based on Reddys third order theory involves the problem of C1 continuity. A four-node quadrilateral element having seven degrees of freedom per node was considered for finite element formulation. In displacement model as present of second derivative of W_0 was indicated that C^1 continuity was required at element boundary, which was circumvented by using the improved discrete Kirchhoff constraint approach. Results obtained using a mesh size 24 X 24 for formulated finite element formulation were compared with 2D analytical results for simply supported plate, 3D exact, 3D approximate and 3D FE results of ANSYS for a square clamped plate and a simply-supported skew plate.

2.2.3 Analysis of Laminated Composite Plates with Piezoelectric material

Hwang and Park[32] studied the vibration control of laminated plate with piezoelectric sensors/actuators. For dynamic analysis equation of motion was formulated using Classical Laminate Theory and Hamilton's principle. The plate was discretized using 4-node quadrilateral plate bending element with 12 degrees of freedom per node and one electrical degree of freedom per element. The piezoelectric sensor was distributed and integrated because output voltage was dependent on the strain rate. For validation static responses of bimorph beam were calculated. For vibration control of plate the responses of plate under given displacements and external loads were obtained using direct time integration of equation of motion using newmark-β method. From finite element formulation code was developed.

Chen et al.[33] presented the studies on vibration control of intelligent structure using finite element analysis. Finite element formulation for vibration control and suppression of intelligent structures with a new piezoelectric plate element was carried out. A method of active vibration control and suppression for intelligent structures was developed based on a negative velocity feedback control law. For finite element formulation, 4-node isoparametric finite element with 12-degree of freedom(mechanical) and one electrical degree of freedom per node was considered. For validation of the presented method two examples were calculated using bimorph beam and intelligent plate.

Shiyekar and Kant[27] presented a studies on a complete analytical solution for cross- ply composite laminates integrated with piezoelectric fiber-reinforced composite (PFRC) actuators under bi-directional bending. A higher order shear and normal deformation theory (HOSNT12) had been used to analyze such hybrid or smart laminates subjected to electromechanical loading. In the presented studies the electrostatic potential had been assumed to be layer wise (LW) linear through the thickness of PFRC. Navier's technique and principle of minimum potential energy had been used to obtain the equations of equilibrium. Transverse shear stresses were presented at the interface of PFRC actuator and laminate under the action of electrostatic potentials. They also observed that actuating effects were more in case of thick than thin laminates. They compared the results with first order shear deformation theory (FOST) and exact solution.

Neto et al.[28] presented the studies on static and dynamic analysis of smart laminated structures. To analyse they presented the three node finite element with piezoelectric coupling. The element was a continuum-based degenerated plate element based on the Reissner-Mindlin theory with six mechanical degrees of freedom per node and one electrical degree of freedom per finite element. The electric field was assumed constant across the thickness of each piezoelectric layer. The bending and membrane consistent mass matrices had been derived for applications on structural dynamics. Since this finite element was firstly developed to allow the active vibration control of the flexible multibody components The numerical results obtained by this finite element correlated well with other published results.

Kogl and Bucalem[29] presented the studies on analysis of smart laminates using piezoelectric MITC plate and shell elements. In the presented studies, recently developed piezoelectric MITC plate and shell elements had been employed for the modelling of multi-layer smart structures. The piezoelectric MITC elements were free of locking and yield very accurate and reliable results. The formulation allowed the incorporation of layers of arbitrary material properties such as viscoelastic bonding layers. By means of numerical examples, the accuracy of the solutions and the suitability of the approach for the modelling of smart structures were demonstrated. Finally, the excellent performance of the MITC-P shell elements was confirmed by investigating harmonic vibrations of an elastic cylindrical shell with two piezoelectric actuators attached to it.

Fukunaga et al.[30]presented the finite element model for analyzing the composite laminates containing the piezoelectrics statically and dynamically. A simple higher order plate theory was used, which can satisfy the free conditions of transverse shear strains on the top and bottom surfaces of the plates. To develop C^0 type FEM scheme, two artificial variables in the displacement field had been introduced to avoid the higher-order plate theory. Also a generalized coupling FEM model for the mechanical and electric fields from the variational framework was proposed. Finally various examples studied in many previous researches had been employed to verify the justification, accuracy and efficiency of the presented model.

Huang and Liu[31]presented the studies which deals with the fully coupled response characteristics of a multilayered composite plate with piezoelectric layers. The response quantities of the plate were coupled by the mechanical field and the electric field. Based on the three-dimensional linear piezoelectricity and the first-order shear deformation theory, the fundamental unknowns, such as the displacements and the electric potential, were assumed to be expandable through the plate thickness coordinate. Numerical results for the static and dynamic response of the laminated composite plates with different lamination schemes and having a PIC-151 piezoelectric material layer were obtained. The effects of the static and dynamic response were presented. Numerical results showed that the plate thickness ratio, plate aspect ratio, lamination scheme, fiber orientations, and piezoelectric coupling significantly influence the static and dynamic responses of the plate. It was observed that the deflections increases and natural frequency decreases with an increase in the plate aspect ratio for all fiber orientations. It has been also observed that the coupling due to piezoelectric layer reduces the transverse deflection and the natural frequency of the plate resistance increases with the presence of piezoelectric coupling.

2.2.4 Analysis of Laminated Composite Plates with Functionally Graded Material

Alieldin et al.[34] investigated the mechanical behaviour of laminated composite and functional graded plates by using, the first-order shear deformation plate (FSDT). Three approaches had been developed to transform the laminated composite plate, with stepped material properties, to an equivalent functionally graded (FG) plate with a continuous property function across the plate thickness. Such transformations were used to determine the details of a functional graded plate equivalent to the original laminated one and to acquire an easy and efficient way to investigate the behaviour of multilayer composite plates, with direct and less computational efforts.

Pendhari et al.[35] presented the studies on mixed semi-analytical and analytical solutions for a rectangular plate made of functionally graded (FG) material. All edges of a plate were considered under simply supported (diaphragm) end conditions and general stress boundary conditions can be applied on both top and bottom surface of a plate during solution. A mixed semi-analytical model consists in defining a two-point boundary value problem governed by a set of first-order ordinary differential equations in the plate thickness direction. Analytical solutions based on shear-normal deformation theories were also established to show the accuracy, simplicity and effectiveness of mixed semi-analytical model. They concluded with the main feature of mixed semi-analytical model that the governing equation system was not transformed into an algebraic equation system, thus the intrinsic behaviour of the physical system was retained to a greater degree of accuracy.

Shiyekar and Kant[36]presented the studies on bidirectional flexure analysis of Functionally Graded (FG) plate integrated with piezoelectric fiber reinforced composites (PFRC). A higher order shear and normal deformation theory (HOSNT12) was used to analyze such hybrid or smart FG plate subjected to electromechanical loading. The displacement function used was approximate. Variations of in-plane and transverse displacements were observed linear and constant. Linear layer wise approximation of the electrostatic potential was proposed in the present model. Elastic constants were varying exponentially along thickness (z axis) for FG material while Poisson's ratio was kept constant. PFRC actuator attached either at top or bottom of FG plate and analyzed under mechanical and coupled mechanical and electrical loading. Comparison of presented HOSNT12 was made with exact and finite element method.

2.3 Summary

In this chapter, literature review related to static and dynamic analysis of laminated composite plate has been briefly reviewed. The review of literature includes the following points:

- Type of theory developed and used in analysis of laminated composites.
- Type of element used in finite element analysis.
- Degrees of Freedom considered based on support conditions.
- Applied Loading Conditions to the laminated composites.
- Comparison of results obtained by presented theory with different available theory solutions.

Chapter 3

Static and Dynamic Analysis of Laminated Composite Plate

3.1 Introduction

For static and dynamic analysis of composite plates Classical Plate Theory(CPT) as well as Finite Element Method(FEM) based on numerical methods can be used. In the present study finite element method is used for analysis of composite plates. Finite element method is based on principle of discretization. By assuming element properties global matrices are formed. From solution of equilibrium equations response of composite plate under static loading can be obtained. Eigen value analysis of assembled stiffness matrix and mass matrix gives natural frequency and mode shapes of composite plates. Element properties depends on stress-strain relationship and strain-displacement relationship. In this chapter element properties are derived based on two displacement models.

3.2 Basic Mechanics of Composite Laminates

3.2.1 Generalized Hooke's law for Nonisotropic Materials

Normal Stress and Strain, Uniaxially Applied Force

For isotropic materials, the relationship between stress and strain is independent of the direction of force, thus only one elastic constant (young's modulus) is required to describe the stress-strain relationship for a uniaxially applied force.

For a nonisotropic material, at least two elastic constants are needed to describe the stress-strain behavior of the material. Fig.3.1 is a schematic of an isotropic and a unidirectional fiber-reinforced material. The stiffness of the isotropic plate can be described by one value, the modulus, E, of the material, regardless of direction of load.

The stiffness of the orthotropic plate must be described by two values, one along the longitudinal direction of the fibers commonly referred to as E_L, and one transverse to the direction of fibers, usually denoted by E_T. Subscripts 1 and 2 will be used such that $E_L = E_1$ and $E_T = E_2$. Thus indices must be added to the stress, strain, and modulus values to describe the direction of the applied force.

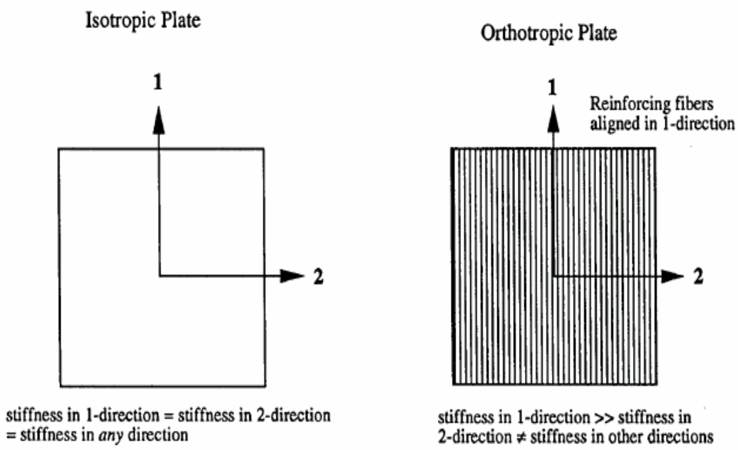

Figure 3.1: Difference between an isotopic plate and an orthotropic plate

For example, for an isotropic material, the stress-strain relationship is written.

$$\sigma = E\varepsilon \tag{3.1}$$

For the orthotropic system the direction must be specified.
For example,

$$\sigma_1 = E_1\varepsilon_1 \quad or \quad \sigma_2 = E_2\varepsilon_2 \tag{3.2}$$

3.2.2 Stress And Strain relations of a thin lamina for specially orthotropic plates

The previous section dealt with an extremely simple type of stress state, uniaxial. In general, plates will experience stresses in more than one direction within the plane. This is referred as the plane stress condition. In this case Poisson's ratio now becomes important. It is the ratio of the strain perpendicular to a given loading direction, to the strain parallel to this given loading direction:
Poisson's ratio, for loading along the fibers

$$\nu_{12} = \frac{\varepsilon_T}{\varepsilon_L} \tag{3.3}$$

for loading perpendicular to fibers

$$\nu_{21} = \frac{\varepsilon_T}{\varepsilon_L} \tag{3.4}$$

The strain components are now stretch due to an applied force, minus the contraction due to Poisson's effect of another force perpendicular to this applied force. Thus,

$$\varepsilon_1 = \frac{\sigma_1}{E_1} - \nu_{21}\varepsilon_2 \;\; and \;\; \varepsilon_2 = \frac{\sigma_2}{E_2} - \nu_{12}\varepsilon_1 \tag{3.5}$$

Using equation,

$$\varepsilon_1 = \frac{\sigma_1}{E_1} - \nu_{21}\frac{\sigma_2}{E_2} \;\; and \;\; \varepsilon_2 = \frac{\sigma_2}{E_2} - \nu_{12}\frac{\sigma_1}{E_1} \tag{3.6}$$

Shear forces can also be present. Shear stress and shear strain are related by a constant. This constant is called the shear modulus and is usually denoted by G. Thus,

$$\tau_{12} = \gamma_{12}G_{12} \tag{3.7}$$

Where τ_{12} is the shear stress (the 1 and 2 indices indicating shear in the 1-2 plane), and γ_{12} is the shear strain. Fig.3.2 gives a definition of shear strain. Since it is known that a relationship exists between Poisson's ratios and the modulii in each of the two axes directions, namely,

$$\nu_{21}E_1 = \nu_{12}E_2 \tag{3.8}$$

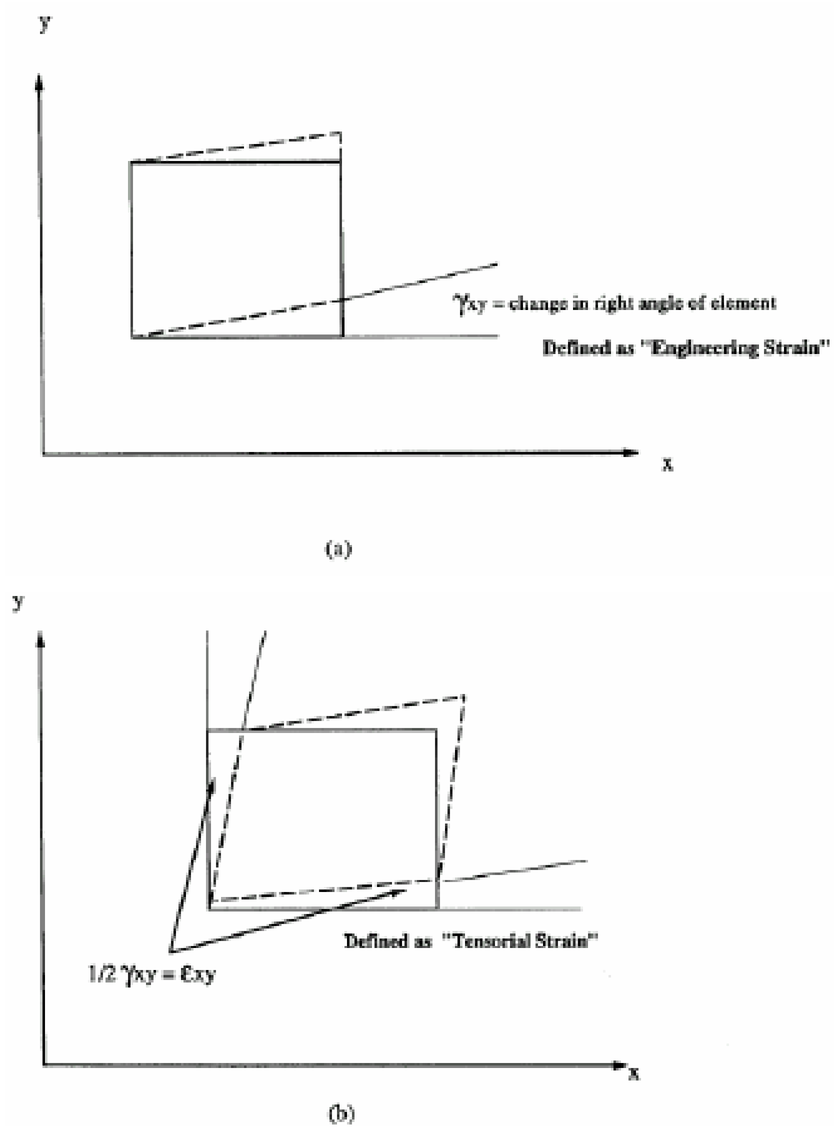

Figure 3.2: Definition of shearing strain

For lamina stress and strain tensors are written as follows:

$\sigma_{11} = \sigma_1, \sigma_{22} = \sigma_2, \sigma_{33} = \sigma_3, \sigma_{23} = \tau_{23} = \sigma_4, \sigma_{31} = \tau_{31} = \sigma_5, \sigma_{12} = \tau_{12} = \sigma_6$

In such a case all stress components out-of-plane direction (3-direction) are zero, that is:

$$\sigma_3 = \tau_{23} = \tau_{31} = 0 \tag{3.9}$$

Equations 3.6 and 3.7 can be written in matrix form as:

$$\begin{vmatrix} \varepsilon_1 \\ \varepsilon_2 \\ \gamma_{12} \end{vmatrix} = \begin{vmatrix} S_{11} & S_{12} & 0 \\ S_{12} & S_{22} & 0 \\ 0 & 0 & S_{33} \end{vmatrix} \begin{vmatrix} \sigma_1 \\ \sigma_2 \\ \tau_{12} \end{vmatrix} \tag{3.10}$$

where

$$S_{11} = \frac{1}{E_1}, S_{22} = \frac{1}{E_2}, S_{12} = \frac{-\nu_{12}}{E_1} = \frac{-\nu_{21}}{E_2}, S_{33} = \frac{1}{G_{12}} \tag{3.11}$$

By inverting the compliance matrix, one can get stress as a function of strain. This turns out to be:

$$\begin{vmatrix} \sigma_1 \\ \sigma_2 \\ \tau_{12} \end{vmatrix} = \begin{vmatrix} Q_{11} & Q_{12} & 0 \\ Q_{12} & Q_{22} & 0 \\ 0 & 0 & Q_{33} \end{vmatrix} \begin{vmatrix} \varepsilon_1 \\ \varepsilon_2 \\ \gamma_{12} \end{vmatrix} \tag{3.12}$$

Where:

$$Q_{11} = \frac{E_1}{1-\nu_{12}\nu_{21}} \; Q_{22} = \frac{E_2}{1-\nu_{12}\nu_{21}} \; Q_{12} = \frac{\nu_{12}E_2}{1-\nu_{12}\nu_{21}} = \frac{\nu_{21}E_1}{1-\nu_{12}\nu_{21}} \; Q_{33} = G_{12} \tag{3.13}$$

The Q_{ij} is referred to as the reduced stiffness component and the matrix is abbreviated as [Q].

3.2.3 Transformation of stress and strain

The stiffness of composite changes with the change of ply orientation. A particular axis system is chosen for conveniently solving the problem - axis system is known as the loading axis or the reference axis. For fibre reinforced composites, another axis system which is parallel and perpendicular to the fibre orientation is convenient for the calculation of material properties. As such the transformation of stresses and strains from one axis system to another is needed.

The principal material axis system is indicated by the 1-2 axis and the reference axis system is shown by the x-y axis Fig.3.3. Fig.3.3(a) indicates an on-axis system, that is, where the principal material axis is coincident with the reference axis. Fig.3.3(b) depicts an off-axis system. Here the reference axis system for a unidirectional composite is different from the material axis system. Counter-clockwise rotation of θ is taken as positive.

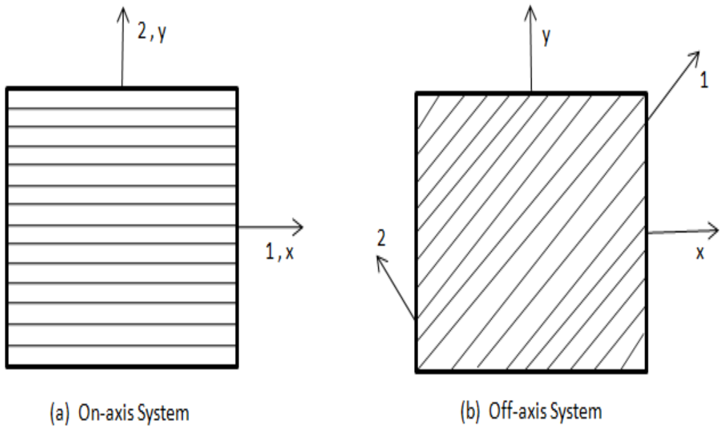

Figure 3.3: Axis system in an unidirectional stressed lamina

Unidirectional stressed lamina in an off-axis system is shown in Fig.3.4 stresses on planes coincident with the material axis system is shown in Fig.3.5 the wedge is considered parallel and perpendicular to the fibre orientation.

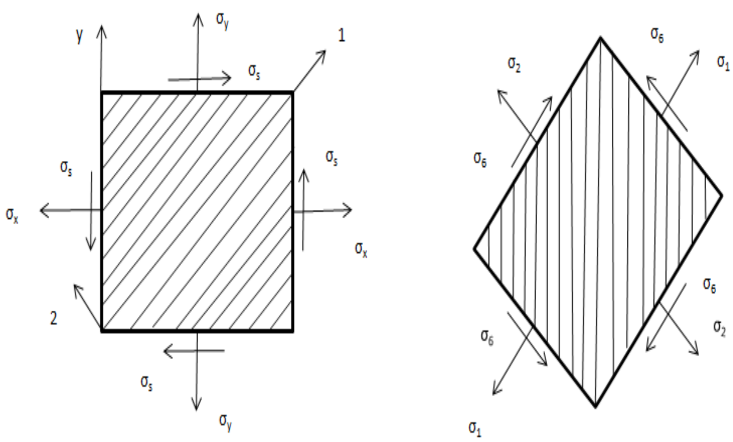

Figure 3.4: Unidirectional stressed lamina

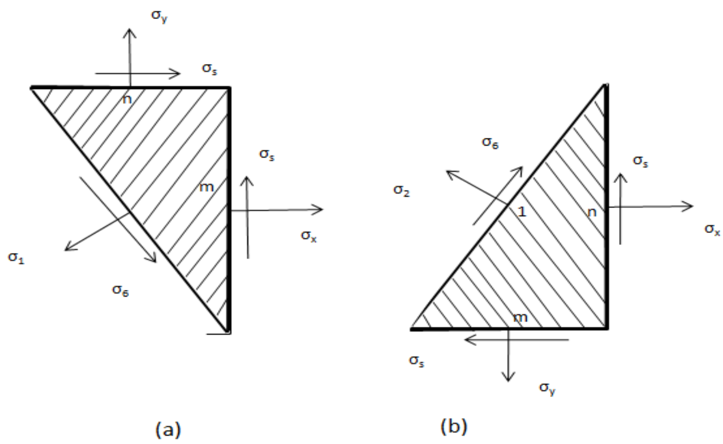

Figure 3.5: Stresses on inclined plane

Referring to Fig.3.5 , the equilibrium of all horizontal and vertical forces of the wedge with unit area on the inclined plane yield the following equations,

$$m\sigma_1 - n\sigma_6 = m\sigma_x + n\sigma_s \tag{3.14}$$

$$n\sigma_1 - m\sigma_6 = n\sigma_y + m\sigma_s \tag{3.15}$$

Where,

$m = \cos\theta$,$n = \sin\theta$ and $\sigma_6 = \tau_{12}$

Solving Equation 3.14 and 3.15 ,yields,

$$\sigma_1 = m^2\sigma_x + n^2\sigma_y + 2mn\sigma_s \tag{3.16}$$

$$\sigma_6 = -mn\sigma_x + mn\sigma_y + (m^2 - n^2)\sigma_s \tag{3.17}$$

Similarly, referring to Fig.3.5(b) and following similar steps as above, we get

$$\sigma_2 = n^2\sigma_x + m^2\sigma_y - 2mn\sigma_s \tag{3.18}$$

Equations 3.16 to 3.17 written in matrix form becomes

$$\begin{vmatrix} \sigma_1 \\ \sigma_2 \\ \sigma_6 \end{vmatrix} = \begin{vmatrix} m^2 & n^2 & 2mn \\ n^2 & m^2 & -2mn \\ -mn & mn & m^2 - n^2 \end{vmatrix} \begin{vmatrix} \sigma_x \\ \sigma_y \\ \sigma_s \end{vmatrix} \tag{3.19}$$

Or,

$$\sigma_{1,2} = [T] \; \sigma_{x,y} \tag{3.20}$$

[T] is known as the transformation matrix.

Same way transformation matrix for strain,

$$\begin{vmatrix} \varepsilon_1 \\ \varepsilon_2 \\ \frac{\varepsilon_6}{2} \end{vmatrix} = \begin{vmatrix} m^2 & n^2 & 2mn \\ n^2 & m^2 & -2mn \\ -mn & mn & m^2 - n^2 \end{vmatrix} \begin{vmatrix} \varepsilon_x \\ \varepsilon_y \\ \frac{\varepsilon_s}{2} \end{vmatrix} \tag{3.21}$$

Or,

$$\varepsilon_{1,2} = [T] \; \varepsilon_{x,y} \tag{3.22}$$

By multiplying both sides of Equation 3.19 and 3.21 by $[T]^{-1}$, we obtain for the stressed lamina,

$$\begin{vmatrix} \sigma_x \\ \sigma_y \\ \sigma_s \end{vmatrix} = [T]^{-1} \begin{vmatrix} \sigma_1 \\ \sigma_2 \\ \sigma_6 \end{vmatrix} \tag{3.23}$$

end

$$\begin{vmatrix} \varepsilon_x \\ \varepsilon_y \\ \frac{\varepsilon_s}{2} \end{vmatrix} = [T]^{-1} \begin{vmatrix} \varepsilon_1 \\ \varepsilon_2 \\ \frac{\varepsilon_6}{2} \end{vmatrix} \tag{3.24}$$

Where

$$[T]^{-1} = [T(-\theta)] = \begin{vmatrix} m^2 & n^2 & -2mn \\ n^2 & m^2 & 2mn \\ mn & -mn & m^2-n^2 \end{vmatrix} \tag{3.25}$$

Transformation of elastic constants

When a lamina is loaded in the reference axis xy, the relationship between stresses in the reference xy-axis and that in the principal material axis is given by Equation 3.23,

Combining 3.12 and 3.23 result in,

$$\begin{vmatrix} \sigma_x \\ \sigma_y \\ \sigma_s \end{vmatrix} = \begin{vmatrix} m^2 & n^2 & -2mn \\ n^2 & m^2 & 2mn \\ mn & -mn & m^2-n^2 \end{vmatrix} \begin{vmatrix} Q_{11} & Q_{12} & 0 \\ Q_{12} & Q_{22} & 0 \\ 0 & 0 & 2Q_{66} \end{vmatrix} \begin{vmatrix} \varepsilon_1 \\ \varepsilon_2 \\ \frac{\varepsilon_6}{2} \end{vmatrix} \tag{3.26}$$

substituting strains in the 1-2 axis in terms of x-y axis from Equation 3.21 into 3.26, yields

$$\begin{vmatrix} \sigma_x \\ \sigma_y \\ \sigma_s \end{vmatrix} = \begin{vmatrix} m^2 & n^2 & -2mn \\ n^2 & m^2 & 2mn \\ mn & -mn & m^2-n^2 \end{vmatrix} \begin{vmatrix} Q_{11} & Q_{12} & 0 \\ Q_{12} & Q_{22} & 0 \\ 0 & 0 & 2Q_{66} \end{vmatrix} \begin{vmatrix} m^2 & n^2 & 2mn \\ n^2 & m^2 & -2mn \\ -mn & mn & m^2-n^2 \end{vmatrix} \begin{vmatrix} \varepsilon_x \\ \varepsilon_y \\ \frac{\varepsilon_s}{2} \end{vmatrix} \tag{3.27}$$

Equation 3.27 is written as

$$\begin{vmatrix} \sigma_x \\ \sigma_y \\ \sigma_s \end{vmatrix} \begin{vmatrix} Q_{xx} & Q_{xy} & 2Q_{xs} \\ Q_{yx} & Q_{yy} & 2Q_{ys} \\ Q_{sx} & Q_{sy} & 2Q_{ss} \end{vmatrix} \begin{vmatrix} \varepsilon_x \\ \varepsilon_y \\ \frac{\varepsilon}{s} \end{vmatrix} \tag{3.28}$$

The relationship between reduced stiffness are as follows,

$Q_{xx} = m^4Q_{11} + n^4Q_{22} + 2m^2n^2Q_{12} + 4m^2n^2Q_{66}$

$Q_{yy} = n^4Q_{11} + m^4Q_{22} + 2m^2n^2Q_{12} + 4m^2n^2Q_{66}$

$Q_{xy} = m^2n^2Q_{11} + m^2n^2Q_{22} + (m^4 + n^4)Q_{12}$ - $4m^2n^2Q_{66}$

$Q_{xs} = m^3nQ_{11}$ - mn^3Q_{22} + $(mn^3 - m^3n)Q_12$ + $2(mn^3 - m^3n)Q_{66}$

$Q_{ys} = mn^3Q_{11}$ - m^3nQ_{22} + $(m^3n - mn^3)Q_12$ + $2(m^3n - mn^3)Q_{66}$

$Q_{ss} = m^2n^2Q_{11} + m^2n^2Q_{22}$ - $2m^2n^2Q_12$ + $(m^2 - n^2)^2Q_{66}$

3.3 Higher Order Shear Deformation Theory

Introduction

Fibre reinforced composite are manufactured in the form of thin layers and by bonding them together laminated composite plate is constructed. The analysis of these plates has been very abundantly studied area in structural engineering for many years because of their application. In most applications, the thickness of a laminate is small compared to the planner dimensions. For analysis of this laminate two dimensional theories are developed from three dimensional elasticity theory by making assumptions of variation of displacements and/or stresses through the thickness of laminate. The classical laminated plate theory(CLPT) is an extension of the classical plate theory to laminated plate. In this theory displacements are assumed to vary linearly through thickness and transverse displacement is assumed constant through the thickness. In most of the case the classical laminated plate theory is found adequate for the laminate with small thickness, and where it is not applicable the refinement of this theory is required. A refined classical laminate plate theory is known as a First Order Shear Deformation Theory(FSDT).[2]

The fist order shear deformation theory is based on displacement field, where the three components of the displacement vector are expanded in power series of the thickness coordinate and unknown functions. It is also known commonly as "The Mindlin Plate Theory". The first order shear deformation theory yields a constant value of transverse shear strain through the thickness of plate by introducing shear correction factors. The shear correction factors are dimensionless quantities introduced to account for the inconsistency between the constant rate of shear strains in the first order theory and the higher-order distribution of shear strains in the elasticity theory.

To account for the transverse shear deformation more correctly, the higher order terms are necessary to incorporate in the displacement field. Higher order theories are derived out of power series expansion of the mid-surface displacements in the power of the thickness co-ordinates as given below. in this study two Displacement models are used to account for membrane, bending and transverse shear deformation.

A coordinate system is adopted such that the x-y plane coincides with the mid plane and the z-axis is perpendicular to the plane as shown in Fig.3.6. The displacements in the x, y and z directions of the symmetrically laminated composite plates subjected to transverse load may be taken as follows. The displacement along the x, y and z directions are expressed in terms of higher order functions of thickness coordinates and mid plane variables.

a. Displacement Model - 1

$$u(x,y,z) = z\theta_x(x,y,0) + z^3\theta_x^*(x,y,0) = z\theta_x + z^3\theta_x^*$$
$$v(x,y,z) = z\theta_y(x,y,0) + z^3\theta_y^*(x,y,0) = z\theta_y + z^3\theta_y^*$$
$$w(x,y,z) = w_0(x,y,0) + z^2w_0^*(x,y,0) = w_0 + z^2w_0^*$$

b. Displacement Model - 2

$$u(x,y,z) = u_0(x,y,0)+z\theta_x(x,y,0)+z^2u_0^*(x,y,0)+z^3\theta_x^*(x,y,0)=u_0+z\theta_x+z^2u_0^*+z^3\theta_x^*$$
$$v(x,y,z) = v_0(x,y,0)+z\theta_y(x,y,0)+z^2v_0^*(x,y,0)+z^3\theta_y^*(x,y,0)=v_0+z\theta_y+z^2v_0^*+z^3\theta_y^*$$
$$w(x,y,z) = w_0(x,y,0) + z\theta_z(x,y,0)+z^2w_0^*(x,y,0) = w_0 + z\theta_z + z^2w_0^*$$

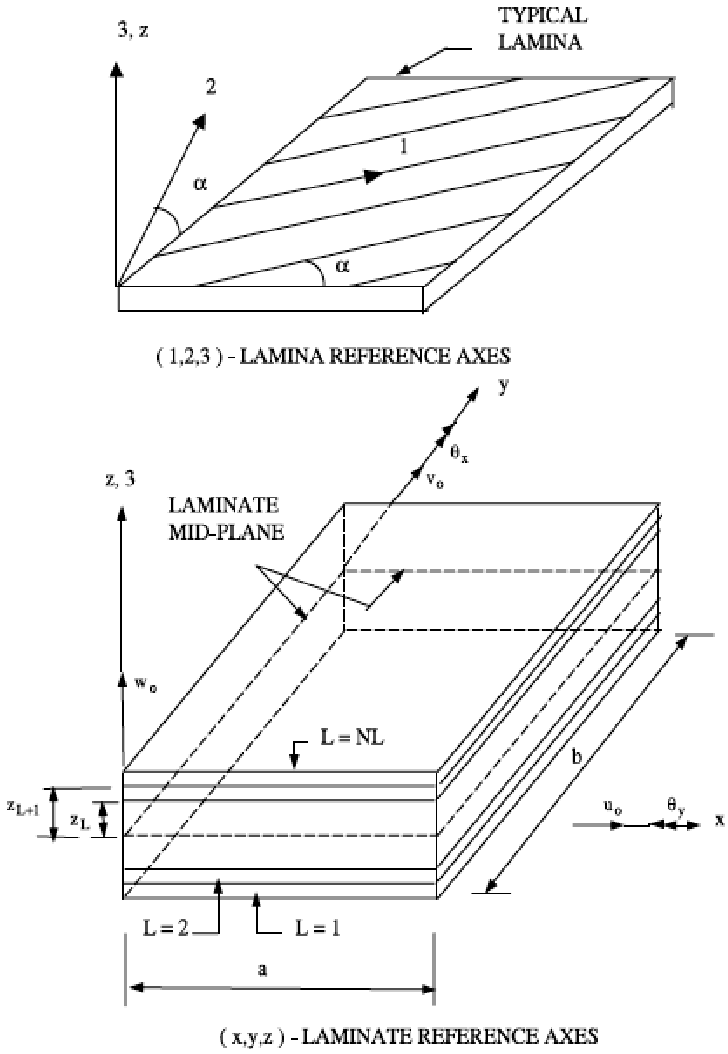

Figure 3.6: Laminate geometry with positive set of lamina reference axis, displacement components and fibre orientation.[21]

3.3.1 Definition of Displacement Field for Model-1

$$u(x, y, z) = z\theta_x(x, y, 0) + z^3\theta_x^*(x, y, 0) = z\theta_x + z^3\theta_x^*$$
$$v(x, y, z) = z\theta_y(x, y, 0) + z^3\theta_y^*(x, y, 0) = z\theta_y + z^3\theta_y^*$$
$$w(x, y, z) = w_0(x, y, 0) + z^2w_0^*(x, y, 0) = w_0 + z^2w_0^*$$

where u, v, and w define the displacements of a point along x, y and z directions respectively, θ_x and θ_y are the rotations of the normal to the mid plane at the same point, and w_0^*, θ_x^*, θ_y^* are the corresponding higher order terms. An advantage of the displacement model under consideration is that the assumed field variables w_0,

θ_x, θ_y, w_0^*, θ_x^*, θ_y^* need only be C^0 continuity. This model includes the effects of the transverse normal strain/stress also.

Strain Displacement Relationship Corresponding to Model

$$\varepsilon_x = \frac{\partial u}{\partial x} = z\frac{\partial \theta_x}{\partial x} + z^3\frac{\partial \theta_x^*}{\partial x} = zK_x + z^3K_x^*$$
$$\varepsilon_y = \frac{\partial v}{\partial y} = z\frac{\partial \theta_y}{\partial y} + z^3\frac{\partial \theta_y^*}{\partial y} = zK_y + z^3K_y^*$$
$$\varepsilon_z = \frac{\partial w}{\partial z} = 2zw_0^* = zK_z$$
$$\gamma_{xy} = \frac{\partial u}{\partial y} + \frac{\partial v}{\partial x} = z\frac{\partial \theta_x}{\partial y} + z^3\frac{\partial \theta_x^*}{\partial y} + z\frac{\partial \theta_y}{\partial x} + z^3\frac{\partial \theta_y^*}{\partial x} = zK_{xy} + z^3K_{xy}^*$$
$$\gamma_{yz} = \frac{\partial v}{\partial z} + \frac{\partial w}{\partial y} = \theta_y + 3z^2\theta_y^* + \frac{\partial w_0}{\partial y} + z^2\frac{\partial w_0^*}{\partial y} = \phi_y + z^2\phi_y^*$$
$$\gamma_{xz} = \frac{\partial u}{\partial z} + \frac{\partial w}{\partial x} = \theta_x + 3z^2\theta_x^* + \frac{\partial w_0}{\partial x} + z^2\frac{\partial w_0^*}{\partial x} = \phi_x + z^2\phi_x^*$$

Where the definitions of the various terms are as follows:

$$K_x = \frac{\partial \theta_x}{\partial x}$$
$$K_y = \frac{\partial \theta_y}{\partial y}$$
$$K_{xy} = \frac{\partial \theta_x}{\partial y} + \frac{\partial \theta_y}{\partial x}$$
$$K_x^* = \frac{\partial \theta_x^*}{\partial x}$$
$$K_y^* = \frac{\partial \theta_y^*}{\partial y}$$
$$K_{xy}^* = \frac{\partial \theta_x^*}{\partial y} + \frac{\partial \theta_y^*}{\partial x}$$
$$\phi_x = \theta_x + \frac{\partial w_0}{\partial x}$$
$$\phi_y = \theta_y + \frac{\partial w_0}{\partial y}$$
$$\phi_x^* = 3\theta_x^* + \frac{\partial w_0^*}{\partial x}$$
$$\phi_y^* = 3\theta_y^* + \frac{\partial w_0^*}{\partial y}$$
$$K_z = 2w_0^*$$

The concise matrix form above equations,

$$\varepsilon_b^k = \begin{vmatrix} \varepsilon_x \\ \varepsilon_y \\ \varepsilon_z \\ \gamma_{xy} \end{vmatrix} = z \begin{vmatrix} K_x \\ K_y \\ K_z \\ K_x y \end{vmatrix} + z^3 \begin{vmatrix} K_x^* \\ K_y^* \\ K_z^* \\ K_x y^* \end{vmatrix} = zK + z^3 K^* \tag{3.29}$$

$$\varepsilon_s^k = \begin{vmatrix} \gamma_{yz} \\ \gamma_{xz} \end{vmatrix} = z \begin{vmatrix} \phi_y \\ \phi_x \end{vmatrix} + z^2 \begin{vmatrix} \phi_y^* \\ \phi_x^* \end{vmatrix} = \phi + z^2 \phi^* \tag{3.30}$$

The above Equation 3.29 and 3.30 are the expressions for the flexure and transverse shear strains respectively, at any point in the k^{th} layer of the laminate located at a distance z from the mid-plane. It should be noted that owing to the nature of Equation 3.30, the transverse shear strains vary parabolically through the plate thickness. For an orthotropic lamina in a 3-D state, the strain-stress relationship at a point in each of the three orthogonal planes is given by,

$$\begin{vmatrix} \varepsilon_1 \\ \varepsilon_2 \\ \varepsilon_3 \\ \gamma_{12} \\ \gamma_{23} \\ \gamma_{13} \end{vmatrix} = \begin{vmatrix} \frac{1}{E_1} & \frac{-\nu_{21}}{E_2} & \frac{-\nu_{31}}{E_3} & 0 & 0 & 0 \\ \frac{-\nu_{12}}{E_1} & \frac{1}{E_2} & \frac{-\nu_{32}}{E_3} & 0 & 0 & 0 \\ \frac{-\nu_{13}}{E_3} & \frac{-\nu_{23}}{E_2} & \frac{1}{E_3} & 0 & 0 & 0 \\ 0 & 0 & 0 & \frac{1}{G_{12}} & 0 & 0 \\ 0 & 0 & 0 & 0 & \frac{1}{G_{23}} & 0 \\ 0 & 0 & 0 & 0 & 0 & \frac{1}{G_{13}} \end{vmatrix} \begin{vmatrix} \sigma_1 \\ \sigma_2 \\ \sigma_3 \\ \tau_{12} \\ \tau_{23} \\ \tau_{13} \end{vmatrix} \tag{3.31}$$

Or

$$\varepsilon = [s]\sigma \tag{3.32}$$

The stress-strain constitutive relations can be obtained by inversion of strain-stress relations given by Equation 3.32 and are written in following matrix form.

$$\sigma = [C]\varepsilon \tag{3.33}$$

where,

$$\sigma = \begin{vmatrix} \sigma_1 \\ \sigma_2 \\ \sigma_3 \\ \tau_{12} \\ \tau_{23} \\ \tau_{13} \end{vmatrix} \tag{3.34}$$

$$[C] = \frac{1}{\Delta} \begin{vmatrix} E_1(1-\nu_{23}\nu 32) & E_1(\nu_{21}+\nu_{31}\nu 23) & E_1(\nu_{31}+\nu_{21}\nu 32) & 0 & 0 & 0 \\ E_2(\nu_{12}+\nu_{13}\nu 32) & E_2(1-\nu_{13}\nu 31) & E_2(\nu_{32}+\nu_{12}\nu 31) & 0 & 0 & 0 \\ E_3(\nu_{13}+\nu_{12}\nu 23) & E_3(\nu_{23}+\nu_{21}\nu 13) & E_3(1-\nu_{12}\nu 21) & 0 & 0 & 0 \\ 0 & 0 & 0 & \Delta G_1 2 & 0 & 0 \\ 0 & 0 & 0 & 0 & \Delta G_2 3 & 0 \\ 0 & 0 & 0 & 0 & 0 & \Delta G_1 3 \end{vmatrix} \tag{3.35}$$

$$\varepsilon = \begin{vmatrix} \varepsilon_1 \\ \varepsilon_2 \\ \varepsilon_3 \\ \gamma_{12} \\ \gamma_{23} \\ \gamma_{13} \end{vmatrix} \tag{3.36}$$

In which,

Δ = (1 - $\nu_{12}\nu_{21}$ - $\nu_{23}\nu_{32}$ - $\nu_{31}\nu_{13}$ - $2\nu_{12}\nu_{23}\nu_{31}$)

In the stress-strain relation Equation 3.29 and 3.30, the subscript k is introduced to designate k_{th} layer of the laminate. The relations given by Equation 3.33 are the stress-strain constitutive relations with reference to lamina axes for a homogeneous orthotropic layer in a general 3-D state of stress and these are adopted here to develop a theory based on the displacement model.

As noted earlier, the relation given by Equation 3.33 is the stress-strain constitutive relation for the orthotropic lamina referred to the laminas principal axes (1,2,3). The principal material axes of a lamina may not coincide with the reference axes for the laminated plate. It is therefore necessary to transform the constitutive relation given by Equation 3.33 from the lamina principal axes (1,2,3) to the reference axes of the laminate (x, y, z).

$$\sigma' = T\sigma \quad and \quad \varepsilon' = T\varepsilon \tag{3.37}$$

The transformation matrix T is given by,

$$T = \begin{vmatrix} c^2 & s^2 & 0 & 2cs & 0 & 0 \\ s^2 & c^2 & 0 & -2cs & 0 & 0 \\ 0 & 0 & 1 & 0 & 0 & 0 \\ -sc & sc & 0 & (c^2 - s^2) & 0 & 0 \\ 0 & 0 & 0 & 0 & c & -s \\ 0 & 0 & 0 & 0 & s & c \end{vmatrix} \tag{3.38}$$

Where, $c = \cos\alpha$ and $s = \sin\alpha$ with a as angle between reference axes and principal axes of laminate.

The relation between engineering and tensor strain vectors is given by,

$$\varepsilon = [R]\varepsilon_{ts} \quad which \;\; can \;\; be \;\; written \;\; as \quad \varepsilon_{ts} = [R]^{-1}\varepsilon \tag{3.39}$$

R matrix is defined as,

$$[R] = \begin{vmatrix} 1 & 0 & 0 & 0 & 0 & 0 \\ 0 & 1 & 0 & 0 & 0 & 0 \\ 0 & 0 & 1 & 0 & 0 & 0 \\ 0 & 0 & 0 & 2 & 0 & 0 \\ 0 & 0 & 0 & 0 & 2 & 0 \\ 0 & 0 & 0 & 0 & 0 & 2 \end{vmatrix} \tag{3.40}$$

The stress-strain constitutive relations with reference to laminate axes are obtained in the following form by making use of relations from Equations 3.33, 3.35 and 3.38.

$$\sigma = [T]^{-1} CRTR^{-1} \varepsilon \tag{3.41}$$

It can easily be proved that,

$$RTR^{-1} = [T]^{-1t} \tag{3.42}$$

Thus, the relation 3.39 can be rewritten as,

$$\sigma = Q\varepsilon \tag{3.43}$$

Where,

$$Q = [T]^{-1} C [T]^{-1t} \tag{3.44}$$

In matrix form,

$$\begin{vmatrix} \sigma_x \\ \sigma_y \\ \sigma_z \\ \tau_{xy} \\ \tau_{yz} \\ \tau_{xz} \end{vmatrix} = \begin{vmatrix} Q_{11} & Q_{12} & Q_{13} & Q_{14} & 0 & 0 \\ Q_{21} & Q_{22} & Q_{23} & Q_{24} & 0 & 0 \\ Q_{31} & Q_{32} & Q_{33} & Q_{34} & 0 & 0 \\ Q_{41} & Q_{42} & Q_{43} & Q_{44} & 0 & 0 \\ 0 & 0 & 0 & 0 & Q_{55} & Q_{56} \\ 0 & 0 & 0 & 0 & Q_{65} & Q_{66} \end{vmatrix} \begin{vmatrix} \varepsilon_x \\ \varepsilon_y \\ \varepsilon_z \\ \gamma_{xy} \\ \gamma_{yz} \\ \gamma_{xz} \end{vmatrix} \tag{3.45}$$

The matrix coefficients Q are defined as,

$$
\begin{aligned}
Q_{11} &= C_{11}c^4 + (2C_{12} + 4C_{44})\ s^2c^2 + C_{22}s^4 \\
Q_{12} &= (s^4 + c^4)\ C_{12} + (C_{11} + C_{22} - 4C_{44})\ s^2c^2 \\
Q_{13} &= c^2C_{13} + s^2C_{23} \\
Q_{14} &= (C_{11} - C_{12} - 2C_{44})\ c^3s + (C_{12} - C_{22} + 2C_{44})s^3c \\
Q_{22} &= C_{11}s^4 + C_{22}c^4 + (2C_{12} + 4C_{44})s^2c^2 \\
Q_{23} &= c^2C_{23} + s^2C_{13} \\
Q_{24} &= (C_{11} - C_{12} - 2C_{44})\ s^3c + (C_{12} - C_{22} + 2C_{44})c^3s \\
Q_{33} &= C_{33} \\
Q_{34} &= (C_{13} - C_{23})\mathrm{sc} \\
Q_{44} &= (C_{11} + C_{22} - 2C_{12} - 2C_{44})s^2c^2 + (c^4 + s^4)C_{44} \\
Q_{55} &= c^2C_{55} + s^2C_{66} \\
Q_{56} &= (C_{66} - C_{55})\mathrm{sc} \\
Q_{66} &= s^2C_{55} + c^2C_{66}
\end{aligned}
$$

And the coefficients of C matrix are defined by Equation 3.33.

Stress-Resultant and Mid-Plane Strains Relationships

Laminate constitutive relations

The laminate constitutive relations with the assumed displacement model can be derived as follows: In this case, from stress-strain relationship equations corresponding to displacement model are substituted in the energy expression. By principle of virtual work,

$$\delta U = \delta W \tag{3.46}$$

$$\int_v (\delta\varepsilon^t\sigma)dV = \int_A \delta^t F dA \tag{3.47}$$

Where δU is the strain energy of the plate, δW represents the work done by externally applied forces and F is the vector of force intensities corresponding to the generalized displacement vector q defined at mid-plane.

The mid-surface displacement vector q, strain vector $\overline{\varepsilon}$ and the stress-resultant vector $\overline{\sigma}$ are defined as,

q $= (w_0,\, \theta_x,\, \theta_y,\, w_0^*,\, \theta_x^*,\, \theta_y^*)$

$\overline{\varepsilon} = (K_x, K_y, K_{xy}, K_x^*, K_y^*, K_{xy}^*, K_z, \phi_x, \phi_y, \phi_x^*, \phi_y^*)$

$\overline{\sigma} = (M_x, M_y, M_{xy}, M_x^*, M_y^*, M_{xy}^*, M_z, Q_x, Q_y, Q_x^*, Q_y^*)$

The component of stress resultant vector $\overline{\sigma}$ are defined as,

$$(M_x, M_y, M_z, M_{xy}) = \sum_{k=1}^{NL} \int_{h_k=1}^{h_k} (\sigma_x, \sigma_y, \sigma_z, \tau_{xy})^k z dz \tag{3.48}$$

$$(M_x^*, M_y^*, M_{xy}^*) = \sum_{k=1}^{NL} \int_{h_k=1}^{h_k} (\sigma_x, \sigma_y, \tau_{xy})^k z^3 dz \tag{3.49}$$

$$(Q_x, Q_y) = \sum_{k=1}^{NL} \int_{h_k=1}^{h_k} (\tau_{xz}, \tau_{yz})^k dz \tag{3.50}$$

$$(Q_x^*, Q_y^*) = \sum_{k=1}^{NL} \int_{h_k=1}^{h_k} (\tau_{xz}, \tau_{yz})^k z^2 dz \tag{3.51}$$

The expressions for the stresses in the k^{th} layer can be rewritten by substitution of strain expressions Equations 3.29 and 3.30 in the lamina constitutive relations Equations 3.43 as follows,

$$\begin{vmatrix} \sigma_x \\ \sigma_y \\ \sigma_z \\ \tau_{xy} \end{vmatrix} = \begin{vmatrix} Q_{11} & Q_{12} & Q_{13} & Q_{14} \\ Q_{21} & Q_{22} & Q_{23} & Q_{24} \\ Q_{31} & Q_{32} & Q_{33} & Q_{34} \\ Q_{41} & Q_{42} & Q_{43} & Q_{44} \end{vmatrix}^k z \begin{vmatrix} K_x \\ K_y \\ K_z \\ K_{xy} \end{vmatrix} + \begin{vmatrix} Q_{11} & Q_{12} & Q_{13} & Q_{14} \\ Q_{21} & Q_{22} & Q_{23} & Q_{24} \\ Q_{31} & Q_{32} & Q_{33} & Q_{34} \\ Q_{41} & Q_{42} & Q_{43} & Q_{44} \end{vmatrix}^k z^3 \begin{vmatrix} K_x^* \\ K_y^* \\ 0 \\ K_{xy}^* \end{vmatrix} \tag{3.52}$$

$$\begin{vmatrix} \tau_{yz} \\ \tau_{xz} \end{vmatrix} = \begin{vmatrix} Q_{55} & Q_{56} \\ Q_{65} & Q_{66} \end{vmatrix}^k \begin{vmatrix} \phi_y \\ \phi_x \end{vmatrix} + \begin{vmatrix} Q_{55} & Q_{56} \\ Q_{65} & Q_{66} \end{vmatrix}^k z^2 \begin{vmatrix} \phi_y^* \\ \phi_x^* \end{vmatrix} \tag{3.53}$$

The substitution of expressions (3.50, 3.51) in Equations (3.46, 3.47, 3.48, 3.49) and the integration through each lamina thickness, results in the following laminate constitutive relations.

$$\begin{vmatrix} M_x \\ M_y \\ M_{xy} \\ M_x^* \\ M_y^* \\ M_{xy}^* \\ M_z \end{vmatrix} = \sum_{k=1}^{NL} \begin{vmatrix} Q_{11}H_3 & Q_{12}H_3 & Q_{14}H_3 & Q_{11}H_5 & Q_{12}H_5 & Q_{14}H_5 & Q_{13}H_3 \\ Q_{12}H_3 & Q_{22}H_3 & Q_{24}H_3 & Q_{12}H_5 & Q_{22}H_5 & Q_{24}H_5 & Q_{23}H_3 \\ Q_{14}H_3 & Q_{24}H_3 & Q_{44}H_3 & Q_{14}H_5 & Q_{24}H_5 & Q_{44}H_5 & Q_{34}H_3 \\ Q_{11}H_5 & Q_{12}H_5 & Q_{14}H_5 & Q_{11}H_7 & Q_{12}H_7 & Q_{14}H_7 & Q_{13}H_5 \\ Q_{12}H_5 & Q_{22}H_5 & Q_{24}H_5 & Q_{12}H_7 & Q_{22}H_7 & Q_{24}H_7 & Q_{23}H_5 \\ Q_{14}H_5 & Q_{24}H_5 & Q_{44}H_5 & Q_{14}H_7 & Q_{24}H_7 & Q_{44}H_7 & Q_{34}H_5 \\ Q_{13}H_3 & Q_{23}H_3 & Q_{34}H_3 & Q_{13}H_5 & Q_{23}H_5 & Q_{34}H_5 & Q_{33}H_3 \end{vmatrix}^k \begin{vmatrix} K_x \\ K_y \\ K_{xy} \\ K_x^* \\ K_y^* \\ K_{xy}^* \\ K_z \end{vmatrix} \tag{3.54}$$

$$\begin{vmatrix} Q_x \\ Q_y \\ Q_x^* \\ Q_y^* \end{vmatrix} = \sum_{k=1}^{NL} \begin{vmatrix} Q_{55}H_1 & Q_{56}H_1 & Q_{55}H_3 & Q_{56}H_3 \\ Q_{56}H_1 & Q_{66}H_1 & Q_{56}H_3 & Q_{66}H_3 \\ Q_{55}H_3 & Q_{56}H_3 & Q_{55}H_5 & Q_{56}H_3 \\ Q_{56}H_3 & Q_{66}H_3 & Q_{56}H_5 & Q_{66}H_3 \end{vmatrix}^k \begin{vmatrix} \phi_x \\ \phi_y \\ \phi_x^* \\ \phi_y^* \end{vmatrix} \tag{3.55}$$

Where, $H_i = \frac{(h_k^i - h_{k-1}^i)}{i}$ i=1,3,5,7

Equation matrix is for flexure rigidity and Equation matrix is foe shear rigidity.

3.3.2 Definition of Displacement Field Model-2

$$u(x,y,z) = u_0(x,y,0) + z\theta_x(x,y,0) + z^2u_0^*(x,y,0) + z^3\theta_x^*(x,y,0) = u_0 + z\theta_x + z^2u_0^* + z^3\theta_x^*$$
$$v(x,y,z) = v_0(x,y,0) + z\theta_y(x,y,0) + z^2v_0^*(x,y,0) + z^3\theta_y^*(x,y,0) = v_0 + z\theta_y + z^2v_0^* + z^3\theta_y^*$$
$$w(x,y,z) = w_0(x,y,0) + z\theta_z(x,y,0) + z^2w_0^*(x,y,0) = w_0 + z\theta_z + z^2w_0^*$$

where u, v, and w define the displacements of a generic point in x, y and z directions respectively, u_0, v_0, w_0 are the associated mid-plane displacements, θ_x and θ_y are the rotations of the transverse normal in the x-z and y-z planes, u_0^*, v_0^*, w_0^*, θ_x^*, θ_y^* and θ_z are the corresponding higher order terms.

Strain Displacement Relationship Corresponding to Model

$\varepsilon_x = \frac{\partial u}{\partial x} = \frac{\partial u_0}{\partial x} + z\frac{\partial \theta_x}{\partial x} + z^2\frac{\partial u_0^*}{\partial x} + z^3\frac{\partial \theta_x^*}{\partial x} = \varepsilon_{0x} + zK_x + z^2\varepsilon_{0x}^* + z^3K_x^*$

$\varepsilon_y = \frac{\partial v}{\partial y} = \frac{\partial v_0}{\partial y} + z\frac{\partial \theta_y}{\partial y} + z^2\frac{\partial v_0^*}{\partial y} + z^3\frac{\partial \theta_y^*}{\partial y} = \varepsilon_{0y} + zK_y + z^2\varepsilon_{0y}^* + z^3K_y^*$

$\varepsilon_z = \frac{\partial w}{\partial z} = \theta_z + 2zw_0^* = \varepsilon_{0z} + zK_z^*$

$\gamma_{xy} = \frac{\partial u}{\partial y} + \frac{\partial v}{\partial x} = \frac{\partial u_0}{\partial y} + z\frac{\partial \theta_x}{\partial y} + z^2\frac{\partial u_0^*}{\partial y} + z^3\frac{\partial \theta_x^*}{\partial y} + \frac{\partial v_0}{\partial x} + z\frac{\partial \theta_y}{\partial x} + z^2\frac{\partial v_0^*}{\partial x} + z^3\frac{\partial \theta_y^*}{\partial x} = \varepsilon_{0xy} + zK_{xy} + z^2\varepsilon_{0xy}^* + z^3K_{xy}^*$

$\gamma_{yz} = \frac{\partial v}{\partial z} + \frac{\partial w}{\partial y} = \theta_y + 2zv_0^* + 3z^2\theta_y^* + \frac{\partial w_0}{\partial y} + z\frac{\partial \theta_z}{\partial y} + z^2\frac{\partial w_0^*}{\partial y} = \phi_y + z\psi_y + z^2\phi_y^*$

$\gamma_{xz} = \frac{\partial u}{\partial z} + \frac{\partial w}{\partial x} = \theta_x + 2zu_0^* + 3z^2\theta_x^* + \frac{\partial w_0}{\partial x} + z\frac{\partial \theta_z}{\partial x} + z^2\frac{\partial w_0^*}{\partial x} = \phi_x + z\psi_x + z^2\phi_x^*$

Where the definitions of the various terms are as follows:

$\varepsilon_{0x} = \frac{\partial u_0}{\partial x}$
$\varepsilon_{0y} = \frac{\partial v_0}{\partial y}$
$\varepsilon_{0xy} = \frac{\partial u_0}{\partial y} + \frac{\partial v_0}{\partial x}$
$\varepsilon_{0x}^* = \frac{\partial u_0^*}{\partial x}$
$\varepsilon_{0y}^* = \frac{\partial v_0^*}{\partial y}$
$\varepsilon_{0xy}^* = \frac{\partial u_0^*}{\partial y} + \frac{\partial v_0^*}{\partial x}$
$\varepsilon_{0z} = \theta_z$
$K_x = \frac{\partial \theta_x}{\partial x}$
$K_y = \frac{\partial \theta_y}{\partial y}$
$K_{xy} = \frac{\partial \theta_x}{\partial y} + \frac{\partial \theta_y}{\partial x}$
$K_x^* = \frac{\partial \theta_x^*}{\partial x}$
$K_y^* = \frac{\partial \theta_y^*}{\partial y}$
$K_{xy}^* = \frac{\partial \theta_x^*}{\partial y} + \frac{\partial {\theta_y}^*}{\partial x}$
$K_z^* = 2w_0^*$

$\phi_x = \theta_x + \frac{\partial w_0}{\partial x}$

$\phi_y = \theta_y + \frac{\partial w_0}{\partial y}$

$\psi_x = 2u_0^* + \frac{\partial \theta_z}{\partial x}$

$\psi_y = 2v_0^* + \frac{\partial \theta_z}{\partial y}$

$\phi_x^* = 3\theta_x^* + \frac{\partial w_0^*}{\partial x}$

$\phi_y^* = 3\theta_y^* + \frac{\partial w_0^*}{\partial y}$

The concise matrix form above equations,

$$\varepsilon_b^k = \begin{vmatrix} \varepsilon_x \\ \varepsilon_y \\ \varepsilon_z \\ \gamma_{xy} \end{vmatrix} = \begin{vmatrix} \varepsilon_{0x} \\ \varepsilon_{0y} \\ \varepsilon_{0z} \\ \varepsilon_{0xy} \end{vmatrix} + z^2 \begin{vmatrix} \varepsilon_{0x}^* \\ \varepsilon_{0y}^* \\ 0 \\ \varepsilon_{0xy}^* \end{vmatrix} + z \begin{vmatrix} K_x \\ K_y \\ 0 \\ K_x y \end{vmatrix} + \begin{vmatrix} z^3 K_x^* \\ z^3 K_y^* \\ z K_z^* \\ z^3 K_{xy}^* \end{vmatrix} \tag{3.56}$$

$$\varepsilon_s^k = \begin{vmatrix} \gamma_{yz} \\ \gamma_{xz} \end{vmatrix} = z \begin{vmatrix} \phi_y \\ \phi_x \end{vmatrix} + z \begin{vmatrix} \psi_y \\ \psi_x \end{vmatrix} + z^2 \begin{vmatrix} \phi_y^* \\ \phi_x^* \end{vmatrix} \tag{3.57}$$

The above Equation 3.54 and 3.55 are the expressions for the flexure and transverse shear strains respectively, at any point in the k^{th} layer of the laminate located at a distance z from the mid-plane. It should be noted that owing to the nature of Equation 3.55, the transverse shear strains vary parabolically through the plate thickness. For an orthotropic lamina in a 3-D state, the strain-stress relationship at a point in each of the three orthogonal planes is given by,

$$\begin{vmatrix} \varepsilon_1 \\ \varepsilon_2 \\ \varepsilon_3 \\ \gamma_{12} \\ \gamma_{23} \\ \gamma_{13} \end{vmatrix} = \begin{vmatrix} \frac{1}{E_1} & \frac{-\nu_{21}}{E_2} & \frac{-\nu_{31}}{E_3} & 0 & 0 & 0 \\ \frac{-\nu_{12}}{E_1} & \frac{1}{E_2} & \frac{-\nu_{32}}{E_3} & 0 & 0 & 0 \\ \frac{-\nu_{13}}{E_3} & \frac{-\nu_{23}}{E_2} & \frac{1}{E_3} & 0 & 0 & 0 \\ 0 & 0 & 0 & \frac{1}{G_{12}} & 0 & 0 \\ 0 & 0 & 0 & 0 & \frac{1}{G_{23}} & 0 \\ 0 & 0 & 0 & 0 & 0 & \frac{1}{G_{13}} \end{vmatrix} \begin{vmatrix} \sigma_1 \\ \sigma_2 \\ \sigma_3 \\ \tau_{12} \\ \tau_{23} \\ \tau_{13} \end{vmatrix} \tag{3.58}$$

Or

$$\varepsilon = [s]\sigma \tag{3.59}$$

The stress-strain constitutive relations can be obtained by inversion of strain-stress relations given by Equation 3.57 and are written in following matrix form.

$$\sigma = [C]\varepsilon \tag{3.60}$$

where,

$$\sigma = \begin{vmatrix} \sigma_1 \\ \sigma_2 \\ \sigma_3 \\ \tau_{12} \\ \tau_{23} \\ \tau_{13} \end{vmatrix} \tag{3.61}$$

$$[C] = \frac{1}{\Delta}\begin{vmatrix} E_1(1-\nu_{23}\nu 32) & E_1(\nu_{21}+\nu_{31}\nu 23) & E_1(\nu_{31}+\nu_{21}\nu 32) & 0 & 0 & 0 \\ E_2(\nu_{12}+\nu_{13}\nu 32) & E_2(1-\nu_{13}\nu 31) & E_2(\nu_{32}+\nu_{12}\nu 31) & 0 & 0 & 0 \\ E_3(\nu_{13}+\nu_{12}\nu 23) & E_3(\nu_{23}+\nu_{21}\nu 13) & E_3(1-\nu_{12}\nu 21) & 0 & 0 & 0 \\ 0 & 0 & 0 & \Delta G_1 2 & 0 & 0 \\ 0 & 0 & 0 & 0 & \Delta G_2 3 & 0 \\ 0 & 0 & 0 & 0 & 0 & \Delta G_1 3 \end{vmatrix} \tag{3.62}$$

$$\varepsilon = \begin{vmatrix} \varepsilon_1 \\ \varepsilon_2 \\ \varepsilon_3 \\ \gamma_{12} \\ \gamma_{23} \\ \gamma_{13} \end{vmatrix} \tag{3.63}$$

In which,

Δ = (1 - $\nu_{12}\nu_{21}$ - $\nu_{23}\nu_{32}$ - $\nu_{31}\nu_{13}$ - $2\nu_{12}\nu_{23}\nu_{31}$)

In the stress-strain relation Equation 3.54 and 3.55, the subscript k is introduced to designate k_{th} layer of the laminate. The relations given by Equation 3.58 are the stress-strain constitutive relations with reference to lamina axes for a homogeneous orthotropic layer in a general 3-D state of stress and these are adopted here to develop a theory based on the displacement model.

As noted earlier, the relation given by Equation 3.58 is the stress-strain constitutive relation for the orthotropic lamina referred to the laminas principal axes (1,2,3). The principal material axes of a lamina may not coincide with the reference axes for the laminated plate. It is therefore necessary to transform the constitutive relation given by Equation 3.58 from the lamina principal axes (1,2,3) to the reference axes of the laminate (x, y, z).

$$\sigma' = T\sigma \quad and \quad \varepsilon' = T\varepsilon \tag{3.64}$$

The transformation matrix T is given by,

$$T = \begin{vmatrix} c^2 & s^2 & 0 & 2cs & 0 & 0 \\ s^2 & c^2 & 0 & -2cs & 0 & 0 \\ 0 & 0 & 1 & 0 & 0 & 0 \\ -sc & sc & 0 & (c^2 - s^2) & 0 & 0 \\ 0 & 0 & 0 & 0 & c & -s \\ 0 & 0 & 0 & 0 & s & c \end{vmatrix} \tag{3.65}$$

Where, $c = \cos\alpha$ and $s = \sin\alpha$ with a as angle between reference axes and principal axes of laminate.

The relation between engineering and tensor strain vectors is given by,

$$\varepsilon = [R]\varepsilon_{ts} \quad \varepsilon_{ts} = [R]^{-1}\varepsilon \tag{3.66}$$

R matrix is defined as,

$$[R] = \begin{vmatrix} 1 & 0 & 0 & 0 & 0 & 0 \\ 0 & 1 & 0 & 0 & 0 & 0 \\ 0 & 0 & 1 & 0 & 0 & 0 \\ 0 & 0 & 0 & 2 & 0 & 0 \\ 0 & 0 & 0 & 0 & 2 & 0 \\ 0 & 0 & 0 & 0 & 0 & 2 \end{vmatrix} \tag{3.67}$$

The stress-strain constitutive relations with reference to laminate axes are obtained in the following form by making use of relations from Equations 3.58, 3.60 and 3.63.

$$\sigma = [T]^{-1}CRTR^{-1}\varepsilon \tag{3.68}$$

It can easily be proved that,

$$RTR^{-1} = [T]^{-1t} \tag{3.69}$$

Thus, the relation 3.64 can be rewritten as,

$$\sigma = Q\varepsilon \tag{3.70}$$

Where,

$$Q = [T]^{-1}C[T]^{-1t} \tag{3.71}$$

In matrix form,

$$\begin{vmatrix} \sigma_x \\ \sigma_y \\ \sigma_z \\ \tau_{xy} \\ \tau_{yz} \\ \tau_{xz} \end{vmatrix} = \begin{vmatrix} Q_{11} & Q_{12} & Q_{13} & Q_{14} & 0 & 0 \\ Q_{21} & Q_{22} & Q_{23} & Q_{24} & 0 & 0 \\ Q_{31} & Q_{32} & Q_{33} & Q_{34} & 0 & 0 \\ Q_{41} & Q_{42} & Q_{43} & Q_{44} & 0 & 0 \\ 0 & 0 & 0 & 0 & Q_{55} & Q_{56} \\ 0 & 0 & 0 & 0 & Q_{65} & Q_{66} \end{vmatrix} \begin{vmatrix} \varepsilon_x \\ \varepsilon_y \\ \varepsilon_z \\ \gamma_{xy} \\ \gamma_{yz} \\ \gamma_{xz} \end{vmatrix} \tag{3.72}$$

The matrix coefficients Q are defined as,

$Q_{11} = C_{11}c^4 + (2C_{12} + 4C_{44})\ s^2c^2 + C_{22}s^4$

$Q_{12} = (s^4 + c^4)\ C_{12} + (C_{11} + C_{22}$ - $4C_{44})\ s^2c^2$

$Q_{13} = c^2C_{13} + s^2C_{23}$

$Q_{14} = (C_{11}$ - C_{12} - $2C_{44})\ c^3s + (C_{12}$ - $C_{22} + 2C_{44})s^3c$

$Q_{22} = C_{11}s^4 + C_{22}c^4 + (2C_{12} + 4C_{44})s^2c^2$

$Q_{23} = c^2C_{23} + s^2C_{13}$

$Q_{24} = (C_{11}$ - C_{12} - $2C_{44})\ s^3c + (C_{12}$ - $C_{22} + 2C_{44})c^3s$

$Q_{33} = C_{33}$

$Q_{34} = (C_{13}$ - $C_{23})$sc

$Q_{44} = (C_{11} + C_{22}$ - $2C_{12}$ - $2C_{44})s^2c^2 + (c^4 + s^4)C_{44}$

$Q_{55} = c^2C_{55} + s^2C_{66}$

$Q_{56} = (C_{66}$ - $C_{55})$sc

$Q_{66} = s^2C_{55} + c^2C_{66}$

And the coefficients of C matrix are defined by Equation 3.60.

Stress-Resultant and Mid-Plane Strains Relationships

Laminate constitutive relations

The laminate constitutive relations with the assumed displacement model can be derived as follows: In this case, from stress-strain relationship equations corresponding to displacement model are substituted in the energy expression. By principle of virtual work,

$$\delta U = \delta W \tag{3.73}$$

$$\int_v (\delta\varepsilon^t \sigma) dV = \int_A \delta^t F dA \tag{3.74}$$

Where δU is the strain energy of the plate, δW represents the work done by externally applied forces and F is the vector of force intensities corresponding to the generalized displacement vector q defined at mid-plane.

The mid-surface displacement vector q, strain vector $\overline{\varepsilon}$ and the stress-resultant vector $\overline{\sigma}$ are defined as,

q $= (u_0,v_0,w_0,\ \theta_x,\ \theta_y,\ \theta_z,\ u_0^*,v_0^*,\ w_0^*,\ \theta_x^*,\ \theta_y^*)$

$\overline{\varepsilon} = (\varepsilon_{0x},\ \varepsilon_{0y},\ \varepsilon_{0xy},\ \varepsilon_{0x}^*,\ \varepsilon_{0y}^*,\ \varepsilon_{0xy}^*,\ \varepsilon_{0z},\ K_x,\ K_y,\ K_{xy},\ K_x^*,\ K_y^*,\ K_{xy}^*,\ K_z^*,\ \phi_x,\ \phi_y,\ \psi_x,\ \psi_y,\ \phi_x^*,\ \phi_x^*)$

$\overline{\sigma} = (N_x,\ N_y,\ N_{xy},\ N_x^*,\ N_y^*,\ N_{xy}^*,\ N_Z,\ M_x,\ M_y,\ M_{xy},\ M_x^*,\ M_y^*,\ M_{xy}^*,\ M_z,\ Q_x,\ Q_y,\ S_x,\ S_y,\ Q_x^*,\ Q_y^*)$

The component of stress resultant vector $\overline{\sigma}$ are defined as,

$$(N_x, N_y, N_{xy}, N_z) = \sum_{k=1}^{NL} \int_{h_k=1}^{h_{k+1}} (\sigma_x, \sigma_y, \tau_{xy}, \sigma_z)^k dz \tag{3.75}$$

$$(N_x^*, N_y^*, N_{xy}^*) = \sum_{k=1}^{NL} \int_{h_k=1}^{h_{k+1}} z^2(\sigma_x, \sigma_y, \tau_{xy})^k dz \tag{3.76}$$

$$(M_x, M_y, M_{xy}, M_z) = \sum_{k=1}^{NL} \int_{h_k=1}^{h_{k+1}} z(\sigma_x, \sigma_y, \tau_{xy}, \sigma_z)^k dz \tag{3.77}$$

$$(M_x^*, M_y^*, M_{xy}^*) = \sum_{k=1}^{NL} \int_{h_k=1}^{h_{k+1}} z^3(\sigma_x, \sigma_y, \tau_{xy})^k dz \tag{3.78}$$

$$(Q_x, Q_y) = \sum_{k=1}^{NL} \int_{h_k=1}^{h_{k+1}} (\tau_{xz}, \tau_{yz})^k dz \tag{3.79}$$

$$(S_x, S_y) = \sum_{k=1}^{NL} \int_{h_k=1}^{h_{k+1}} z(\tau_{xz}, \tau_{yz})^k dz \tag{3.80}$$

$$(Q_x^*, Q_y^*) = \sum_{k=1}^{NL} \int_{h_k=1}^{h_{k+1}} z^2(\tau_{xz}, \tau_{yz})^k dz \tag{3.81}$$

The expressions for the stresses in the k^{th} layer can be rewritten by substitution of strain expressions Equations 3.54 and 3.55 in the lamina constitutive relations Equations 3.68 as follows,

$$\begin{vmatrix} \sigma_x \\ \sigma_y \\ \sigma_z \\ \tau_{xy} \end{vmatrix} = \begin{vmatrix} Q_{11} & Q_{12} & Q_{13} & Q_{14} & Q_{11} & Q_{12} & Q_{13} & Q_{14} \\ Q_{21} & Q_{22} & Q_{23} & Q_{24} & Q_{21} & Q_{22} & Q_{23} & Q_{24} \\ Q_{31} & Q_{32} & Q_{33} & Q_{34} & Q_{31} & Q_{32} & Q_{33} & Q_{34} \\ Q_{41} & Q_{42} & Q_{43} & Q_{44} & Q_{41} & Q_{42} & Q_{43} & Q_{44} \end{vmatrix}^k \begin{vmatrix} \varepsilon_{0x} \\ \varepsilon_{0y} \\ 0 \\ \varepsilon_{0xy} \\ zK_x \\ zK_y \\ 0 \\ zK_{xy} \end{vmatrix} \tag{3.82}$$

$$+\begin{vmatrix} Q_{11} & Q_{12} & Q_{13} & Q_{14} & Q_{11} & Q_{12} & Q_{13} & Q_{14} \\ Q_{21} & Q_{22} & Q_{23} & Q_{24} & Q_{21} & Q_{22} & Q_{23} & Q_{24} \\ Q_{31} & Q_{32} & Q_{33} & Q_{34} & Q_{31} & Q_{32} & Q_{33} & Q_{34} \\ Q_{41} & Q_{42} & Q_{43} & Q_{44} & Q_{41} & Q_{42} & Q_{43} & Q_{44} \end{vmatrix}^k \begin{vmatrix} z^2\varepsilon^*_{0x} \\ z^2\varepsilon^*_{0y} \\ 0 \\ z^2\varepsilon^*_{0xy} \\ z^3K^*_x \\ z^3K^*_y \\ 0 \\ z^3K^*_{xy} \end{vmatrix} \tag{3.83}$$

$$\begin{vmatrix} \tau_{xz} \\ \tau_{yz} \end{vmatrix} = \begin{vmatrix} Q_{66} & Q_{65} & Q_{66} & Q_{65} \\ Q_{56} & Q_{55} & Q_{56} & Q_{55} \end{vmatrix}^k \begin{vmatrix} \phi_x \\ \phi_y \\ z\psi_x \\ z\psi_y \end{vmatrix} + \begin{vmatrix} Q_{66} & Q_{65} \\ Q_{56} & Q_{55} \end{vmatrix}^k z^2 \begin{vmatrix} \phi^*_x \\ \phi^*_y \end{vmatrix} \tag{3.84}$$

The substitution of expressions (3.79, 3.80) in Equations (3.71, 3.72, 3.73, 3.74, 3.75, 3.76, 3.77) and the integration through each lamina thickness, results in the following laminate constitutive relations.

$$\begin{vmatrix} N \\ N^* \\ M \\ M^* \\ Q \\ Q^* \end{vmatrix} = \begin{vmatrix} D_m & D_c & 0 \\ D_c & D_b & 0 \\ 0 & 0 & D_s \end{vmatrix} \begin{vmatrix} \varepsilon_0 \\ \varepsilon^*_0 \\ K \\ K^* \\ \phi \\ \phi^* \end{vmatrix} \tag{3.85}$$

where, $N = [N_x, N_y, N_{xy}]^T$, $N^* = [N^*_x, N^*_y, N^*_{xy}, N_z]^T$,
$M = [M_x, M_y, M_{xy}]^T$, $M^* = [M^*_x, M^*_y, M^*_{xy}, M_z]^T$, $Q = [Q_x, Q_y]^T$, $Q^* = [S_x, S_y, Q^*_x, Q^*_y]$,

$\varepsilon_0 = [\frac{\partial u_0}{\partial x}, \frac{\partial v_0}{\partial y}, \frac{\partial u_0}{\partial y} + \frac{\partial v_0}{\partial x}]^T$, $\varepsilon^*_0 = [\frac{\partial u^*_0}{\partial x}, \frac{\partial v^*_0}{\partial y}, \frac{\partial u^*_0}{\partial y} + \frac{\partial v^*_0}{\partial x}, \theta_z]^T$,

$K = [\frac{\partial \theta_x}{\partial x}, \frac{\partial \theta_y}{\partial y}, \frac{\partial \theta_x}{\partial y} + \frac{\partial \theta_y}{\partial x}]^T$, $K^* = [\frac{\partial \theta^*_x}{\partial x}, \frac{\partial \theta^*_y}{\partial y}, \frac{\partial \theta^*_x}{\partial y} + \frac{\partial \theta^*_y}{\partial x}, 2w^*_0]^T$,

$\phi = [\theta_x + \frac{\partial w_0}{\partial x}, \theta_y + \frac{\partial w_0}{\partial y}]^T$, $\phi^* = [2u_0^* + \frac{\partial \theta_z}{\partial x}, 2v_0^* + \frac{\partial \theta_z}{\partial y}, 3\theta_x^* + \frac{\partial w_0^*}{\partial x}, 3\theta_y^* + \frac{\partial w_0^*}{\partial y}]^T$

The rigidity matrices are as follow:

$$D_m = \sum_{k=1}^{n} \begin{vmatrix} Q_{11}H_1 & Q_{12}H_1 & Q_{14}H_1 & Q_{11}H_3 & Q_{12}H_3 & Q_{14}H_3 & Q_{13}H_1 \\ Q_{12}H_1 & Q_{22}H_1 & Q_{24}H_1 & Q_{12}H_3 & Q_{22}H_3 & Q_{24}H_3 & Q_{23}H_1 \\ Q_{14}H_1 & Q_{24}H_1 & Q_{44}H_1 & Q_{14}H_3 & Q_{24}H_3 & Q_{44}H_3 & Q_{34}H_1 \\ Q_{11}H_3 & Q_{12}H_3 & Q_{14}H_3 & Q_{11}H_5 & Q_{12}H_5 & Q_{14}H_5 & Q_{13}H_3 \\ Q_{12}H_3 & Q_{22}H_3 & Q_{24}H_3 & Q_{12}H_5 & Q_{22}H_5 & Q_{24}H_5 & Q_{23}H_3 \\ Q_{14}H_3 & Q_{24}H_3 & Q_{44}H_3 & Q_{14}H_5 & Q_{24}H_5 & Q_{44}H_5 & Q_{34}H_3 \\ Q_{13}H_1 & Q_{23}H_1 & Q_{34}H_1 & Q_{13}H_3 & Q_{23}H_3 & Q_{34}H_3 & Q_{33}H_1 \end{vmatrix}^k \tag{3.86}$$

$$D_c = \sum_{k=1}^{n} \begin{vmatrix} Q_{11}H_2 & Q_{12}H_2 & Q_{14}H_2 & Q_{11}H_4 & Q_{12}H_4 & Q_{14}H_4 & Q_{13}H_2 \\ Q_{12}H_2 & Q_{22}H_2 & Q_{24}H_2 & Q_{12}H_4 & Q_{22}H_4 & Q_{24}H_4 & Q_{23}H_2 \\ Q_{14}H_2 & Q_{24}H_2 & Q_{44}H_2 & Q_{14}H_4 & Q_{24}H_4 & Q_{44}H_4 & Q_{34}H_2 \\ Q_{11}H_4 & Q_{12}H_4 & Q_{14}H_4 & Q_{11}H_6 & Q_{12}H_6 & Q_{14}H_6 & Q_{13}H_4 \\ Q_{12}H_4 & Q_{22}H_4 & Q_{24}H_4 & Q_{12}H_6 & Q_{22}H_6 & Q_{24}H_6 & Q_{23}H_4 \\ Q_{14}H_4 & Q_{24}H_4 & Q_{44}H_4 & Q_{14}H_6 & Q_{24}H_6 & Q_{44}H_6 & Q_{34}H_4 \\ Q_{13}H_2 & Q_{23}H_2 & Q_{34}H_2 & Q_{13}H_4 & Q_{23}H_4 & Q_{34}H_4 & Q_{33}H_2 \end{vmatrix}^k \tag{3.87}$$

$$D_b = \sum_{k=1}^{n} \begin{vmatrix} Q_{11}H_3 & Q_{12}H_3 & Q_{14}H_3 & Q_{11}H_5 & Q_{12}H_5 & Q_{14}H_5 & Q_{13}H_3 \\ Q_{12}H_3 & Q_{22}H_3 & Q_{24}H_3 & Q_{12}H_5 & Q_{22}H_5 & Q_{24}H_5 & Q_{23}H_3 \\ Q_{14}H_3 & Q_{24}H_3 & Q_{44}H_3 & Q_{14}H_5 & Q_{24}H_5 & Q_{44}H_5 & Q_{34}H_3 \\ Q_{11}H_5 & Q_{12}H_5 & Q_{14}H_5 & Q_{11}H_7 & Q_{12}H_7 & Q_{14}H_7 & Q_{13}H_5 \\ Q_{12}H_5 & Q_{22}H_5 & Q_{24}H_5 & Q_{12}H_7 & Q_{22}H_7 & Q_{24}H_7 & Q_{23}H_5 \\ Q_{14}H_5 & Q_{24}H_5 & Q_{44}H_5 & Q_{14}H_7 & Q_{24}H_7 & Q_{44}H_7 & Q_{34}H_5 \\ Q_{13}H_3 & Q_{23}H_3 & Q_{34}H_3 & Q_{13}H_5 & Q_{23}H_5 & Q_{34}H_5 & Q_{33}H_3 \end{vmatrix}^k \tag{3.88}$$

$$D_s = \sum_{k=1}^{n} \begin{vmatrix} Q_{66}H_1 & Q_{65}H_1 & Q_{66}H_2 & Q_{65}H_2 & Q_{66}H_3 & Q_{56}H_3 \\ Q_{65}H_1 & Q_{55}H_1 & Q_{56}H_3 & Q_{55}H_3 & Q_{56}H_3 & Q_{55}H_3 \\ Q_{66}H_3 & Q_{56}H_3 & Q_{66}H_5 & Q_{65}H_3 & Q_{66}H_3 & Q_{65}H_3 \\ Q_{65}H_3 & Q_{55}H_3 & Q_{65}H_5 & Q_{55}H_3 & Q_{56}H_3 & Q_{55}H_3 \\ Q_{66}H_3 & Q_{56}H_3 & Q_{66}H_5 & Q_{56}H_3 & Q_{66}H_3 & Q_{65}H_3 \\ Q_{56}H_3 & Q_{55}H_3 & Q_{65}H_5 & Q_{55}H_3 & Q_{65}H_3 & Q_{55}H_3 \end{vmatrix}^k \tag{3.89}$$

In all above relations, n is the number of layers and $H_i = \frac{(h_k^i - h_{k-1}^i)}{i}$ i=1,2....,7.

3.4 Finite Element Formulation

The solution of the fundamental equations of the displacement model based on higher order shear deformation theory for laminates anisotropic plates, can conveniently be obtained by using the finite element displacement formulation.Element properties are derived by assuming a displacement function, which ensures completeness within the element and compatibility across the element boundaries. The finite element theory is developed in this section for application to linear equilibrium problems of isotropic, orthotropic and multilayer anisotropic plates with various loading and boundary conditions. In present work, 8-node isoparametric quadrilateral element Fig.3.7 is used. The finite element formulation starts with writing the shape functions, followed by the derivation of the strain-displacement matrix [B], and calculation of element stiffness matrix. Here for both assumed displacement models the finite element formulation is formulated.

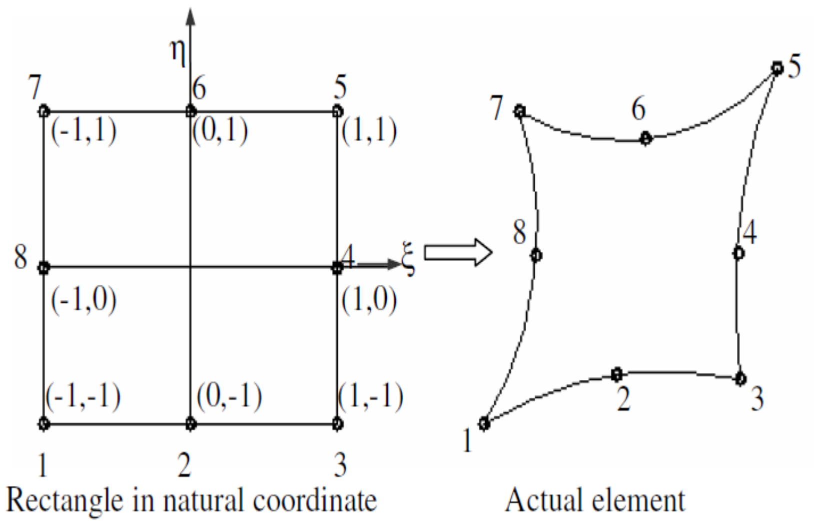

Figure 3.7: Eight Node Isoparametric Element

3.4.1 Displacement Model-1

$$u(x, y, z) = z\theta_x(x, y, 0) + z^3\theta_x^*(x, y, 0) = z\theta_x + z^3\theta_x^*$$
$$v(x, y, z) = z\theta_y(x, y, 0) + z^3\theta_y^*(x, y, 0) = z\theta_y + z^3\theta_y^*$$
$$w(x, y, z) = w_0(x, y, 0) + z^2w_0^*(x, y, 0) = w_0 + z^2w_0^*$$

The vector,

q = $[w_{01}, \theta_{x1}, \theta_{y1}, w^*_{01}, \theta^*_{x1}, \theta^*_{y1}, w_{02}, \theta_{x2}, \theta_{y2}, w^*_{02}, \theta^*_{x2}, \theta^*_{y2}, \ldots\ldots\ldots\ldots, \theta^*_{y8}]$ denotes the element displacement vector. Thus the degrees of freedom at each node are:

w_0 = Transverse displacement at the geometrical mid-plane.

θ_x, θ_y = Rotations of the normal to the geometrical mid-plane in x-z and y-z plane respectively.

w^*_0 = Higher order term of transverse displacement w_0 at the geometrical mid-plane.

θ^*_x, θ^*_y = Higher order terms of rotations of the normal to the geometrical mid-plane in x-z and y-z plane i.e. qx and qy respectively.

Therefore, Nodal degree of freedom for element : 6

Number of nodes in the element : 8

Total degree of freedom for the element : 6x8 = 48

Shape Functions

The shape functions for this element in terms of the non-dimensional coordinate system can be written as:

$$N_1 = \frac{\xi(\xi-1)\eta(\eta-1)}{4} \tag{3.90}$$

$$N_2 = \frac{(1-\xi^2)\eta(\eta-1)}{2} \tag{3.91}$$

$$N_3 = \frac{\xi(\xi+1)\eta(\eta-1)}{4} \tag{3.92}$$

$$N_4 = \frac{\xi(\xi+1)(1-\eta^2)}{2} \tag{3.93}$$

$$N_5 = \frac{\xi(\xi+1)\eta(\eta+1)}{4} \tag{3.94}$$

$$N_6 = \frac{(1-\xi^2)\eta(\eta+1)}{2} \tag{3.95}$$

$$N_7 = \frac{\xi(\xi-1)\eta(\eta+1)}{4} \tag{3.96}$$

$$N_8 = \frac{\xi(\xi-1)(1-\eta^2)}{2} \tag{3.97}$$

Where, ξ and η are the non-dimensional coordinates Fig.3.7 of a given point on the element.

Now the displacement field is expressed in terms of the nodal values. Thus, if d = $[w_0,\ \theta_x,\ \theta_y,\ w_0^*,\ \theta_x^*,\ \theta_y^*]$ represents the displacement components of a point located at (ξ,η), and q is the element displacement vector, then

$w_0 = N_1 w_{01} + N_2 w_{02} + ...+ N_8 w_{08}$

$\theta_x = N_1 \theta_{x1} + N_2 \theta_{x2} + ...+ N_8 \theta_{x8}$

$\theta_y = N_1 \theta_{y1} + N_2 \theta_{y2} + ...+ N_8 \theta_{y8}$

$w_0^* = N_1 w_{01}^* + N_2 w_{02}^* + ...+ N_8 w_{08}^*$

$\theta_x^* = N_1 \theta_{x1}^* + N_2 \theta_{x2}^* + ...+ N_8 \theta_{x8}^*$

$\theta_y^* = N_1 \theta_{y1}^* + N_2 \theta_{y2}^* + ...+ N_8 \theta_{y8}^*$

Where,

$$[N]_{6\times 48} = \Sigma \begin{vmatrix} N_i & 0 & 0 & 0 & 0 & 0 \\ 0 & N_i & 0 & 0 & 0 & 0 \\ 0 & 0 & N_i & 0 & 0 & 0 \\ 0 & 0 & 0 & N_i & 0 & 0 \\ 0 & 0 & 0 & 0 & N_i & 0 \\ 0 & 0 & 0 & 0 & 0 & N_i \end{vmatrix} \tag{3.98}$$

Strain-Displacement Matrix

The strain-displacement matrix relating strain components to element nodal variables can be formed as:

$$[\varepsilon] = [B][\delta] \tag{3.99}$$

Where each $\delta_i^T = [w_0,\ \theta_x,\ \theta_y,\ w_0^*,\ \theta_x^*,\ \theta_y^*]$ for i = 1 to 8.

Now, considering the flexure strain terms and shear strain terms separately and from [C] matrix, writing the strain-displacement relationship in terms of the bending curvature-displacement relation $[B_b]$ and shear rotation-displacement relation $[B_s]$.

From Equations 3.29 and 3.30,

$$\begin{vmatrix} \varepsilon_x \\ \varepsilon_y \\ \varepsilon_z \\ \gamma_{xy} \end{vmatrix} = \begin{vmatrix} z & 0 & 0 & z^3 & 0 & 0 & 0 \\ 0 & z & 0 & 0 & z^3 & 0 & 0 \\ 0 & 0 & 0 & 0 & 0 & 0 & z \\ 0 & 0 & z & 0 & 0 & z^3 & 0 \end{vmatrix} \begin{vmatrix} K_x \\ K_y \\ K_{xy} \\ K_x^* \\ K_y^* \\ K_{xy}^* \\ K_z \end{vmatrix} = [H_b(z)][K] \tag{3.100}$$

$$\begin{vmatrix} \gamma_{yz} \\ \gamma_{xz} \end{vmatrix} = \begin{vmatrix} 1 & 0 & z^2 & 0 \\ 0 & 1 & 0 & z^2 \end{vmatrix} \begin{vmatrix} \phi_y \\ \phi_x \\ \phi_y^* \\ \phi_x^* \end{vmatrix} = [H_s(z)][\phi] \tag{3.101}$$

Where, the shear rotation displacement relations $[\phi]$ are,

$$\phi = \begin{vmatrix} \phi_x \\ \phi_y \\ \phi_x^* \\ \phi_y^* \end{vmatrix} = \begin{vmatrix} \theta_x + \frac{\partial w_0}{\partial x} \\ \theta_y + \frac{\partial w_0}{\partial y} \\ 3\theta_x^* + \frac{\partial w_0^*}{\partial x} \\ 3\theta_y^* + \frac{\partial w_0^*}{\partial y} \end{vmatrix} \tag{3.102}$$

And the bending curvature-displacement relations [K] are,

$$K = \begin{vmatrix} K_x \\ K_y \\ K_{xy} \\ K_x^* \\ K_y^* \\ K_{xy^*} \\ K_z \end{vmatrix} = \begin{vmatrix} \frac{\partial\theta_x}{\partial x} \\ \frac{\partial\theta_y}{\partial y} \\ \frac{\partial\theta_x}{\partial y} + \frac{\partial\theta_y}{\partial x} \\ \frac{\partial\theta_x^*}{\partial x} \\ \frac{\partial\theta_y^*}{\partial y} \\ \frac{\partial\theta_x^*}{\partial y} + \frac{\partial\theta_y^*}{\partial x} \\ 2w_0^* \end{vmatrix} \tag{3.103}$$

Curvature-nodal displacement Relationships

The curvature vectors [K] and [ϕ] may be related to the nodal displacements by:

$$[K] = \begin{vmatrix} K_x \\ K_y \\ K_{xy} \\ K_x^* \\ K_y^* \\ K_{xy^*} \\ K_z \end{vmatrix} = \sum_{i=1}^{NN} \begin{vmatrix} 0 & \frac{\partial N_i}{\partial x} & 0 & 0 & 0 & 0 \\ 0 & 0 & \frac{\partial N_i}{\partial y} & 0 & 0 & 0 \\ 0 & \frac{\partial N_i}{\partial y} & \frac{\partial N_i}{\partial x} & 0 & 0 & 0 \\ 0 & 0 & 0 & 0 & \frac{\partial N_i}{\partial x} & 0 \\ 0 & 0 & 0 & 0 & 0 & \frac{\partial N_i}{\partial y} \\ 0 & 0 & 0 & 0 & \frac{\partial N_i}{\partial y} & \frac{\partial N_i}{\partial x} \\ 0 & 0 & 0 & 2N_i & 0 & 0 \end{vmatrix} \begin{vmatrix} w_0 \\ \theta_x \\ \theta_y \\ w_0^* \\ \theta_x^* \\ \theta_y^* \end{vmatrix} = [B_b(x,y)]_{7\times 48}[d_i] \tag{3.104}$$

$$[\phi] = \begin{vmatrix} \phi_x \\ \phi_y \\ \phi_x^* \\ \phi_y^* \end{vmatrix} = \sum_{i=1}^{NN} \begin{vmatrix} \frac{\partial N_i}{\partial x} & N_i & 0 & 0 & 0 & 0 \\ \frac{\partial N_i}{\partial y} & 0 & N_i & 0 & 0 & 0 \\ 0 & 0 & 0 & \frac{\partial N_i}{\partial x} & 3N_i & 0 \\ 0 & 0 & 0 & \frac{\partial N_i}{\partial y} & 0 & 3N_i \end{vmatrix} \begin{vmatrix} w_0 \\ \theta_x \\ \theta_y \\ w_0^* \\ \theta_x^* \\ \theta_y^* \end{vmatrix} [B_s(x,y)]_{4\times 48}[d_i] \tag{3.105}$$

3.4.2 Displacement Model-2

$u(x,y,z) = u_0(x,y,0)+z\theta_x(x,y,0)+z^2u_0^*(x,y,0)+z^3\theta_x^*(x,y,0)=u_0+z\theta_x+z^2u_0^*+z^3\theta_x^*$

$v(x,y,z) = v_0(x,y,0)+z\theta_y(x,y,0)+z^2v_0^*(x,y,0)+z^3\theta_y^*(x,y,0)=v_0+z\theta_y+z^2v_0^*+z^3\theta_y^*$

$w(x,y,z) = w_0(x,y,0) + z\theta_z(x,y,0)+z^2w_0^*(x,y,0) = w_0 + z\theta_z + z^2w_0^*$

The vector,

q = [u_{01}, v_{01}, w_{01}, θ_{x1}, θ_{y1}, θ_{z1}, u_{01}^*, v_{01}^*, w_{01}^*, θ_{x1}^*, θ_{y1}^*, u_{02}, v_{02}, w_{02}, θ_{x2}, θ_{y2}, θ_{z2}, u_{02}^*, v_{02}^*, w_{02}^*, θ_{x2}^*, θ_{y2}^*,,............,θ_{y8}^*] denotes the element displacement vector. Thus the degrees of freedom at each node are:

u_0, v_0, w_0 = Mid plane displacements in x, y , z direction.

θ_x, θ_y = Rotations of the transverse normal in the x-z and y-z plane respectively.

u_0^*, v_0^*, w_0^* = Higher order term of transverse displacements u_0, v_0, w_0 respectively at the geometrical mid-plane.

θ_x^*, θ_y^* = Higher order terms of rotations of the normal to the geometrical mid-plane in x-z and y-z plane i.e. qx and qy respectively.

Therefore, Nodal degree of freedom for element : 11

Number of nodes in the element : 8

Total degree of freedom for the element : 11x8 = 88

Shape Functions

The shape functions for this element in terms of the non-dimensional coordinate system can be written as:

$$N_1 = \frac{\xi(\xi-1)\eta(\eta-1)}{4} \tag{3.106}$$

$$N_2 = \frac{(1-\xi^2)\eta(\eta-1)}{2} \tag{3.107}$$

$$N_3 = \frac{\xi(\xi+1)\eta(\eta-1)}{4} \tag{3.108}$$

$$N_4 = \frac{\xi(\xi+1)(1-\eta^2)}{2} \tag{3.109}$$

$$N_5 = \frac{\xi(\xi+1)\eta(\eta+1)}{4} \tag{3.110}$$

$$N_6 = \frac{(1-\xi^2)\eta(\eta+1)}{2} \tag{3.111}$$

$$N_7 = \frac{\xi(\xi-1)\eta(\eta+1)}{4} \tag{3.112}$$

$$N_8 = \frac{\xi(\xi-1)(1-\eta^2)}{2} \tag{3.113}$$

Where, ξ and η are the non-dimensional coordinates Fig.3.7 of a given point on the element.

Now the displacement field is expressed in terms of the nodal values. Thus, if d = [u_0, v_0, w_0, θ_x, θ_y, θ_z, u_0^*, v_0^*, w_0^*, θ_x^*, θ_y^*] represents the displacement components of a point located at (ξ,η), and q is the element displacement vector, then

$u_0 = N_1 u_{01} + N_2 u_{02} + ...+ N_8 u_{08}$

$v_0 = N_1 v_{01} + N_2 v_{02} + ...+ N_8 v_{08}$

$w_0 = N_1 w_{01} + N_2 w_{02} + ...+ N_8 w_{08}$

$\theta_x = N_1 \theta_{x1} + N_2 \theta_{x2} + ...+ N_8 \theta_{x8}$

$\theta_y = N_1 \theta_{y1} + N_2 \theta_{y2} + ...+ N_8 \theta_{y8}$

$\theta_z = N_1 \theta_{z1} + N_2 \theta_{z2} + ...+ N_8 \theta_{z8}$

$u_0^* = N_1 u_{01}^* + N_2 u_{02}^* + ...+ N_8 u_{08}^*$

$v_0^* = N_1 v_{01}^* + N_2 v_{02}^* + ...+ N_8 v_{08}^*$

$w_0^* = N_1 w_{01}^* + N_2 w_{02}^* + ...+ N_8 w_{08}^*$

$\theta_x^* = N_1 \theta_{x1}^* + N_2 \theta_{x2}^* + ...+ N_8 \theta_{x8}^*$

$\theta_y^* = N_1 \theta_{y1}^* + N_2 \theta_{y2}^* + ...+ N_8 \theta_{y8}^*$

Where,

$$[N]_{11\times 88} = \Sigma \begin{vmatrix} N_i & 0 & 0 & 0 & 0 & 0 & 0 & 0 & 0 & 0 & 0 \\ 0 & N_i & 0 & 0 & 0 & 0 & 0 & 0 & 0 & 0 & 0 \\ 0 & 0 & N_i & 0 & 0 & 0 & 0 & 0 & 0 & 0 & 0 \\ 0 & 0 & 0 & N_i & 0 & 0 & 0 & 0 & 0 & 0 & 0 \\ 0 & 0 & 0 & 0 & N_i & 0 & 0 & 0 & 0 & 0 & 0 \\ 0 & 0 & 0 & 0 & 0 & N_i & 0 & 0 & 0 & 0 & 0 \\ 0 & 0 & 0 & 0 & 0 & 0 & N_i & 0 & 0 & 0 & 0 \\ 0 & 0 & 0 & 0 & 0 & 0 & 0 & N_i & 0 & 0 & 0 \\ 0 & 0 & 0 & 0 & 0 & 0 & 0 & 0 & N_i & 0 & 0 \\ 0 & 0 & 0 & 0 & 0 & 0 & 0 & 0 & 0 & N_i & 0 \\ 0 & 0 & 0 & 0 & 0 & 0 & 0 & 0 & 0 & 0 & N_i \end{vmatrix} \tag{3.114}$$

Strain-Displacement Matrix

The strain-displacement matrix relating strain components to element nodal variables can be formed as:

$$[\varepsilon] = [B][\delta] \tag{3.115}$$

Where each $\delta_i^T = [u_0, v_0, w_0, \theta_x, \theta_y, \theta_z, u_0^*, v_0^*, w_0^*, \theta_x^*, \theta_y^*]$ for i = 1 to 8.

Now, considering the flexure strain terms and shear strain terms separately and from [C] matrix, writing the strain-displacement relationship in terms of the bending curvature-displacement relation $[B_b]$ and shear rotation-displacement relation $[B_s]$.

From Equations 3.29 and 3.30,

$$
\begin{vmatrix} \varepsilon_x \\ \varepsilon_y \\ \varepsilon_z \\ \gamma_{xy} \end{vmatrix} = \begin{vmatrix} 1 & 0 & 0 & z^2 & 0 & 0 & 0 & z & 0 & 0 & z^3 & 0 & 0 & 0 \\ 0 & 1 & 0 & 0 & z^2 & 0 & 0 & 0 & z & 0 & 0 & z^3 & 0 & 0 \\ 0 & 0 & 0 & 0 & 0 & 0 & 1 & 0 & 0 & 0 & 0 & 0 & 0 & z \\ 0 & 0 & 1 & 0 & 0 & z^2 & 0 & 0 & 0 & z & 0 & 0 & z^3 & 0 \end{vmatrix} \begin{vmatrix} \varepsilon_{0x} \\ \varepsilon_{0y} \\ \varepsilon_{0xy} \\ \varepsilon_{0x}^* \\ \varepsilon_{0y}^* \\ \varepsilon_{0xy}^* \\ \varepsilon_{0z} \\ K_x \\ K_y \\ K_{xy} \\ K_x^* \\ K_y^* \\ K_{xy}^* \\ K_z^* \end{vmatrix} = [H_b(z)][K] \tag{3.116}
$$

$$
\begin{vmatrix} \gamma_{yz} \\ \gamma_{xz} \end{vmatrix} = \begin{vmatrix} 1 & 0 & z & 0 & z^2 & 0 \\ 0 & 1 & 0 & z & 0 & z^2 \end{vmatrix} \begin{vmatrix} \phi_y \\ \phi_x \\ \psi_y \\ \psi_x \\ \phi_y^* \\ \phi_x^* \end{vmatrix} = [H_s(z)][\phi] \tag{3.117}
$$

Where, the shear rotation displacement relations [ϕ] are,

$$\phi = \begin{vmatrix} \phi_x \\ \phi_y \\ \psi_x \\ \psi_y \\ \phi_x^* \\ \phi_y^* \end{vmatrix} = \begin{vmatrix} \theta_x + \frac{\partial w_0}{\partial x} \\ \theta_y + \frac{\partial w_0}{\partial y} \\ 2u_0^* + \frac{\partial \theta_z}{\partial x} \\ 2v_0^* + \frac{\partial \theta_z}{\partial y} \\ 3\theta_x^* + \frac{\partial w_0^*}{\partial x} \\ 3\theta_y^* + \frac{\partial w_0^*}{\partial y} \end{vmatrix} \tag{3.118}$$

And the bending curvature-displacement relations [K] are,

$$K = \begin{vmatrix} \varepsilon_{0x} \\ \varepsilon_{0y} \\ \varepsilon_{0xy} \\ \varepsilon_{0x}^* \\ \varepsilon_{0y}^* \\ \varepsilon_{0xy}^* \\ \varepsilon_{0z} \\ K_x \\ K_y \\ K_{xy} \\ K_x^* \\ K_y^* \\ K_{xy}^* \\ K_z^* \end{vmatrix} = \begin{vmatrix} \frac{\partial u_0}{\partial x} \\ \frac{\partial v_0}{\partial y} \\ \frac{\partial u_0}{\partial y} + \frac{\partial v_0}{\partial x} \\ \frac{\partial u_0^*}{\partial x} \\ \frac{\partial v_0^*}{\partial y} \\ \frac{\partial u_0^*}{\partial y} + \frac{\partial v_0^*}{\partial x} \\ \theta_z \\ \frac{\partial \theta_x}{\partial x} \\ \frac{\partial \theta_y}{\partial y} \\ \frac{\partial \theta_x}{\partial y} + \frac{\partial \theta_y}{\partial x} \\ \frac{\partial \theta_x^*}{\partial x} \\ \frac{\partial \theta_y^*}{\partial y} \\ \frac{\partial \theta_x^*}{\partial y} + \frac{\partial \theta_y^*}{\partial x} \\ 2w_0^* \end{vmatrix} \tag{3.119}$$

Curvature-nodal displacement Relationships

The curvature vectors [ε_0], [K] and [ϕ] may be related to the nodal displacements by:

$$\begin{vmatrix} \varepsilon_0 \\ K \end{vmatrix} = \begin{vmatrix} \varepsilon_{0x} \\ \varepsilon_{0y} \\ \varepsilon_{0xy} \\ \varepsilon_{0x}^* \\ \varepsilon_{0y}^* \\ \varepsilon_{0xy}^* \\ \varepsilon_{0z} \\ K_x \\ K_y \\ K_{xy} \\ K_x^* \\ K_y^* \\ K_{xy}^* \\ K_z^* \end{vmatrix} = \sum_{i=1}^{NN} \begin{vmatrix} \frac{\partial N_i}{\partial x} & 0 & 0 & 0 & 0 & 0 & 0 & 0 & 0 & 0 & 0 \\ 0 & \frac{\partial N_i}{\partial y} & 0 & 0 & 0 & 0 & 0 & 0 & 0 & 0 & 0 \\ \frac{\partial N_i}{\partial y} & \frac{\partial N_i}{\partial x} & 0 & 0 & 0 & 0 & 0 & 0 & 0 & 0 & 0 \\ 0 & 0 & 0 & 0 & 0 & 0 & \frac{\partial N_i}{\partial x} & 0 & 0 & 0 & 0 \\ 0 & 0 & 0 & 0 & 0 & 0 & 0 & \frac{\partial N_i}{\partial y} & 0 & 0 & 0 \\ 0 & 0 & 0 & 0 & 0 & 0 & \frac{\partial N_i}{\partial y} & \frac{\partial N_i}{\partial x} & 0 & 0 & 0 \\ 0 & 0 & 0 & 0 & 0 & N_i & 0 & 0 & 0 & 0 & 0 \\ 0 & 0 & 0 & \frac{\partial N_i}{\partial x} & 0 & 0 & 0 & 0 & 0 & 0 & 0 \\ 0 & 0 & 0 & 0 & \frac{\partial N_i}{\partial y} & 0 & 0 & 0 & 0 & 0 & 0 \\ 0 & 0 & 0 & \frac{\partial N_i}{\partial y} & \frac{\partial N_i}{\partial x} & 0 & 0 & 0 & 0 & 0 & 0 \\ 0 & 0 & 0 & 0 & 0 & 0 & 0 & 0 & 0 & \frac{\partial N_i}{\partial x} & 0 \\ 0 & 0 & 0 & 0 & 0 & 0 & 0 & 0 & 0 & 0 & \frac{\partial N_i}{\partial y} \\ 0 & 0 & 0 & 0 & 0 & 0 & 0 & 0 & 0 & \frac{\partial N_i}{\partial y} & \frac{\partial N_i}{\partial x} \\ 0 & 0 & 0 & 0 & 0 & 0 & 0 & 0 & 2N_i & 0 & 0 \end{vmatrix} \begin{vmatrix} u_0 \\ v_0 \\ w_0 \\ \theta_x \\ \theta_y \\ \theta_z \\ u_0^* \\ v_0^* \\ w_0^* \\ \theta_x^* \\ \theta_y^* \end{vmatrix} \tag{3.120}$$

$$\begin{vmatrix} \varepsilon_0 \\ K \end{vmatrix} = [B_b(x,y)]_{14\times 88}[d_i] \tag{3.121}$$

$$[\phi] = \begin{vmatrix} \phi_x \\ \phi_y \\ \psi_x \\ \psi_y \\ \phi_x^* \\ \phi_y^* \end{vmatrix} = \sum_{i=1}^{NN} \begin{vmatrix} 0 & 0 & \frac{\partial N_i}{\partial x} & N_i & 0 & 0 & 0 & 0 & 0 & 0 & 0 \\ 0 & 0 & \frac{\partial N_i}{\partial y} & 0 & N_i & 0 & 0 & 0 & 0 & 0 & 0 \\ 0 & 0 & 0 & 0 & \frac{\partial N_i}{\partial x} & 0 & 2N_i & 0 & 0 & 0 & 0 \\ 0 & 0 & 0 & 0 & 0 & \frac{\partial N_i}{\partial y} & 0 & 2N_i & 0 & 0 & 0 \\ 0 & N_i & 0 & 0 & 0 & 0 & 0 & 0 & \frac{\partial N_i}{\partial x} & 3N_i & 0 \\ 0 & N_i & 0 & 0 & 0 & 0 & 0 & 0 & \frac{\partial N_i}{\partial y} & 0 & 3N_i \end{vmatrix} \begin{vmatrix} u_0 \\ v_0 \\ w_0 \\ \theta_x \\ \theta_y \\ \theta_z \\ u_0^* \\ v_0^* \\ w_0^* \\ \theta_x^* \\ \theta_y^* \end{vmatrix} \tag{3.122}$$

$$[\phi] = [B_s(x,y)]_{6\times 88}[d_i] \tag{3.123}$$

3.4.3 Stiffness Matrix formulation

Here, the Virtual Work Principle has been used to derive the element stiffness matrix and the consistent load vector. If we have, $\partial U = \partial W$, where the internal virtual strain energy ∂U and the external virtual work ∂W can be written in terms of the nodal displacements as,

$$\delta U = \int_v \delta[\varepsilon_b]^T[\sigma_b] \quad + \quad \delta[\gamma_s]^T[\tau_s] \quad dv \tag{3.124}$$

$$\delta U = \int_v \delta[d_i]^T[B_b(x,y)]^T \; [H_b(z)]_n^T[Q_b]_n[H_b(z)]_n[B_b(x,y)][d_i]$$

$$+\delta[d_i]^T[B_s(x,y)]^T \; [H_s(z)]_n^T[Q_s]_n[H_s(z)]_n[B_s(x,y)][d_i] \quad dv \tag{3.125}$$

$$\delta W = \delta[d_i]^T[p_i^e] \tag{3.126}$$

where $[p_i^e]$ are the nodal actions due to the externally applied loads. Next, canceling $\delta[d_i]^T$ from both sides of the equation $\delta U = \delta W$ results in$[K^e][d_i] = [p_i^e]$, where $[K^e]$ is the element stiffness matrix given by,

$$[K^e] = \int_v [B_b(x,y)]^T[H_b(z)]_n^T[Q_b]_n[H_b(z)]_n[B_b(x,y)]$$

$$+[B_s(x,y)]^T[H_s(z)]_n^T[Q_s]_n[H_s(z)]_n[B_s(x,y)] \qquad dA \tag{3.127}$$

further by replacing flexure and shear stiffness matrix by $[D_b]$ and $[D_s]$, the element stiffness matrix can be written in following form,

$$[K^e] = \int_v [B_b(x,y)]^T D_b[B_b(x,y)] + [B_s(x,y)]^T D_s[B_s(x,y)]dA \tag{3.128}$$

Here $[D_b]$ and $[D_s]$ matrix can be obtained from stress-strain relationship elasticity matrix using constitutive law matrix as follows,

$$[D] = \begin{vmatrix} D_b & 0 \\ 0 & D_s \end{vmatrix} \tag{3.129}$$

Where $[D_b]$ is,

$$[D_b] = \int_{-h/2}^{h/2} [H_b(z)]_n^T[Q_b]_n[H_b(z)]_n dz \tag{3.130}$$

and $[D_s]$ is,

$$[D_s] = \int_{-h/2}^{h/2} [H_s(z)]_n^T [Q_s]_n [H_s(z)]_n dz \tag{3.131}$$

Note that the matrices $[B_b]$ and $[B_s]$ are evaluated based on the shape functions given above. Upon evaluating matrices $[D_b]$, $[D_s]$, $[B_b]$ and $[B_s]$ the element stiffness matrix can be evaluated for displacement model-1 and model-2 respectively. However, since the shape functions and, thus, the matrices $[B_b]$ and $[B_s]$ are defined in terms of the nondimensional coordinate system, the element stiffness matrix must be evaluated as follows:

$$[K^e] = \int_{-1}^{+1} \int_{-1}^{+1} \; [B_b(\xi,\eta)]^T \; [D_b] \; [B_b(\xi,\eta)] + [B_s(\xi,\eta)]^T \; [D_b] \; [B_s(\xi,\eta)] \; [J] \; d\xi \; d\eta \tag{3.132}$$

The Gauss-Quadrature integration technique is used to evaluate the integrals. In the present formulation a selective integration scheme is used to evaluate element stiffness matrix. For the bending stiffness terms and shear stiffness terms 3x3 integration scheme has been adopted. Thus the stiffness matrix has been evaluated as follows:

$$[K^e] = \sum_{a=1}^{NG} \sum_{b=1}^{NG} [B_b(\xi,\eta)]^T \; [D_b] \; [B_b(\xi,\eta)] + [B_s(\xi,\eta)]^T \; [D_b] \; [B_s(\xi,\eta)] \; |J| \; W_a \; W_b \tag{3.133}$$

Where Wa and Wb are the weighting factors corresponding to Gauss sampling points and NG is the number of Gauss points selected for the integration schemes.

3.4.4 Evaluation of Consistent Load Vector

The components of the consistent load vector are the equivalent load applied at the nodal points of the element due to the loads applied at the intermediate points of a finite element. In the evaluation of the load vector the entire laminate is considered as a single layer of thickness t_i. The applied external forces may consist of independent or combination of the following load cases:

Gravity Load :

The gravity loads, generally the self-weight of the element, always act in the global z-direction. Let r be the uniform mass density of the element material and g be the acceleration due to gravity in z-direction. The element load vector at node i is given by,

$$P_{gi} = \int_A \rho \ g \ t \ [N_i]^T \ dA \tag{3.134}$$

$$[P_g^e] = \sum_{a=1}^{NG} \sum_{b=1}^{NG} \rho \ g \ t \ [N_i]^T \ [J] W_a W_b \tag{3.135}$$

The above equation represents the element load vector for all the nodes.

Uniform normal surface pressure:

To evaluate the nodal loads due to normal surface pressure P_0, the displacement normal to the surface of the element is required. As here, there is only the transverse displacement, the transverse normal pressure acting either innermost or outermost surface is considered. The load vector at node i is given by,

$$P_{pi} = \int_A \ P_0 \ [N_i]^T \ dA \tag{3.136}$$

$$[P_{pi}] = \sum_{a=1}^{NG} \sum_{b=1}^{NG} \ P_0 \ [N_i]^T \ [J] W_a W_b \tag{3.137}$$

The above equation represents the element load vector for all the nodes.

Sinusoidal normal surface pressure:

The load vector at node i due to sinusoidal distributed normal pressure is obtained from Equation 3.137 by replacing P_0 by,

$$P_0 \frac{\sin m\pi x}{a} \frac{\sin n\pi y}{b} \tag{3.138}$$

Where, P_0 is amplitude of loading in the z-direction and the element load vector is given by Equation 3.138

Uniformly distributed load f_z in the transverse direction:

The load vector at node I due to uniformly distributed load f_z is given by,

$$P_{ui} = \int_A f_z \; [N_i]^T \; dA \tag{3.139}$$

$$[P_{ui}] = \sum_{a=1}^{NG} \sum_{b=1}^{NG} f_z \; [N_i]^T \; [J] W_a W_b \tag{3.140}$$

Equation 3.140 gives the element load vector for the uniformly distributed loads in the transverse direction.

Point load along the transverse direction:

When the point of application is not coincident with nodal point and P_{pt} be the point load normal to the surface of the element, the load vector at node i is given by,

$$[P_{pti}] = P_{pt} \; [N_i]^T \tag{3.141}$$

3.5 Static Analysis of Laminated Composite Plate

General

Static Analysis is required to calculate the displacements along x, y and z points and interlaminar stresses in laminated composite plate under different type of loadings. After obtain global stiffness matrix and load vector from governing equation the static analysis has been done using numerical method.

Assembly and Solution

After obtaining the individual element stiffness matrices and nodal load vectors matrices, they are assembled according to the element node relationship.

Boundary Condition:

The finite element formulation developed above is based on the assumed displacement functions only. Thus only displacement boundary condition can be specified.

3.5.1 Governing Equation

Solution Procedure

We follow the standard finite element solution procedure, where first the element stiffness matrices and the consistent load vectors are assembled to form the global stiffness matrix and the global load vector. Substitution of a minimum number of boundary conditions results in the system governing equation given by,

$$[K][q] = [P] \tag{3.142}$$

Where, [K] and [P] are the stiffness matrix and the consistent load vector, respectively, for the entire solution domain. The above equations can be solved for nodal displacements [q] for a given external load using numerical method.

3.6 Dynamic Analysis of Laminated Composite Plate

Dynamic consideration is required when the loads are of variable nature, the mass and acceleration effects come into the picture. If a solid body deformed elastically and suddenly released, it tends to vibrate about its equilibrium position. This periodic motion due to the restoring strain energy is called Free Vibration. The number of cycles per unit time is called the frequency. In this chapter Free Vibration Analysis of Laminated Composite Plate is presented based on assumed two displacement functions same as used for static snalysis. Based on displacement functions further Finite Element formulation is carried out.

3.6.1 Displacement Model-1

Displacement model considered for mass matrix is as follows,

$$
\begin{aligned}
u(x,y,z) &= z\theta_x(x,y,0) + z^3\theta_x^*(x,y,0) = z\theta_x + z^3\theta_x^* \\
v(x,y,z) &= z\theta_y(x,y,0) + z^3\theta_y^*(x,y,0) = z\theta_y + z^3\theta_y^* \\
w(x,y,z) &= w_0(x,y,0) + z^2w_0^*(x,y,0) = w_0 + z^2w_0^*
\end{aligned}
$$

The displacement along the x, y and z directions are expressed in terms of higher order functions of thickness coordinates and mid plane variables.

Finite Element Formulation of Mass Matrix

The Lagrangean is define by

$$L = T - \prod$$

Where T is the kinetic energy and $\prod$ is the potential energy.

From **Hamilton's Prnciple** for an arbitrary time interval from t_1 to t_2, the state of motion of a body extremizes the functional,

$$I = \int_{t_1}^{t_2} L \quad dt \tag{3.143}$$

For solid body the kinetic energy term is given by,

$$T = \frac{1}{2}\int_v \dot{u}_T \dot{u}\rho \quad dV \tag{3.144}$$

Where ρ is the density(mass per unit volume) of the maerial and $\dot{u} = [\dot{u}, \dot{v}, \dot{w}]^T$ is the velocity vector. In the finite element method the body is devided into elements, and in each elements, we express **u** in terms of the nodal displacements **q**, using shape functions **N**. Thus,

$$u = Nq \tag{3.145}$$

In dynamic analysis, the elements **q** are dependent on time, while **N** represents shape functions defined on a master element.The velocity vector is then given by

$$\dot{u} = N\dot{q} \tag{3.146}$$

By substituting Equation 3.146 in Equation 3.144, the kinetic energy T_e in element e is,

$$T_e = \frac{1}{2}\dot{q}^T \left[\int_e \rho N^T N \quad dV\right]\dot{q} \tag{3.147}$$

where the bracketed expression is the mass matrix

$$M_e = \left[\int_e \rho N^T m N \quad dV \right] \tag{3.148}$$

Where N is shape function and m is inertia matrix given by,

$$N = \sum_{i=1}^{N} N_i \tag{3.149}$$

$$N = [N_i \vdots \ldots\ldots \vdots N_{NN}] \tag{3.150}$$

$$m = \begin{vmatrix} I_1 & & & & & \\ & I_2 & & 0 & & \\ & & I_2 & & & \\ & & & I_4 & & \\ & & 0 & & I_4 & \\ & & & & & I_6 \end{vmatrix} \tag{3.151}$$

$$[I_1, I_2, I_3, I_4, I_5, I_6] = \sum_{L=1}^{n} \int_{h_{l-1}}^{h_l} [1, z^2, z^4, z^6] \rho^l dz \tag{3.152}$$

here ρ^l is the material density of the L^{th} layer. I_1, I_2, I_4,I_6 are the normal inertia, rotary inertia and higher order inertia terms respectively.

This mass matrix is consistent with the shape functions chosen and is called the consistent mass matrix.

$$[M^e] = \int_{-1}^{+1} \int_{-1}^{+1} [N]^T \; [m] \; [N] \; [J] \; d\xi \; d\eta \tag{3.153}$$

The Gauss-Quadrature integration technique is used to evaluate the integrals. In the present formulation a selective 3x3 integration scheme is used to evaluate element mass matrix. For the bending stiffness terms and shear stiffness terms integration scheme has been adopted. Thus the mass matrix has been evaluated as follows:

$$[M^e] = \sum_{a=1}^{NG} \sum_{b=1}^{NG} [N]^T \; [m] \; [N] \; |J| \; W_a \; W_b \tag{3.154}$$

Where Wa and Wb are the weighting factors corresponding to Gauss sampling points and NG is the number of Gauss points selected for the integration schemes.

On summing over all the elements, we get

$$T = \sum_e \; T_e \;\; = \sum_e \frac{1}{2} \; \dot{q}^T M^e \dot{q} \;\; = \;\; \frac{1}{2} \dot{Q}^T M \dot{Q} \tag{3.155}$$

Thus the potential energy is given by

$$\prod = \frac{1}{2} \; Q^T K Q \;\; - \;\; Q^T F \tag{3.156}$$

3.6.2 Displacement Model-2

Displacement model considered for mass matrix is as follows,

$$u(x, y, z) = u_0(x, y, 0) + z\theta_x(x, y, 0) + z^2 u_0^*(x, y, 0) + z^3 \theta_x^*(x, y, 0) = u_0 + z\theta_x + z^2 u_0^* + z^3 \theta_x^*$$
$$v(x, y, z) = v_0(x, y, 0) + z\theta_y(x, y, 0) + z^2 v_0^*(x, y, 0) + z^3 \theta_y^*(x, y, 0) = v_0 + z\theta_y + z^2 v_0^* + z^3 \theta_y^*$$

$w(x,y,z) = w_0(x,y,0) + z\theta_z(x,y,0) + z^2 w_0^*(x,y,0) = w_0 + z\theta_z + z^2 w_0^*$

The displacement along the x, y and z directions are expressed in terms of higher order functions of thickness coordinates and mid plane variables.

Finite Element Formulation of Mass Matrix

The Lagrangean is define by

$$L = T - \prod$$

Where T is the kinetic energy and $\prod$ is the potential energy.

From **Hamilton's Prnciple** for an arbitrary time interval from t_1 to t_2, the state of motion of a body extremizes the functional,

$$I = \int_{t_1}^{t_2} L \quad dt \tag{3.157}$$

For solid body the kinetic energy term is given by,

$$T = \frac{1}{2}\int_v \dot{u}_T \dot{u} \rho \quad dV \tag{3.158}$$

Where ρ is the density(mass per unit volume) of the maerial and $\dot{u} = [\dot{u}, \dot{v}, \dot{w}]^T$ is the velocity vector. In the finite element method the body is divided into elements, and in each elements, we express **u** in terms of the nodal displacements **q**, using shape functions **N**. Thus,

$$u = Nq \tag{3.159}$$

In dynamic analysis, the elements **q** are dependent on time, while **N** represents shape functions defined on a master element.The velocity vector is then given by

$$\dot{u} = N\dot{q} \tag{3.160}$$

By substituting Equation 3.160 in Equation 3.158, the kinetic energy T_e in element e is,

$$T_e = \frac{1}{2}\dot{q}^T \left[\int_e \rho N^T N \quad dV \right] \dot{q} \tag{3.161}$$

where the bracketed expression is the mass matrix

$$M_e = \left[\int_e \rho N^T m N \;\; dV \right] \tag{3.162}$$

Where N is shape function and m is inertia matrix given by,

$$N = \sum_{i=1}^{N} N_i \tag{3.163}$$

$$N = [N_i \vdots \ldots\ldots \vdots N_{NN}] \tag{3.164}$$

$$m = \begin{vmatrix} I_1 & & & & & & & & & & \\ & I_1 & & & & & & & & & \\ & & I_1 & & & & & 0 & & & \\ & & & I_2 & & & & & & & \\ & & & & I_2 & & & & & & \\ & & & & & I_2 & & & & & \\ & & & & & & I_3 & & & & \\ & & & & & & & I_3 & & & \\ & & & 0 & & & & & I_3 & & \\ & & & & & & & & & I_4 & \\ & & & & & & & & & & I_4 \end{vmatrix} \tag{3.165}$$

$$[I_1, I_2, I_3, I_4] = \sum_{L=1}^{n} \int_{h_{l-1}}^{h_l} [1, z^2, z^4, z^6]\rho^l dz \tag{3.166}$$

here ρ^l is the material density of the L^{th} layer. I_1, I_2, I_3,I_4 are the normal inertia, rotary inertia and higher order inertia terms respectively.

This mass matrix is consistent with the shape functions chosen and is called the consistent mass matrix.

$$[M^e] = \int_{-1}^{+1} \int_{-1}^{+1} [N]^T \; [m] \; [N] \; [J] \; d\xi \; d\eta \tag{3.167}$$

The Gauss-Quadrature integration technique is used to evaluate the integrals. In the present formulation a selective 3x3 integration scheme is used to evaluate element mass matrix. For the bending stiffness terms and shear stiffness terms integration scheme has been adopted. Thus the mass matrix has been evaluated as follows:

$$[M^e] = \sum_{a=1}^{NG} \sum_{b=1}^{NG} [N]^T \ [m] \ [N] \ |J| \ W_a \ W_b \tag{3.168}$$

Where Wa and Wb are the weighting factors corresponding to Gauss sampling points and NG is the number of Gauss points selected for the integration schemes.

On summing over all the elements, we get

$$T = \sum_e \ T_e \ = \sum_e \frac{1}{2} \ \dot{q}^T M^e \dot{q} \ = \ \frac{1}{2} \dot{Q}^T M \dot{Q} \tag{3.169}$$

Thus the potential energy is given by

$$\prod = \frac{1}{2} \ Q^T K Q \ - \ Q^T F \tag{3.170}$$

3.6.3 Free Vibration Solution

Using the Lagrangean $L = T - \prod$, obtained equation of motion is:

$$M\ddot{Q} + KQ = F \tag{3.171}$$

For free vibrations the force F is zero. Thus,

$$M\ddot{Q} + KQ = 0 \tag{3.172}$$

For steady state condition, starting from the equilibrium state, we set

$$Q = U sin\omega t \tag{3.173}$$

Where U is the vector of nodal amplitudes of vibration and ω (rad/sec) is the circular frequency (cycles/sec). Introducing Equation 3.173 in Equation 3.172, we have

$$KU = \omega^2 MU \tag{3.174}$$

This generalized eigenvalue problem

$$KU = \lambda MU \tag{3.175}$$

where U is the eigenvector, representing the vibrating mode, corresponding to the eigenvalue λ. The eigenvalue λ is the square of the circular frequency ω. The frequency f in hertz(cycles/sec) is obtained from $f = \frac{\omega}{2\pi}$. The eigenvalue problem is solved by using Inverse Iteration method [4]. To make the solution procedure less time consuming and to solve nos of problem computer program is developed.

3.7 Summary

In this chapter a basic mechanics of composite laminates is discussed. For analysis of Laminated Composites a Higher Order Shear Deformation Theory is studied and presented. A two displacement models with six degrees of freedom and eleven degrees of freedom per node respectively are assumed and based on higher order shear deformation theory using 8-noded isoparametric finite element finite element solution is formulated for Static and Dynamic analysis of laminated composite plates. A global stiffness matrix is calculated using 3x3 Gauss Integration scheme. For Dynamic analysis mass matrix is calculated using 3x3 Gauss Integration scheme. To solve the numerical problem free vibration analysis solution is formulated using Eigen Value analysis.

Chapter 4

Computer Program Development

4.1 Introduction

In this chapter the study of computer program developed in C++ environment for analysis of laminated composite plates is discussed. The programm is capable to perform a meshing of laminated plate and to generate a input data file for analysis of laminated plate. The core program is to perform a static and dynamic analysis of laminated composite plate using a finite element formulation with displacement model-1 and 2 based on higher order shear deformation theory.

4.2 Static Analysis

4.2.1 Features of Computer Program

Features of computer program are as follows:

1. Automatic Mesh generation
2. Generation of element stiffness matrix
3. Generation of load vector
4. Generation of overall stiffness matrix and load vector in banded form

5. Incorporating Boundary conditions

6. Static solution using governing equation

7. Calculation of stresses

4.2.2 Flow of Computer Program

Automatic Mesh Generation with Input Data:

The meshing of laminated plate is performed automatically. The laminated plate is divided in number of elements by assigning the number of divisions in along length and width direction. Numbering to the elements are assigned automatically moving in the direction from left to right and bottom to top. Each element has 8 nodes, which are numbered sequentially from left to right and bottom to top as shown in Fig.4.1.

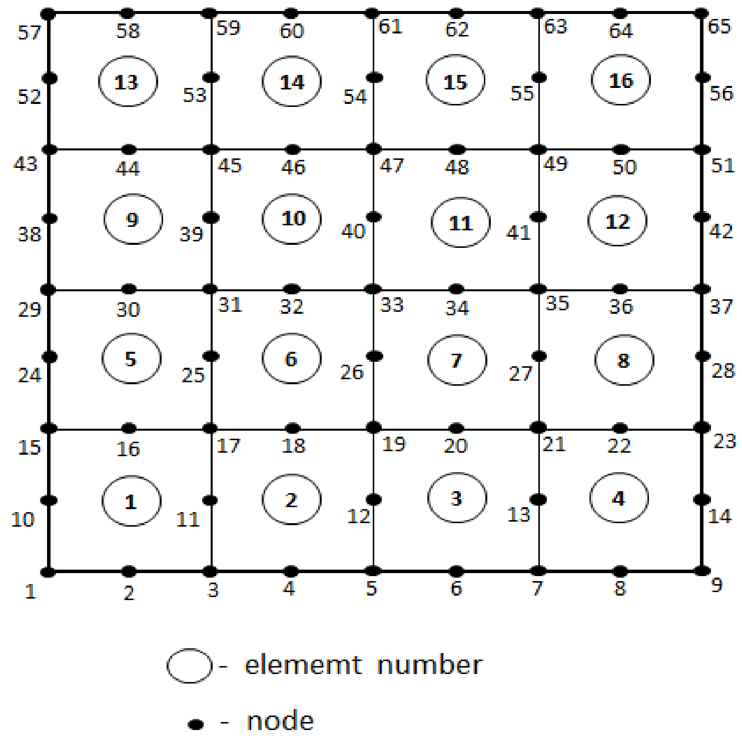

Figure 4.1: Meshing of laminated plate

a. Plate Dimension

b. Number of Materials with properties

c. Number of Laminate

d. Laminate id with angle of orientation and thickness

e. Assigning of Load

After material properties the element incidences and element coordinates are evaluated automatically. And based on support condition the boundary condition is assigned to each node.

Generation of Constitutive Law Matrix:

A formulation of constitutive law matrix is executed in computer program based on the finite element formulation discussed in **Chapter 3**. Constitutive law matrix is formulated using the entered material properties.

Generation of [B] Matrix:

Matrix [B] is formulated using shape functions and curvature - nodal displacement relationship. As shown in flow chart Fig.4.3 for each element [B] matrix for bending and shear is generated using subroutine.

Generation of Overall Stiffness Matrix and Load Vector:

The element stiffness matrix for the laminate is generated by laminate constitutive relation and [B] matrix. Then generated element stiffness matrices for the laminate are assembled in banded form. The integration for stiffness matrix is evaluated by 3x3 Gauss integration scheme. For load vector each element load vector is generated by reading loading type and value from input data. Then element load vectors are assembled in banded form.

Incorporating Boundary conditions:

In input data file at each node based on displacement model according to degrees of freedom 0 or 1 value is assigned to each displacement fields. From this data file boundary condition is assigned to overall stiffness matrix in core program.

Static Solution Using Governing Equation:

After assigning boundary condition to overall stiffness matrix from governing equation displacement is calculated using subroutine based on Gauss Elimination method.The governing equation is $[K]\{u\} = \{F\}$

where $[K]$ = Overall stiffness matrix, $\{u\}$ = displacement vector and $\{F\}$= Overall load vector

Calculation of stresses:

Stresses are calculated from the stress-resultant and mid-plane strains relationships as derived in **Chapter 3** using subroutine of stress calculation in the program as shown in flow chart Fig.4.3. Stresses are calculated for each lamina at top, at middle and at bottom.

Output:

Output data file is consist of following data and results:

a. Plate Dimension

b. Number of elements, nodes and materials

c. Material Properties

d. Laminate data: id, angle of orientation, thickness

e. Element incidences

f. Joint Coordinates

g. Boundary condition

h. Lamina thickness

i. Overall stiffness matrix

j. Overall load vector

k. Displacement vector

l. Stresses

Flow Chart for the program of meshing of laminated composite plate with Input Data

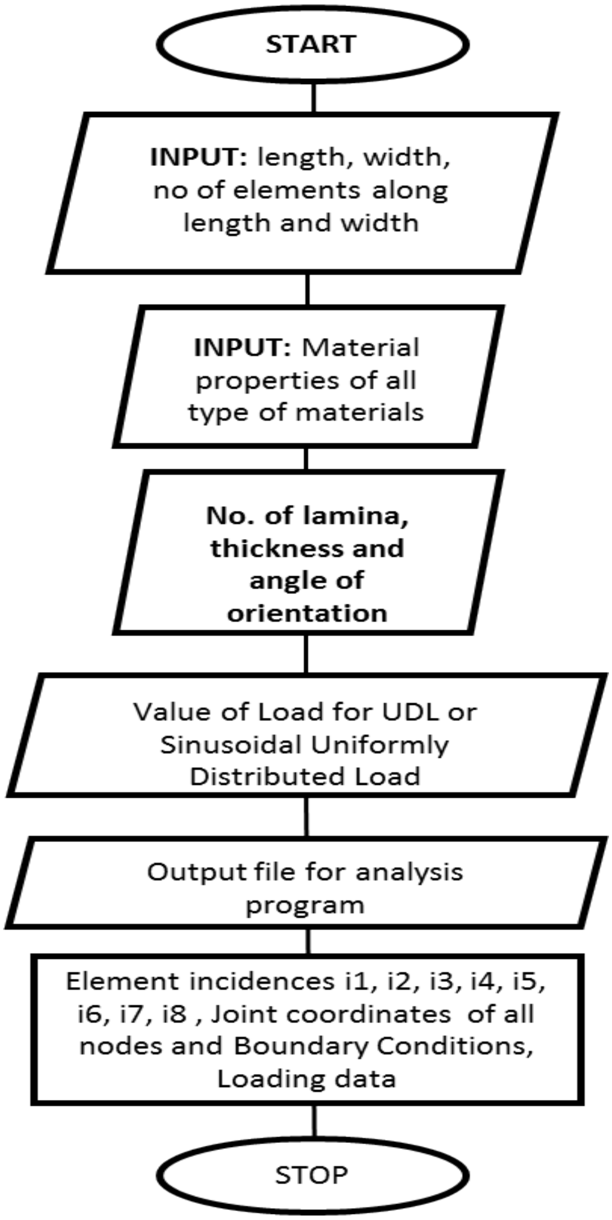

Figure 4.2: Input data with meshing of laminated plate

Flow Chart for Static Analysis Program

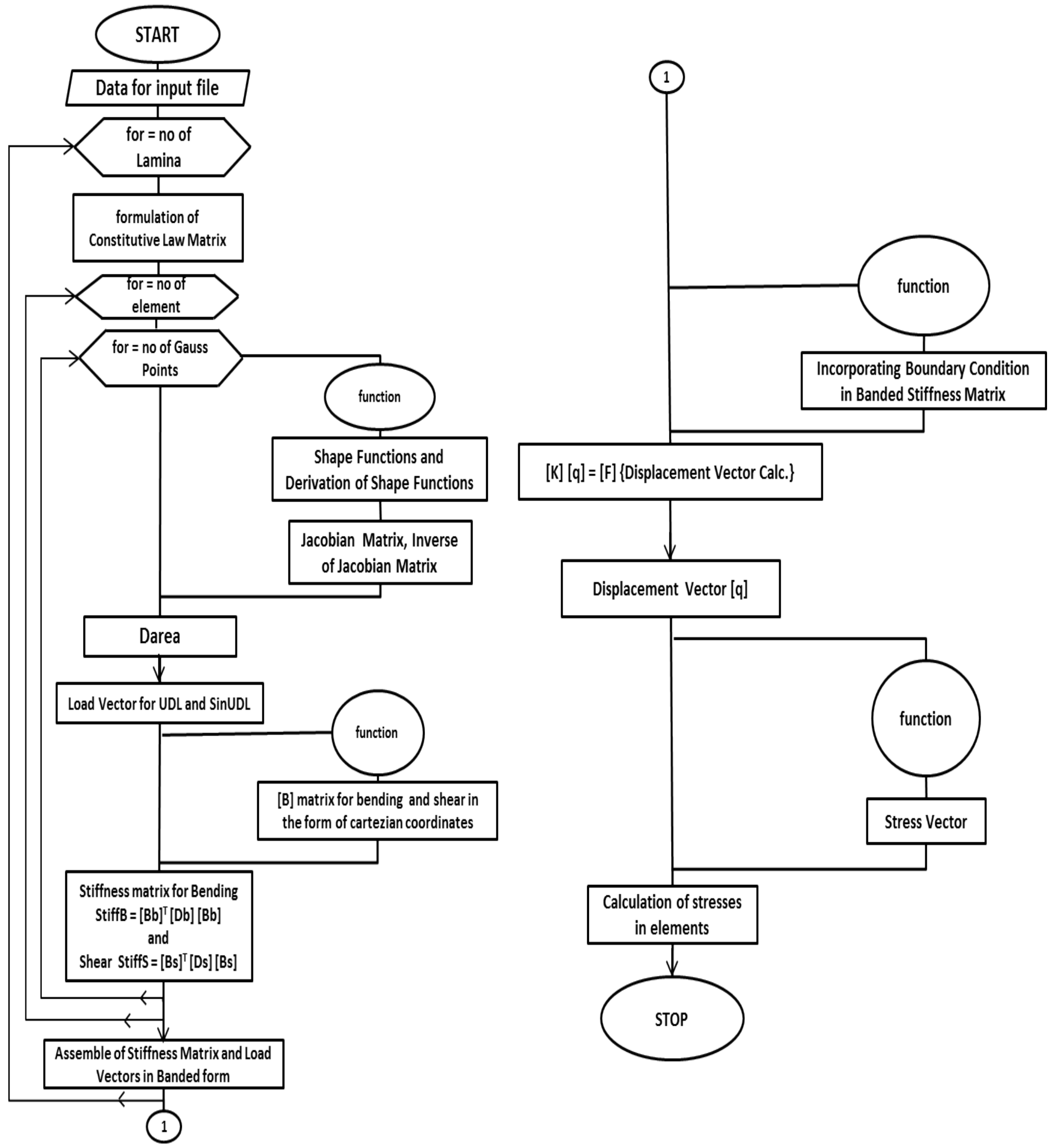

Figure 4.3: Static analysis of laminated composite plate

4.3 Dynamic Analysis

4.3.1 Features of Computer Program

In dynamic analysis of laminated composite plate program flow of computer program for the generation of automatic mesh and overall stiffness matrix are same as executed in static analysis. Here generation of overall mass matrix and subroutine for free vibration solution are incorporated in analysis program as shown in Fig.4.4.

4.3.2 Flow of Computer Program

Generation of consistent Mass Matrix:
From Hamilton's principle the element mass matrix for the laminate is generated by shape function and inertia matrix. Then generated element mass matrices for the laminate are assembled in banded form. The integration for mass matrix is evaluated by 3x3 Gauss integration scheme.

Incorporating Boundary conditions:
In input data file at each node based on displacement model according to degrees of freedom 0 or 1 value is assigned to each displacement fields. From this data file boundary condition is assigned to overall stiffness matrix mass matrix in core program.

Dynamic Solution Using Governing Equation:
From Lagrangian principle the equation of motion is obtained and converted in to generalized eigen value problem. Natural frequency is calculated for plate by solving eigen value problem using subroutine of inverse iteration method [4] in core program.

Output:
Output data file is consist of following data and results:

a. Plate Dimension

b. Number of elements, nodes and materials

c. Material Properties

d. Laminate data: id, angle of orientation, thickness

e. Element incidences

f. Joint Coordinates

g. Boundary condition

h. Overall stiffness matrix

i. Overall mass matrix

j. Eigen value, Iteration number, Eigen vector, omega and frequency

Flow Chart for the Dynamic Analysis Program

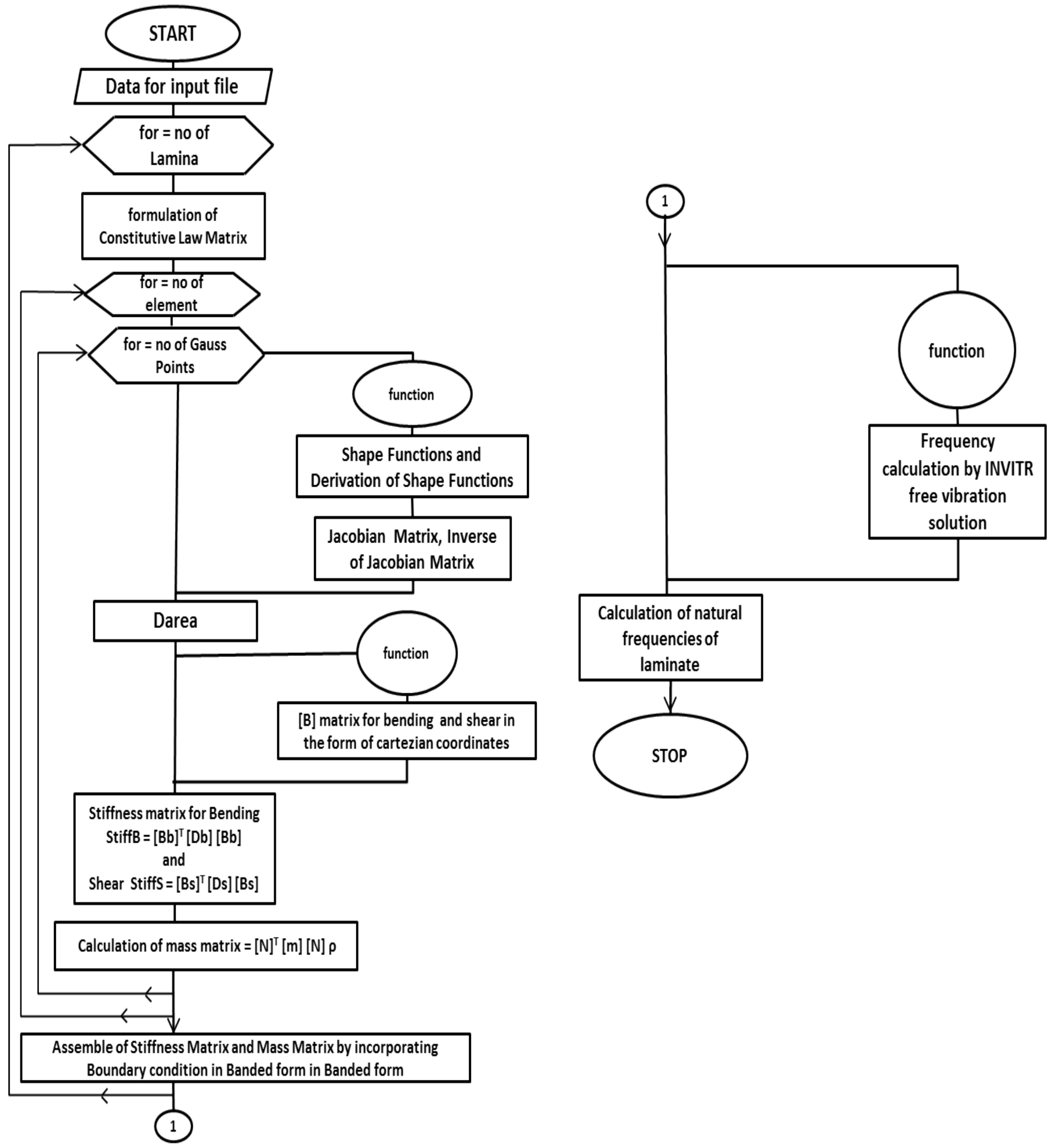

Figure 4.4: Dynamic analysis of laminated composite plate

4.4 Summary

Developed computer programs are used to solve the various numerical problems to validate the finite element formulation by comparing obtained displacements and frequencies with available results in literatures. From this study it can be conclude that the developed computer programs are capable to carryout static and dynamic analysis of laminated composite plates with varying width-to-thickness ratio, material anisotropy, number of layers and support conditions.

Chapter 5

Static Analysis: Results and Discussion

5.1 General

The Finite Element Method formulation based on Higher Order Shear Deformation Theory is discussed in **Chapter 3**. Computer program is developed for static analysis of composite plates using finite element model as discussed in **Chapter 4**. in this chapter finite element method is employed for analysis of laminated composite plate under different static loadings with different support conditions, widh/thickness ratio, material anisotropy. Using computer program analysis results are obtained and nondimensionalized displacement and stresses are calculated. In order to establish the reliability and accuracy of the present finite element formulation various examples available in literature are solved and discussed.

5.2 Problem Descritization

From convergence study in general unless otherwise stated for all examples considered, the plate is descritized with sixteen elements (4x4 mesh size) in the quarter part of plate as shown in Fig.5.1. The maximum displacement and stresses at a particular point as shown in Fig.5.2 are found out by using developed program for sinusoidal loading and uniformly distributed loading as shown in Fig.5.3 with different boundary conditions as shown in Fig.5.4.

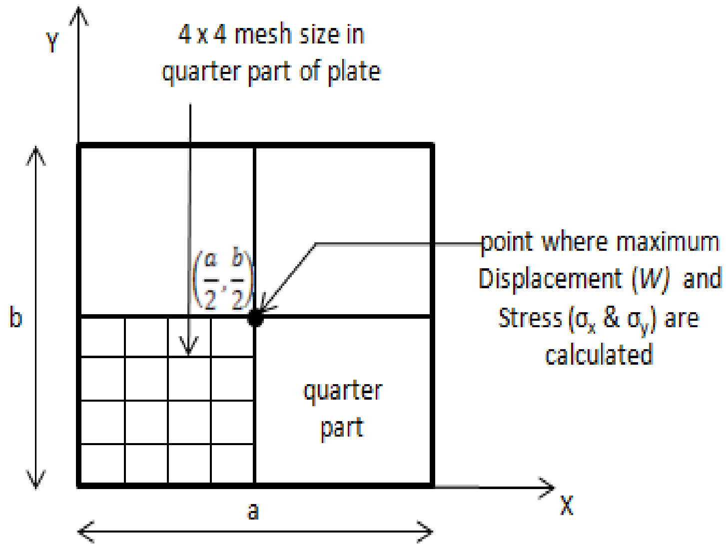

Figure 5.1: (4x4) Meshing in quarter part of plate

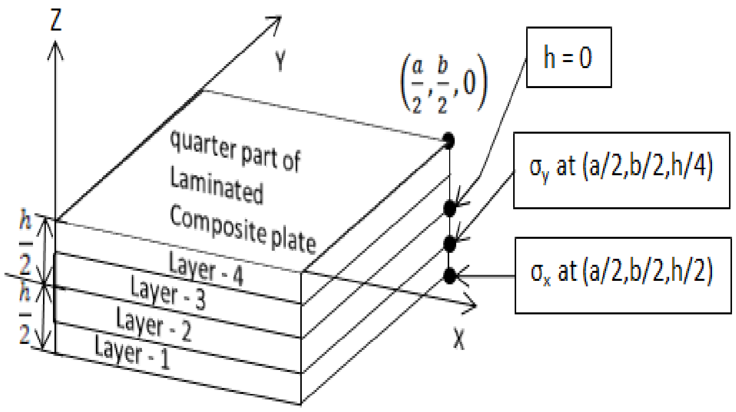

Figure 5.2: Sectional view of quarter part of plate

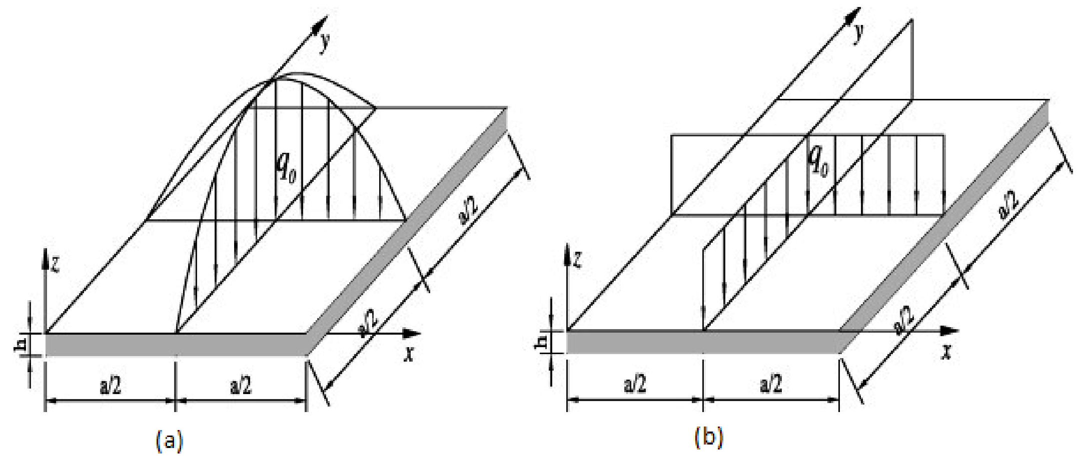

Figure 5.3: Loading conditions: (a) sinusoidal loading and (b) uniformly distributed loading

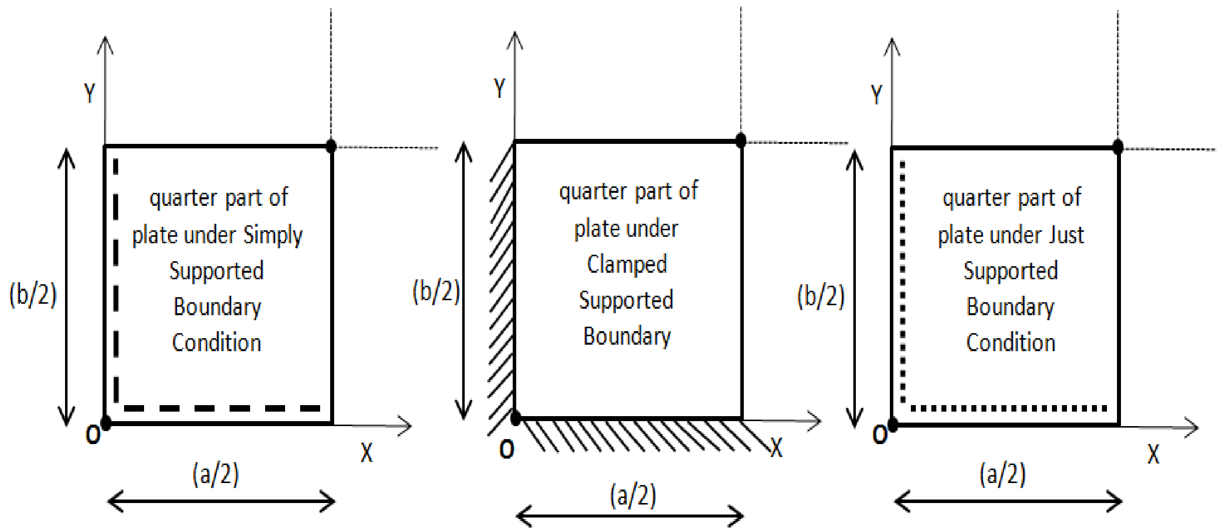

Figure 5.4: Support conditions for quarter part of plate

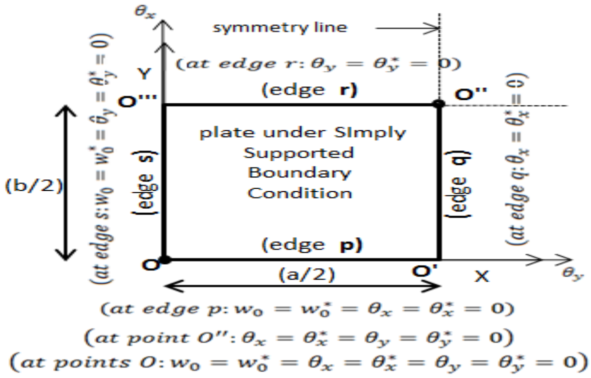

Figure 5.5: quarter part of plate under Simply supported boundary condition for model-1

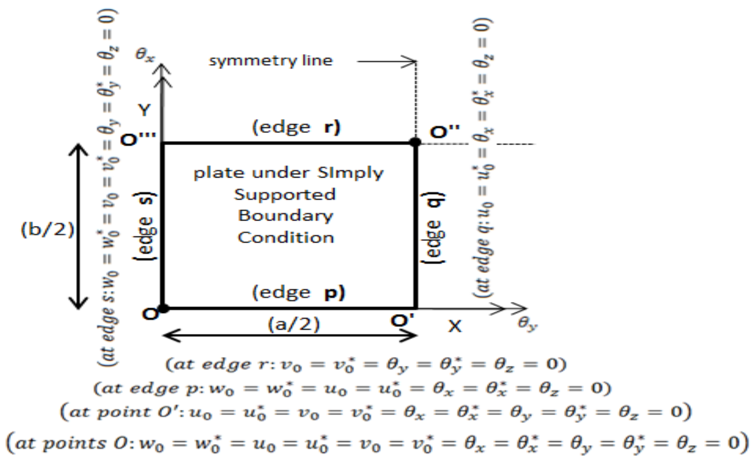

Figure 5.6: quarter part of plate under Simply supported boundary condition for model-2

Boundary condition: simply supported on four side

For displacement model-1(Fig.5.5):

$W_0 = W_0^* = \theta_y = \theta_y^* = 0$ at X=0 and X=a

$W_0 = W_0^* = \theta_x = \theta_x^* = 0$ at Y=0 and Y=a

For displacement model-2(Fig.5.6):

$W_0 = W_0^* = V_0 = V_0^* = \theta_y = \theta_y^* = \theta_z = 0$ at X=0 and X=a

$W_0 = W_0^* = U_0 = U_0^* = \theta_x = \theta_x^* = \theta_z = 0$ at Y=0 and Y=a

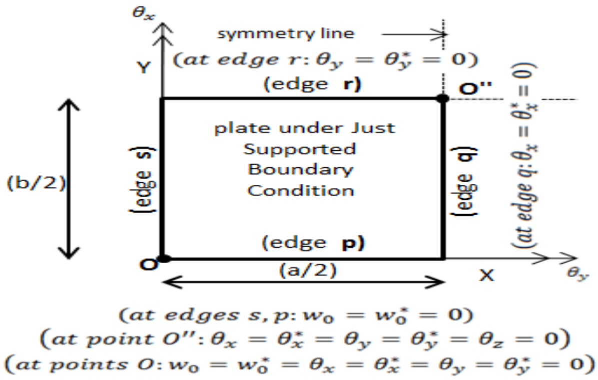

Figure 5.7: quarter part of plate under Just supported boundary condition for model-1

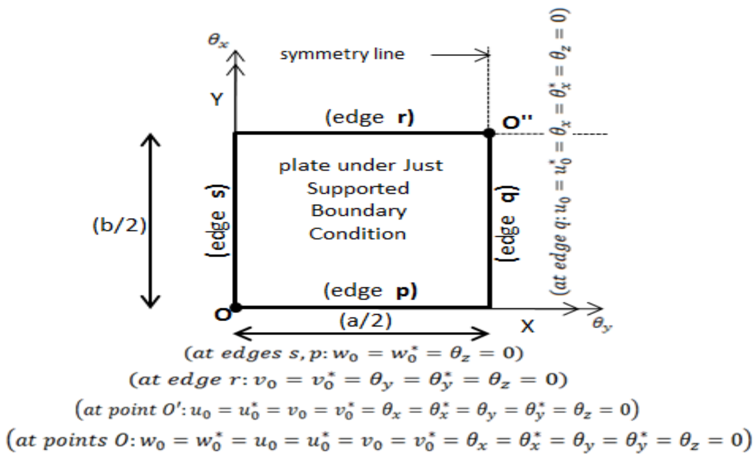

Figure 5.8: quarter part of plate under Just supported boundary condition for model-2

Boundary condition: just supported on four side

For displacement model-1(Fig.5.7):

$W_0 = W_0^* = 0$ at X=0 and X=a

$W_0 = W_0^* = 0$ at Y=0 and Y=a

For displacement model-2(Fig.5.8):

$W_0 = W_0^* = \theta_z = 0$ at X=0 and X=a

$W_0 = W_0^* = \theta_z = 0$ at Y=0 and Y=a

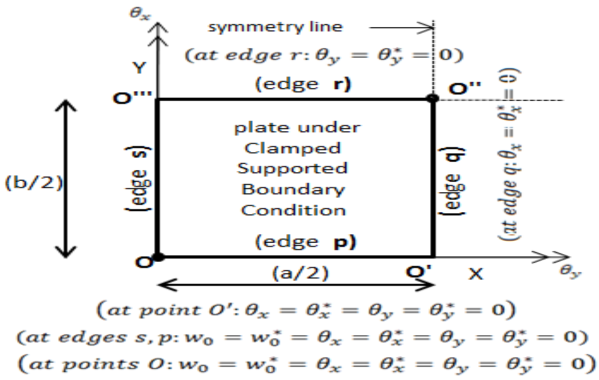

Figure 5.9: quarter part of plate under Clamped supported boundary condition for model-1

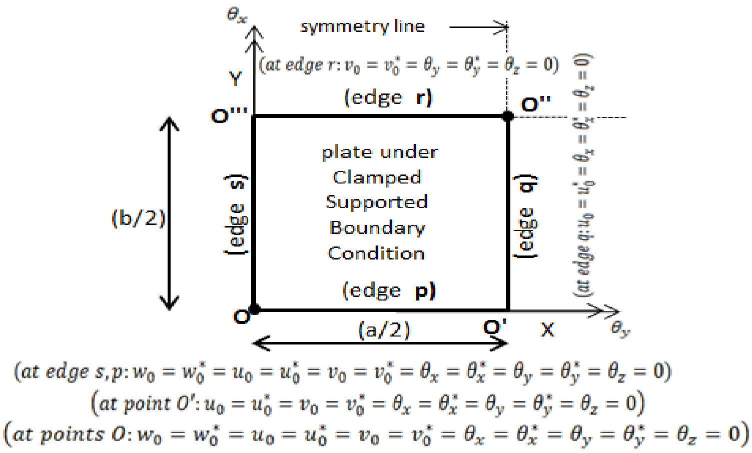

Figure 5.10: quarter part of plate under Clamped supported boundary condition for model-2

Boundary condition: clamped supported on four side

For displacement model-1(Fig.5.9):

$W_0 = W_0^* = \theta_x = \theta_x^* = \theta_y = \theta_y^* = 0$ at X=0 and X=a

$W_0 = W_0^* = \theta_x = \theta_x^* = \theta_y = \theta_y^* = 0$ at Y=0 and Y=a

For displacement model-2(Fig.5.10):

$W_0 = W_0^* = U_0 = U_0^* = V_0 = V_0^* = \theta_x = \theta_x^* = \theta_y = \theta_y^* = \theta_z = 0$ at X=0 and X=a

$W_0 = W_0^* = U_0 = U_0^* = V_0 = V_0^* = \theta_x = \theta_x^* = \theta_y = \theta_y^* = \theta_z = 0$ at Y=0 and Y=a

The numerical results of displacement due to different loadings are presented in nondimensional form as defined follows,

$$m_1 = \frac{100E_2h^3}{P_0a^4} \tag{5.1}$$

Non-dimensional displacement($\overline{W}$)= m_1 * Actual Displacement(W)

The non-dimensional stresses are defined as follows,

$$Non-dimensional \quad stresses(\overline{\sigma}_x, \overline{\sigma}_y, \overline{\tau}_{xy}) = \frac{h^2}{P_0a^2} \quad * \quad ActualStresses(\sigma_x, \sigma_y, \tau_{xy}) \tag{5.2}$$

Unless otherwise stated the displacements($\overline{W}$) is calculated at ($\frac{a}{2}$,$\frac{b}{2}$,0)

The stresses($\overline{\sigma}_x$) are calculated at ($\frac{a}{2}$,$\frac{b}{2}$,$\frac{h}{2}$)

The stresses($\overline{\sigma}_y$) are calculated at ($\frac{a}{2}$,$\frac{b}{2}$,$\frac{h}{4}$)

In solving of problems following material properties sets are considered,

Material Set-1;

$$\frac{E_1}{E_2} = \frac{E_1}{E_3} = 25, E_2 = E_3 = 10^6, \frac{G_{12}}{E_2} = \frac{G_{13}}{E_3} = 0.5, \frac{G_{23}}{E_3} = 0.2, \nu_{12} = \nu_{23} = \nu_{13} = 0.25 \tag{5.3}$$

Material Set-2;

$$\frac{E_1}{E_2} = 40, \frac{G_{12}}{E_2} = 0.6, \frac{G_{23}}{E_2} = 0.5, E_2 = E_3 = 10^6, G_{13} = G_{12}, \nu_{12} = \nu_{23} = \nu_{13} = 0.25 \tag{5.4}$$

Material Set-3;

$$FaceSheets \qquad \frac{E_1}{E_2} = \frac{E_1}{E_3} = 25, \frac{G_{12}}{E_2} = \frac{G_{13}}{E_3} = 0.5, \frac{G_{23}}{E_3} = 0.2, \nu_{12} = \nu_{23} = \nu_{13} = 0.25 \tag{5.5}$$

$$Core \quad \frac{E_1}{E_3} = \frac{E_2}{E_3} = 0.08, E_3 = 0.5{*}10^6, \frac{G_{13}}{E_3} = \frac{G_{23}}{E_3} = 0.12, \nu_{12} = 0.25, \nu_{23} = \nu_{13} = 0.02 \tag{5.6}$$

Material Set-4;

$$E = 210 * 10^3, G = 80769.23, \nu = 0.3 \tag{5.7}$$

5.3 Comparison of Results

The developed finite element formulation is validated and assessed for its performance considering following cases of Laminated plate with different type of orientation scheme of lamina as shown in Fig.5.11 and 5.12.

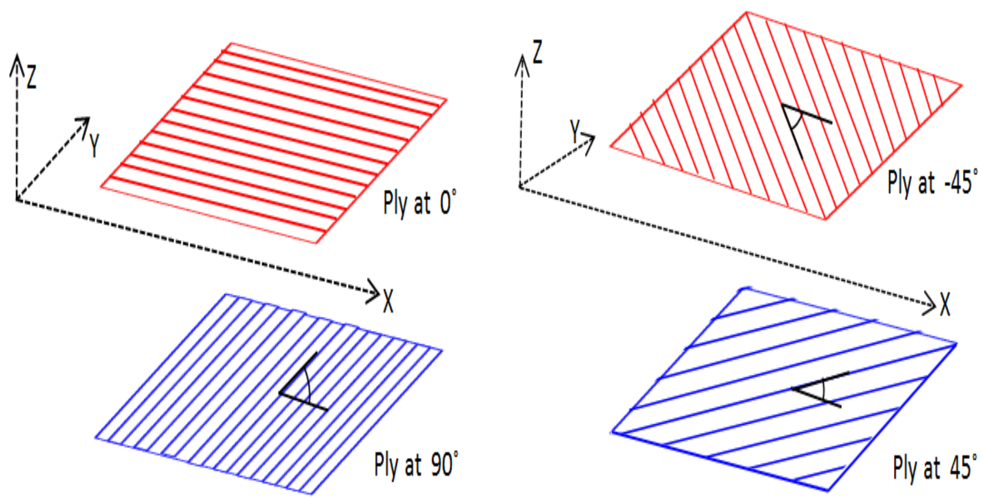

Figure 5.11: Orientation scheme of Lamina : (a) Cross Ply (b) Angle Ply

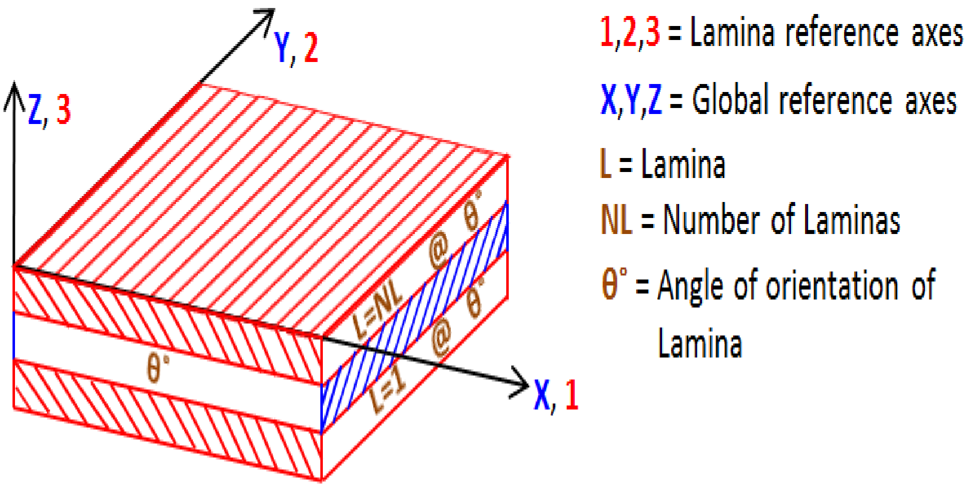

Figure 5.12: Cross Ply - Laminated Composite Plate

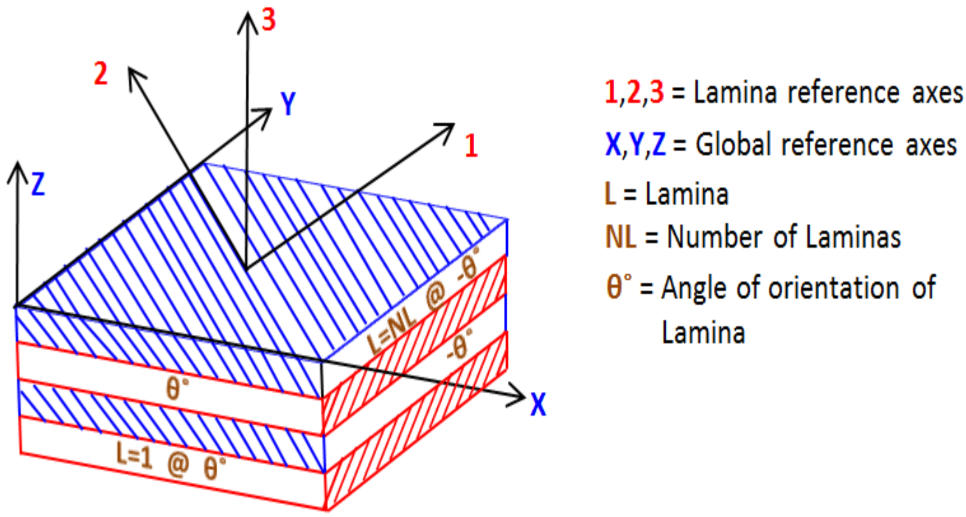

Figure 5.13: Angle Ply - Laminated Composite Plate

Convergence Study:

A simply supported square laminated cross-ply plate (0/90/90/0) made up of four equally thick laminas (Material set-1) subjected to a sinusoidal transverse load is considered for convergence study and results are presented in Table 5.1.

Table 5.1: Convergence of deflections and stresses in a simply supported four layer cross-ply (0/90/90/0) square laminate under sinusoidal transverse load (hi = h/4, i = 1 , . . . , 4 and a/h = 10)

Mesh Size	**Source**	$\overline{W}$	$\overline{\sigma}_x$	$\overline{\sigma}_y$
1x1	Present Model 1	0.5749	0.4653	0.2690
2x2		0.6401	0.5072	0.3030
3x3		0.6411	0.5147	0.3074
4x4		0.6409	0.5175	0.3090
5x5		0.6408	0.5187	0.3097
6x6		0.6408	0.5187	0.3097
1x1	Present Model 2	0.6460	0.5342	0.3635
2x2		0.7156	0.5614	0.3924
3x3		0.7176	0.5616	0.3917
4x4		0.7179	0.5611	0.3912
5x5		0.7179	0.5608	0.3908
6x6		0.7179	0.5605	0.3906
1x1	Higher order theory [8]	0.72402	0.5701	0.3944
2x2		0.7185	0.5676	0.3948
3x3		0.71809	0.5635	0.3924
4x4		0.71801	0.5619	0.3914
	Elasticity [13]	0.7370	0.5590	0.4010

In above example convergence of results is studied by descritizing quarter part of plate in different scheme of meshing. As from study it is concluded that at 4x4 meshing scheme convergence is obtained. Therefore further in solving of all problems uniform 4x4 meshing is considered.

Case : 1

The study of numerical problems are carried out for the laminated plate with equal layer thickness as well as also variation of thickness is considered. In this case simply supported boundary condition is considered along all four edges, where laminated plate is subjected to sinusoidal load. The results of solved problem for different a/h ratios and material sets are presented in tabular form and compared with available results in literature. Schematic diagram of solved problem of laminated plate is shown in Fig.5.12.

Table 5.2 shows the numerical values of nondimensional displacements and stresses for simply supported laminate under sinusoidal loading. The results are obtained for different width-to-thickness ratios. The obtained solutions are compared with available solutions based on higher order shear deformation theory (HOSDT) and first order shear deformation theory (FOSDT) in literature. The comparisons show that the solutions given by displacement model-1 and 2 are fairly close to higher order theory model -2 and 3.

Table 5.2: Comparison of non-dimensional deflection and stresses in a four- equal layer thickness (0/90/90/0) square simply supported laminate under sinusoidal load using Material set-1

a/h	**Source**	$\overline{W}$	$\overline{\sigma}_x$	$\overline{\sigma}_y$
4	Present Model 1	1.6870	0.4900	0.3726
	Present Model 2	1.8737	0.7076	0.6192
	Higher order theory model-1 [7]	1.6813	0.4111	0.5951
	Higher order theory model-2 [7]	1.8688	0.7306	0.6506
	Higher order theory model-3 [7]	1.8750	0.7163	0.6250
	Higher order theory [8]	1.8744	0.7163	0.6250
	Mindlin Theory [8]	1.7054	0.4121	0.5829
	FSDT [11]	1.7100	0.4059	0.5765
	3D-FEM [12]	0.5061	0.5393	0.3043
10	Present Model 1	0.6409	0.5175	0.3011
	Present Model 2	0.7178	0.5611	0.3912
	Higher order theory model-1 [7]	0.6388	0.5067	0.3721
	Higher order theory model-2 [7]	0.6961	0.5730	0.4038
	Higher order theory model-3 [7]	0.7185	0.5676	0.3948
	Higher order theory [8]	0.7185	0.5676	0.3948
	Mindlin Theory [8]	0.6613	0.5063	0.3653
	FSDT [11]	0.6682	0.4989	0.3615
	3D-FEM [12]	0.7147	0.5456	0.3888
20	Present Model 1	0.4843	0.5297	0.2802
	Present Model 2	0.5072	0.5440	0.3055
	Higher order theory model-1 [7]	0.4674	0.5363	0.3018
	Higher order theory model-2 [7]	0.4840	0.5535	0.3120
	Higher order theory model-3 [7]	0.5076	0.5503	0.3083
	FSDT [11]	0.4912	0.5273	0.2957
	3D-FEM [12]	1.8937	0.6651	0.6322
100	Present Model 1	0.4334	0.5350	0.2681
	Present Model 2	0.4326	0.5351	0.2676
	Higher order theory model-1 [7]	0.4097	0.5459	0.2742
	Higher order theory model-2 [7]	0.4104	0.5466	0.2747
	Higher order theory model-3 [7]	0.4346	0.5442	0.2734
	Higher order theory [8]	0.4346	0.5442	0.2734
	Mindlin Theory [8]	0.4322	0.5416	0.2704
	FSDT [11]	0.4337	0.5382	0.2705

In Table 5.3 results are presented for rectangular laminate and property of laminate is given by material set-1. The result are obtained for different a/h ratios. The present numerical results are compared with the existing three dimensional elasticity solutions and other higher order theory models. From comparison study the percentage difference between present results and 3-D solutions are, for thick plate (a/h=10): present model-1 = 8.78% , model-2 = 5.82%. For moderately thin plate (a/h=50): present model-1=0.63% , model-2=2.57%. For thin plate (a/h=100): present model-1 =0.27% , model-2 = 3.28%. It is clear that Present Model-1 make better predictions of displacements for moderately thin plate and thin plate, whereas present model-2 make better predictions of displacements for thick plate.

Table 5.3: Comparison of non-dimensional deflection and stresses in a three-equal layer thickness (0/90/0) rectangular(b=3a) simply supported laminate under $10kN/cm^2$ sinusoidal load using material set-1

a/h	**Source**	$\overline{W}$	$\overline{\sigma}_x$	$\overline{\sigma}_y$
10	Present Model 1	0.8383	0.6280	0.0385
	Present Model 2	0.8655	0.7163	0.4011
	Higher order theory model-1 [7]	0.7731	0.6361	0.0382
	Higher order theory model-2 [7]	0.8379	0.7310	0.0409
	Higher order theory model-3 [7]	0.8665	0.7249	0.0402
	Elasticity [11]	0.9190	0.7250	0.0435
50	Present Model 1	0.5167	0.6239	0.02514
	Present Model 2	0.5066	0.6110	0.02507
	Higher order theory model-1 [7]	0.4862	0.6316	0.0259
	Higher order theory model-2 [7]	0.4883	0.6344	0.0259
	Higher order theory model-3 [7]	0.5183	0.6340	0.0257
	Elasticity [11]	0.5200	0.6280	0.0259
100	Present Model 1	0.5066	0.6135	0.02469
	Present Model 2	0.4913	0.5877	0.02414
	Higher order theory model-1 [7]	0.4772	0.6307	0.0255
	Higher order theory model-2 [7]	0.4773	0.6308	0.0255
	Higher order theory model-3 [7]	0.5073	0.6304	0.0253
	Elasticity [11]	0.5080	0.6240	0.0253

In Table 5.4 solution of the square simply supported laminate under sinusoidal loading is presented. The obtained results are compared with the 3-D elasticity solution and closed form solution. The presented results of model-1 are in good agreement with closed form solution(CFS) with maximum error less than 3.42% and of model-2 are fairly close to the 3-D elasticity solution with maximum error less than 5.1%.

Table 5.4: Comparison of non-dimensional maximum deflection and stresses in a three-layer (0/90/0) of varying thickness ($t_1 = t_3 = t/4, t_2 = t/2$) square simply supported laminate under sinusoidal loading using material set-1

a/h	**Source**	$\overline{W}$	$\overline{\sigma}_x$	$\overline{\sigma}_y$
10	Present Model 1	6.4010	0.5072	0.3030
	Present Model 2	7.1548	0.5614	0.3924
	CFS(Closed Form Solution)[11]	6.6270	0.4960	0.3590
	3-DES [11]	7.4340	0.5990	0.4030
20	Present Model 1	4.8442	0.5194	0.2746
	Present Model 2	5.0444	0.5412	0.3024
	CFS(Closed Form Solution)[11]	4.9110	0.5240	0.2940
	3-DES [11]	5.1730	0.5430	0.3080
100	Present Model 1	4.3312	0.5234	0.2622
	Present Model 2	4.1615	0.5023	0.2481
	CFS(Closed Form Solution)[11]	4.3370	0.5350	0.2690
	3-DES [11]	4.3850	0.2710	0.0214

Deflection and stresses are compared in Table 5.5 for five layer cross ply square plate under sinusoidal loading. The results of present model-1 differ considerably by 1.82% from the CFS solution, while the results of present model-2 differ considerably by 12.44% from the 3-D elasticity solution, which is relatively more for the five-layer case compared to the three layer case shown in Table 5.4.

Table 5.5: Comparison of non-dimensional maximum deflection and stresses in a three-layer (0/90/0/90/0) of varied thickness ($t_1 = t_3 = t_3 = t/6, t_2 = t_2 = t/4$) square simply supported laminate under sinusoidal loading using material set-1

a/h	**Source**	$\overline{W}$	$\overline{\sigma}_x$	$\overline{\sigma}_y$
2	Present Model 1	47.4700	0.6780	0.5718
	Present Model 2	46.7700	0.9417	0.4114
	CFS(Closed Form Solution)[11]	48.3500	0.3910	0.5370
	3-DES [13]	53.4150	1.3320	1.0010
4	Present Model 1	15.6530	0.5527	0.4320
	Present Model 2	15.9098	0.6126	0.3876
	CFS(Closed Form Solution)[11]	15.6230	0.4250	0.4890
	3-DES [13]	18.6680	0.6850	0.6330
10	Present Model 1	6.1421	0.5237	0.3707
	Present Model 2	6.2569	0.5389	0.3289
	CFS(Closed Form Solution)[11]	6.2130	0.4880	0.4000
	3-DES [13]	6.8300	0.5450	0.4300
20	Present Model 1	4.7749	0.5239	0.3557
	Present Model 2	4.7855	0.5357	0.3021
	CFS(Closed Form Solution)[11]	4.7960	0.5241	0.3520
	3-DES [13]	4.9810	0.5220	0.3520
50	Present Model 1	4.3911	0.5244	0.3506
	Present Model 2	4.8927	0.5206	0.2820
	CFS(Closed Form Solution)[11]	4.390	0.5234	0.3490
	3-DES [13]	4.4510	0.5240	0.3500
100	Present Model 1	4.3273	0.5235	0.3492
	Present Model 2	4.1346	0.4981	0.2684
	CFS(Closed Form Solution)[11]	4.3320	0.5240	0.3500
	3-DES [13]	4.3770	0.5390	0.3600

The solution of a simply supported square laminated cross-ply plate made up of four equally thick laminas subjected to a sinusoidal load is considered. Numerical results are presented and compared in Table 5.6 and 5.7 for width-to-thickness ratios of 10 and 100. Convergence of deflection is studied using different meshing scheme in quarter part of plate.

Table 5.6: Comparison of deflections and stresses using convergence in a simply supported four layer cross-ply (0/90/90/0) square laminate under sinusoidal load for a/h = 10.

Mesh Size	**Source**	$\overline{W}$	$\overline{\sigma}_x$	$\overline{\sigma}_y$
1x1	Present Model 1	0.5749	0.4653	0.2690
2x2		0.6401	0.5072	0.3030
3x3		0.6411	0.5147	0.3074
4x4		0.6409	0.5175	0.3090
1x1	Present Model 2	0.6460	0.5342	0.3635
2x2		0.7156	0.5614	0.3924
3x3		0.7176	0.5616	0.3917
4x4		0.7179	0.5611	0.3912
1x1	Higher order theory [8]	0.72402	0.5701	0.3944
2x2		0.7185	0.5676	0.3948
3x3		0.71809	0.5635	0.3924
4x4		0.71801	0.5619	0.3914
	Elasticity [13]	0.7370	0.5590	0.4010

Table 5.7: Comparison of deflections and stresses using convergence in a simply supported four layer cross-ply (0/90/90/0) square laminate under sinusoidal load for a/h = 100.

Mesh Size	**Source**	$\overline{W}$	$\overline{\sigma}_x$	$\overline{\sigma}_y$
1x1	Present Model 1	0.2940	0.3222	0.1834
2x2		0.4332	0.5234	0.2622
3x3		0.4335	0.5320	0.2666
4x4		0.4334	0.5348	0.2681
1x1	Present Model 2	0.1356	0.1542	0.0752
2x2		0.4162	0.5023	0.2481
3x3		0.4299	0.5290	0.2634
4x4		0.4326	0.5351	0.2676
1x1	Higher order theory [8]	0.43659	0.5411	0.2718
2x2		0.4346	0.5442	0.2734
3x3		0.43443	0.5418	0.2723
4x4		0.43439	0.5406	0.2717
	Elasticity [13]	0.4347	0.5390	0.2710

In Table 5.8 a numerical results for a laminate made up of seven layers having variation in thickness according to the orientation of laminas. The comparative study shows that the present model-1 and 2 gives solution in good agreement with other higher order theories and Mindlin's plate theory.

Table 5.8: Comparison of non-dimensional maximum deflection and stresses in a seven-layer (0/90/0/90/0/90/0) thickness of ($h_0 = h/8, h_90 = h/6$) square simply supported laminate under sinusoidal loading using material set-1.

a/h	**Source**	$\overline{W}$	$\overline{\sigma}_x$	$\overline{\sigma}_y$
4	Present Model 1	1.5259	0.5876	0.1676
	Present Model 2	1.5281	0.6219	0.1959
	Higher order theory [8]	1.5334	0.6275	0.5530
	Mindlin Theory [8]	1.5341	0.4664	0.5092
10	Present Model 1	0.6078	0.5325	0.2141
	Present Model 2	0.6123	0.5451	0.2327
	Higher order theory [8]	0.6159	0.5494	0.4482
	Mindlin Theory [8]	0.6114	0.5159	0.4457
100	Present Model 1	0.4326	0.5236	0.2181
	Present Model 2	0.4130	0.4971	0.2068
	Higher order theory [8]	0.4332	0.5439	0.4084
	Mindlin Theory [8]	0.4315	0.5412	0.4060

In Table 5.9 a simply-supported square cross-ply plate under sinusoidal load is considered for comparisons of maximum deflection and stress-resultants and to understand the behaviour of plate. The results of presented displacement model-2 are in good agreement with other higher order models than displacement model-1.

Table 5.9: Maximum deflection and stress resultants for a simply-supported unsymmetric cross-ply (0/90) square plate under sinusoidal load using material set-1.

a/h	**Source**	$\overline{W}$	$\overline{\sigma}_x$	$\overline{\sigma}_y$
4	Present Model 1	0.1468	0.7245	0.0456
	Present Model 2	0.2020	0.7899	0.1029
	Kant and Pandya [9]	0.2055	0.8056	0.0969
	Kant and Pandya [9]	0.2020	0.8000	0.1038
10	Present Model 1	0.0602	0.5688	0.0298
	Present Model 2	0.1219	0.7286	0.0877
	Kant and Pandya [9]	0.1224	0.7390	0.0871
	Kant and Pandya [9]	0.1220	0.7367	0.0884

In Table 5.10 solutions are presented for a simply supported square isotropic plate subjected to sinusoidal load. The results of both present models are in good agreement with Trigonometric shear deformation theory(TSDT).

Table 5.10: Comparison of non-dimensional maximum deflection and stresses for square isotropic simply supported plate under sinusoidal loading using material set-4.

a/h	**Source**	$\overline{\overline{W}}$	$\overline{\sigma}_x$	$\overline{\sigma}_y$
0.1	Present Model 1	2.9410	0.2004	0.2004
	Present Model 2	2.9410	0.2004	0.2004
	TSDT [16]	2.9420	0.3070	0.3070

In Table 5.11 solution for a simply supported three-layered symmetric cross-ply square plate under sinusoidal transverse load is presented. The numerical results of maximum displacements are compared with the higher order refined theory. The results clearly show that the values obtained using Model-2 are in close agreement for all a/h ratios. Whereas Model-1 under predicts deflection by maximum error of 3.87% for higher order refined theory. Also present model-1 gives results in good agreement with closed form solution and FEM solution.

Table 5.11: Comparison of nondimensionalized deflections and stresses in a three-layer simply supported square plate (0/90/0) under sinusoidal transverse load using material set-1.

a/h	**Source**	$\overline{W}$	$\overline{\sigma}_x$	$\overline{\sigma}_y$
2	Present Model 1	5.4029	0.4999	0.3661
	Present Model 2	4.9023	1.1352	0.5346
	Higher order refined theory-1 [10]	4.9147	1.1355	0.5356
	Higher order refined theory-2 [10]	5.2158	1.0912	0.6334
4	Present Model 1	1.8974	0.4933	0.4258
	Present Model 2	1.8966	0.7672	0.4957
	Higher order refined theory-1 [10]	1.8948	0.7648	0.4939
	Higher order refined theory-2 [10]	1.9261	0.7670	0.5079
10	Present Model 1	0.6969	0.5226	0.2541
	Present Model 2	0.7166	0.5861	0.2717
	CFS(Closed Form Solution)[11]	0.6690	0.4990	0.2470
	FEM 4Q8-R [11]	0.6690	0.5100	0.2520
	Higher order refined theory-1 [10]	0.7151	0.5836	0.2705
	Higher order refined theory-2 [10]	0.7176	0.5847	0.2712
20	Present Model 1	0.4964	0.5291	0.1988
	Present Model 2	0.5024	0.5490	0.2045
	CFS(Closed Form Solution)[11]	0.4920	0.5170	0.1940
	FEM 4Q8-R [11]	0.4920	0.5280	0.1280
	Higher order refined theory-1 [10]	0.5053	0.5504	0.2049
	Higher order refined theory-2 [10]	0.5058	0.5507	0.2050
50	Present Model 1	0.4416	0.5339	0.1817
	Present Model 2	0.4416	0.5389	0.1825
	Higher order refined theory-1 [10]	0.4432	0.5406	0.1838
	Higher order refined theory-2 [10]	0.4433	0.5406	0.1838
100	Present Model 1	0.4338	0.5360	0.1796
	Present Model 2	0.4162	0.5363	0.1785
	CFS(Closed Form Solution)[11]	0.4340	0.524	0.176
	FEM 4Q8-R [11]	0.4340	0.535	0.179
	Higher order refined theory-1 [10]	0.4343	0.5392	0.1807
	Higher order refined theory-2 [10]	0.4343	0.5392	0.1807

Case : 2

The study of numerical problems are carried out for the laminated plate with equal layer thickness as well as also variation of thickness is considered. In this case simply supported boundary condition is considered, where laminated plate is subjected to uniformly distributed load. Here results of solved problem for different a/h ratios and material sets are presented in following tables and compared with available results in literatures.Schematic diagram of solved problem of laminated plate is shown in Fig.5.13.

Similarly the solution for a simply supported square laminated cross-ply plate made up of three equal thickness of laminas is presented in Table 5.12. The results of deflections and stresses are in good agreement with other higher order theory solutions.

Table 5.12: Comparison of non-dimensional maximum deflection and stresses in a three-layer (0/90/0) square simply supported laminate under uniformly distributed loading using material set-1.

a/h	**Source**	$\overline{W}$	$\overline{\sigma}_x$	$\overline{\sigma}_y$
4	Present Model 1	2.8830	0.7189	0.6383
	Present Model 2	2.9134	1.1110	0.7358
	Higher order theory [8]	2.8765	1.1094	0.7244
	Mindlin Theory [8]	2.6559	0.6650	0.6625
5	Present Model 1	2.1419	0.7444	0.5506
	Present Model 2	2.2019	1.0085	0.6131
	3D-FEM [12]	2.3218	1.0215	0.6629
10	Present Model 1	1.0631	0.7716	0.3185
	Present Model 2	1.0977	0.8691	0.3427
	Higher order theory [8]	1.0968	0.8739	0.3945
	Mindlin Theory [8]	1.0211	0.7851	0.3844
	3D-FEM [12]	1.1541	0.8709	0.3621
20	Present Model 1	0.7702	0.7994	0.2278
	Present Model 2	0.7808	0.8252	0.2323
	3D-FEM [12]	0.7951	0.8247	0.2391
100	Present Model 1	0.6712	0.7934	0.2015
	Present Model 2	0.6555	0.7740	0.2286
	Higher order theory [8]	0.6713	0.8191	0.3134
	Mindlin Theory [8]	0.6701	0.8190	0.2923

In Table 5.13 a simply-supported square cross-ply plate under uniform transverse load is considered for comparisons of maximum deflection and stress-resultants and to understand the behaviour of plate. The results of present model-2 are in good agreement with other higher order models. While results of present model-1 shows max difference of 43.82% in central deflections by comparing those to the other models, which is increase with increase of a/h ratio. Further to understand the behaviour of laminate made up by square angle ply the numerical results are presented in Table 5.14. For angle ply at lower a/h ratio model-1 predicts deflections more accurately, whereas at higher a/h ratio model-2 predicts deflections more accurately.

Table 5.13: Maximum deflection and stress resultants for a simply-supported unsymmetric cross-ply (0/90) square plate under uniformly distributed load using material set-2.

a/h	**Source**	$\overline{\overline{W}}$
5	Present Model 1	0.10830
	Present Model 2	0.19330
	Kant and Pandya [9]	0.19279
	Kant and Pandya [9]	0.19072
10	Present Model 1	0.06072
	Present Model 2	0.14180
	Kant and Pandya [9]	0.14190
	Kant and Pandya [9]	0.14150
40	Present Model 1	0.04574
	Present Model 2	0.12550
	Kant and Pandya [9]	0.12598
	Kant and Pandya [9]	0.12595

Table 5.14: Maximum deflection and stress resultants for a simply-supported unsymmetric angle-ply (15/-15) square plate under uniformly distributed load using material set-2.

a/h	**Source**	$\overline{W}$
5	Present Model 1	0.12260
	Present Model 2	0.20900
	Kant and Pandya [9]	0.15403
	Kant and Pandya [9]	0.15192
10	Present Model 1	0.05858
	Present Model 2	0.05528
	Kant and Pandya [9]	0.09187
	Kant and Pandya [9]	0.09142
40	Present Model 1	0.03662
	Present Model 2	0.05329
	Kant and Pandya [9]	0.07154
	Kant and Pandya [9]	0.07150

Table 5.15 shows a results of displacements and stresses of a simply supported orthotropic square plate with length a = 20 cm and thickness t subjected to a uniformly distributed load q = 100 kN/m^2. Present model-2 gives values in good agreement, whereas present model-1 gives values in reasonable agreement in comparing those with 3D-FEM solution for thin plate t/a=0.01, moderately thick plate t/a=0.1 and thick plate t/a=0.2.

Table 5.15: Comparison study of deflections and stresses for a orthotropic simply supported square 20 cm length plate under 100 kN/m^2 uniformly distributed loading using material set-1.

t/a	**Source**	$\overline{W}$	$\overline{\sigma}_x$	$\overline{\sigma}_y$
0.05	Present Model 1	0.8430	0.8105	0.0328
	Present Model 2	0.7264	0.7983	0.0275
	3D-FEM [12]	0.7255	0.7961	0.0277
0.1	Present Model 1	1.3882	0.8740	0.0572
	Present Model 2	0.9512	0.8258	0.0355
	3D-FEM [12]	0.9478	0.8227	0.0370
0.2	Present Model 1	3.1669	1.0090	0.1325
	Present Model 2	1.7991	0.9268	0.0615
	3D-FEM [12]	1.7783	0.9234	0.0667

Further comparison study of obtained central displacements and stresses for a simply supported square laminate with varying number of stacks of lamina subjected to uniformly distributed load is carried out. The results of laminated plates made up of four and five equal thickness stack of laminas for different t/a ratios are presented in Table 5.16 and 5.17 respectively. From comparison study it is clear that from present models, model-2 predicts accurate results in agreement with 3D-FEM solutions. Whereas results of present model-1 are differs for four layers: by 11.85%, five layers: by 9.19%.

Table 5.16: Comparison study of nondimensionalized deflections and stresses for a simply supported square three layer (0/90/90/0) plate under uniformly distributed load using material set-1.

t/a	**Source**	$\overline{W}$	$\overline{\sigma}_x$	$\overline{\sigma}_y$
0.05	Present Model 1	0.7563	0.8057	0.3763
	Present Model 2	0.7950	0.8245	0.4123
	3D-FEM [12]	0.8029	0.8228	0.4168
0.1	Present Model 1	0.9842	0.7783	0.4266
	Present Model 2	1.1149	0.8316	0.5481
	3D-FEM [12]	1.1401	0.8280	0.5617
0.2	Present Model 1	1.8769	0.7329	0.5215
	Present Model 2	2.1829	0.9142	0.8293
	3D-FEM [12]	2.2383	0.9080	0.8610

Table 5.17: Comparison study of nondimensionalized deflections and stresses for a simply supported square three layer (0/90/90/90/0) plate under uniformly distributed load using material set-1.

t/a	**Source**	$\overline{W}$	$\overline{\sigma}_x$	$\overline{\sigma}_y$
0.05	Present Model 1	0.7527	0.8146	0.3038
	Present Model 2	0.7893	0.8149	0.3406
	3D-FEM [12]	0.7794	0.8207	0.4870
0.1	Present Model 1	0.9591	0.8003	0.3030
	Present Model 2	1.0790	0.7943	0.4175
	3D-FEM [12]	1.0576	0.8201	0.5605
0.2	Present Model 1	1.7920	0.7799	0.2916
	Present Model 2	2.0705	0.8235	0.5463
	3D-FEM [12]	2.1044	0.8995	0.7386

Case : 3

The study of numerical problem is carried out for the sandwich laminated plate with different material properties of face sheet and the core portion of laminate. In this case simply supported boundary condition is considered, where laminated plate is subjected to sinusoidal load. Here results of solved problem for different a/h ratios are presented in Table 5.18 and compared with available results in literatures.Schematic diagram of solved problem of sandwich laminated plate is shown in Fig.5.13.

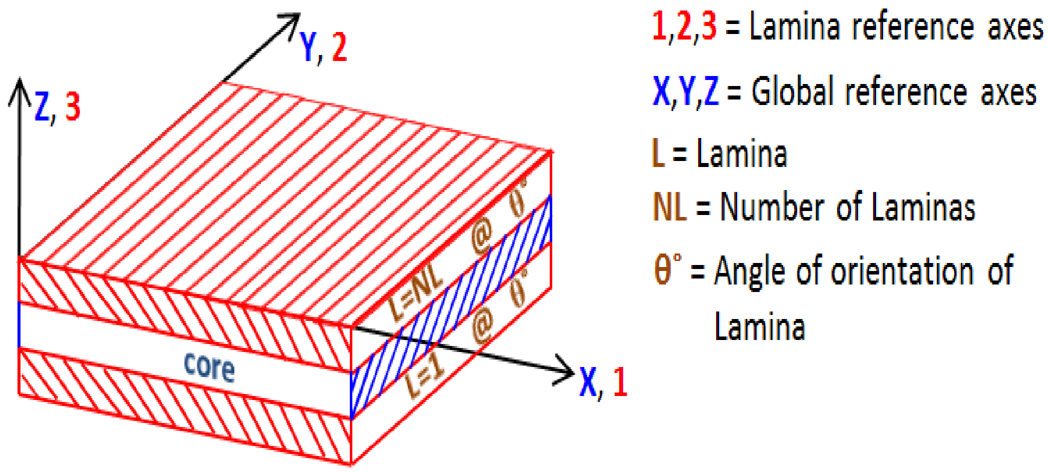

Figure 5.14: Sandwich laminated composite plate

In Table 5.18 numerical results of transverse displacement and in-plane stresses for various aspect ratios (a/h) are presented for a simply supported three-layered symmetric square sandwich plate with the thickness of each face sheet equal to h/10 is considered. Form comparative study it is clear that both displacement model-1 and 2 give sufficient accurate results for displacement and stresses.

Table 5.18: Comparison of nondimensionalized deflections and stresses in a three-layer simply supported square sandwich plate (0/core/0) under sinusoidal transverse load using material set-3.

a/h	Source	$\overline{W}$	$\overline{\sigma}_x$	$\overline{\sigma}_y$
4	Present Model 1	7.3272	1.3651	0.2779
	Present Model 2	7.0566	1.5162	0.2648
	Higher order redefine theory-1 [10]	7.0551	1.5137	0.2648
	Higher order redefine theory-2 [10]	7.1539	1.5030	0.2391
10	Present Model 1	2.1471	1.1199	0.1128
	Present Model 2	2.0795	1.1539	0.1100
	Higher order redefine theory-1 [10]	2.0798	1.1523	0.1100
	Higher order redefine theory-2 [10]	2.0848	1.1495	0.1042
20	Present Model 1	1.2119	1.0971	0.0709
	Present Model 2	1.1930	1.1124	0.0704
	Higher order redefine theory-1 [10]	1.1933	1.1110	0.0705
	Higher order redefine theory-2 [10]	1.1939	1.1091	0.0682
50	Present Model 1	0.9327	1.0920	0.0576
	Present Model 2	0.9288	1.1007	0.0575
	Higher order redefine theory-1 [10]	0.9296	1.1005	0.0578
	Higher order redefine theory-2 [10]	0.9294	1.0989	0.0566
100	Present Model 1	0.8921	1.0913	0.0556
	Present Model 2	0.8892	1.0958	0.0553
	Higher order redefine theory-1 [10]	0.8913	1.09901	0.0560
	Higher order redefine theory-2 [10]	0.8910	1.0975	0.0549

Case : 4

The study of numerical problems are carried out for the laminated plate with equal layer thickness as well as also variation of thickness is considered. In this case just supported boundary condition is considered at all four edges, where laminated plate is subjected to sinusoidal or uniformly distributed load. Here results of solved problem for different a/h ratios and material sets are presented in following tables and compared with available results in literatures.

In Table 5.19 and 5.20 solutions are presented for a just supported square laminated plate having seven stacks of lamina and three stacks of lamina respectively. The results of laminate having seven layer of lamina with unequal thickness for preset model-1 and 2 are overestimated by 75% in comparison with Mindlin's theory and higher order theory. Whereas the results of present model-1 and 2 presented in Table 5.20 are in good agreement in comparison with Mindlin's theory and other higher order theories.

Table 5.19: Comparison of non-dimensional maximum deflection and stresses in a seven-layer (0/90/0/90/0/90/0) cross ply (h_0=h/8, h_{90}=h/6) just supported square laminate under sinusoidal loading using material set-1.

a/h	**Source**	$\overline{W}$	$\overline{\sigma}_x$	$\overline{\sigma}_y$
4	Present Model 1	1.5257	0.6088	0.3052
	Present Model 2	1.5408	0.6283	0.3426
	Higher order theory [8]	1.5421	0.6475	0.5677
	Mindlin Theory [8]	1.5495	0.4824	0.5241
10	Present Model 1	1.0848	0.8382	0.5085
	Present Model 2	1.0841	0.8513	0.5147
	Higher order theory [8]	0.6196	0.5623	0.4562
	Mindlin Theory [8]	0.6188	0.5255	0.4531
100	Present Model 1	0.4337	0.5358	0.3125
	Present Model 2	0.4312	0.5341	0.3117
	Higher order theory [8]	0.4354	0.5595	0.4207
	Mindlin Theory [8]	0.4343	0.5581	0.4192

In Table 5.21 solutions are presented for a just supported square laminated plate made up of three stacks of laminas subjected to uniformly distributed load. The results of both present models are in good agreement in comparison with Mindlin's theory and higher order theory.

Table 5.20: Comparison of non-dimensional maximum deflection and stresses in a three-layer (0/90/0) just supported square laminate under sinusoidal loading using material set-1.

a/h	**Source**	$\overline{W}$	$\overline{\sigma}_x$	$\overline{\sigma}_y$
4	Present Model 1	1.9256	0.5088	0.4376
	Present Model 2	1.9246	0.7845	0.5062
	Higher order theory [8]	1.9359	0.8113	0.5179
	Mindlin Theory [8]	1.8157	0.4693	0.4986
10	Present Model 1	0.7031	0.5281	0.2556
	Present Model 2	0.7222	0.5908	0.2730
	Higher order theory [8]	0.7229	0.6078	0.2754
	Mindlin Theory [8]	0.6773	0.5316	0.2588
100	Present Model 1	0.4361	0.5367	0.1796
	Present Model 2	0.4340	0.5364	0.1785
	Higher order theory [8]	0.4362	0.5604	0.1871
	Mindlin Theory [8]	0.4345	0.5590	0.1858

Table 5.21: Comparison of non-dimensional maximum deflection and stresses in a three-layer (0/90/0) just supported square laminate under uniformly distributed load using material set-1.

a/h	**Source**	$\overline{W}$	$\overline{\sigma}_x$	$\overline{\sigma}_y$
4	Present Model 1	2.9382	0.7545	0.6660
	Present Model 2	2.9679	1.1315	0.7486
	Higher order theory [8]	2.9449	1.1681	0.7563
	Mindlin Theory [8]	2.7325	0.7063	0.7194
10	Present Model 1	1.0766	0.7927	0.3219
	Present Model 2	1.1107	0.8731	0.3401
	Higher order theory [8]	1.1094	0.9013	0.4296
	Mindlin Theory [8]	1.0375	0.8026	0.4161
100	Present Model 1	0.6734	0.8063	0.1936
	Present Model 2	0.6722	0.8079	0.2003
	Higher order theory [8]	0.6741	0.8480	0.3192
	Mindlin Theory [8]	0.6741	0.8519	0.3096

Case : 5

The study of numerical problems are carried out for the laminated plate with equal layer thickness as well as also variation of thickness is considered. In this case clamped supported boundary condition is considered at all four edges, where laminated plate is subjected to sinusoidal and uniformly distributed load. Here results of solved problem for different a/h ratios and material sets are presented in following tables and compared with available results in literatures.

In Table 5.22 and 5.23 solutions are presented for a clamped supported square laminated plate having seven stacks of lamina and three stacks of lamina respectively. The results of laminate having seven layer of lamina with unequal thickness for preset model-1 and 2 are overestimated by 55.19% in comparison with Mindlin's theory and higher order theory. Whereas the results of present model-1 and 2 presented in Table 5.23 are in good agreement in comparison with Mindlin's theory and other higher order theories.

Table 5.22: Comparison of non-dimensional maximum deflection and stresses in a seven-layer (0/90/0/90/0/90/0) cross ply (h_0=h/8, h_{90}=h/6) clamped supported square laminate under sinusoidal loading using material set-1.

a/h	**Source**	$\overline{W}$	$\overline{\sigma}_x$	$\overline{\sigma}_y$
4	Present Model 1	1.1741	0.2731	0.1093
	Present Model 2	1.1626	0.3159	0.1249
	Higher order theory [8]	1.1636	0.5126	0.5108
	Mindlin Theory [8]	1.1978	0.3253	0.2181
10	Present Model 1	0.4437	0.8382	0.5085
	Present Model 2	0.4419	0.3393	0.2242
	Higher order theory [8]	0.2893	0.3721	0.3367
	Mindlin Theory [8]	0.2859	0.2766	0.2942
100	Present Model 1	0.1092	0.2195	0.1247
	Present Model 2	0.1067	0.2175	0.1247
	Higher order theory [8]	0.1097	0.3379	0.2610
	Mindlin Theory [8]	0.1067	0.3297	0.2575

Table 5.23: Comparison of non-dimensional maximum deflection and stresses in a three-layer (0/90/0) clamped supported square laminate under sinusoidal loading using material set-1.

a/h	**Source**	$\overline{W}$	$\overline{\sigma}_x$	$\overline{\sigma}_y$
4	Present Model 1	1.4527	0.1559	0.0751
	Present Model 2	1.3129	0.4215	0.2801
	Higher order theory [8]	1.3146	0.6900	0.3754
	Mindlin Theory [8]	1.3376	0.2113	0.4735
10	Present Model 1	0.3720	0.2014	0.1670
	Present Model 2	0.3732	0.2634	0.1836
	Higher order theory [8]	0.3752	0.4909	0.2932
	Mindlin Theory [8]	0.3452	0.2784	0.2859
100	Present Model 1	0.1079	0.2166	0.0590
	Present Model 2	0.1064	0.2171	0.0605
	Higher order theory [8]	0.1081	0.3292	0.1352
	Mindlin Theory [8]	0.1054	0.3162	0.1390

In Table 5.24 solutions are presented for a just supported square laminated plate made up of three stacks of laminas subjected to uniformly distributed load. The results of both present models are in good agreement in comparison with Mindlin's theory and higher order theory.

Table 5.24: Comparison of non-dimensional maximum deflection and stresses in a three-layer (0/90/0) clamped supported square laminate under uniformly distributed load using material set-1.

a/h	**Source**	$\overline{W}$	$\overline{\sigma}_x$	$\overline{\sigma}_y$
4	Present Model 1	2.0997	0.2435	0.3211
	Present Model 2	1.9023	0.5158	0.3568
	Higher order theory [8]	1.8891	1.0306	0.5593
	Mindlin Theory [8]	1.9203	0.3106	0.7175
10	Present Model 1	0.5208	0.2574	0.1883
	Present Model 2	0.5213	0.3304	0.2051
	Higher order theory [8]	0.5247	0.7282	0.4596
	Mindlin Theory [8]	0.4829	0.3996	0.4600
100	Present Model 1	0.1419	0.2743	0.0405
	Present Model 2	0.1428	0.2765	0.0483
	Higher order theory [8]	0.1421	0.4537	0.2498
	Mindlin Theory [8]	0.1388	0.4365	0.2548

5.4 Summary

In this chapter Results of Static Analysis(free vibration analysis) of laminated composite plate are discussed. Nondimensional displacements and stresses are calculated using developed computer program. In solving of problems 4x4 uniform mesh size is considered based on convergence study. To validate the finite element formulation comparison study of obtained numerical results is carried out with available results reported in literature. The computer program developed under consideration of the present two displacement models gives sufficiently accurate results for laminated composite plate with varying width-to-thickness ratio, material anisotropy, stacking sequence, orientation of fibres and support conditions.

Chapter 6

Dynamic Analysis: Results and Discussion

6.1 General

The Finite Element Method is formulated based on A Higher Order Shear Deformation Theory as discussed in **Chapter 3** and employed for dynamic analysis of laminated composite plate with different support conditions, widh/thickness ratio, material anisotropy for symmetric plate and also the plate with cutout at centre. The computer program is developed for analysis of plate and nondimensionalized frequency is calculated. In order to establish the reliability and accuracy of the present finite element formulation various examples available in literature are solved and discussed.

6.2 Problem Discretization

In general unless otherwise stated for all problems considered, the plate is discretized with sixteen elements (8x8 mesh size) in the full part of plate as shown in Fig.6.1 and different boundary conditions are considered as shown in Fig.6.3.

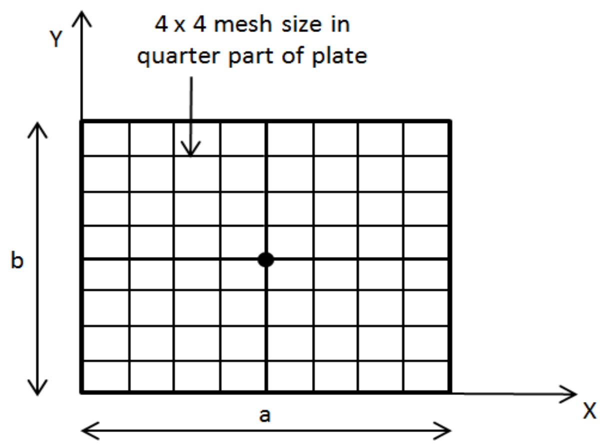

Figure 6.1: (8x8) Meshing in full part of plate

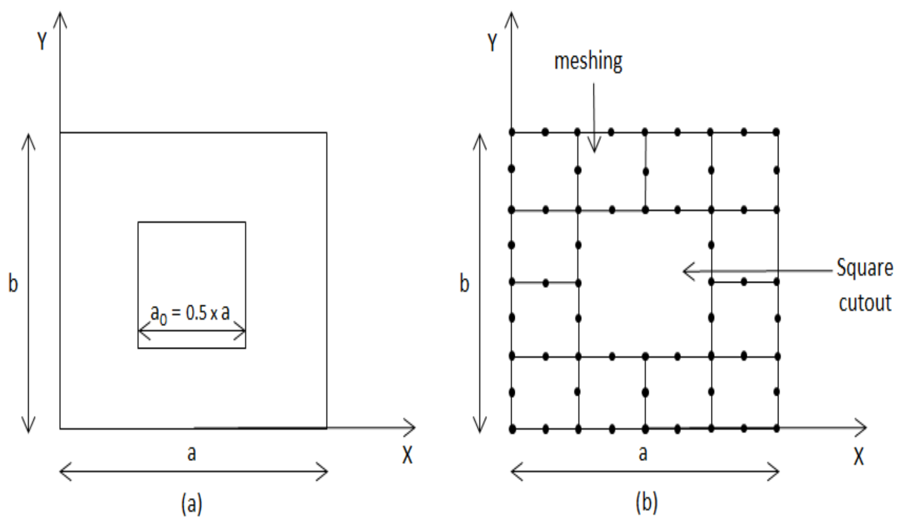

Figure 6.2: (a) Plate with square cutout at centre (b) Meshing of plate with square cutout at centre

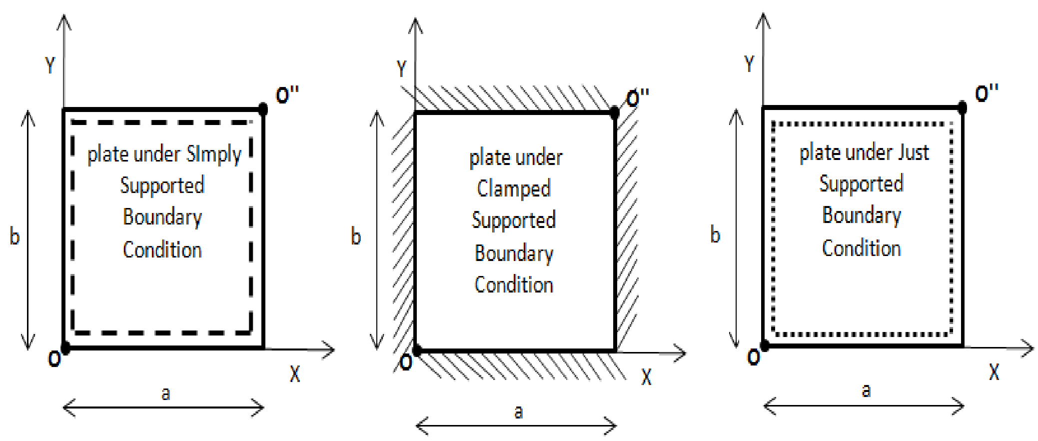

Figure 6.3: Support Conditons

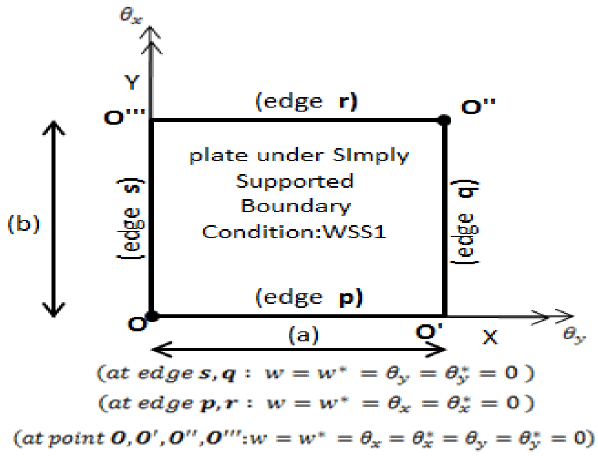

Figure 6.4: Plate under Simply supported boundary condition for model-1

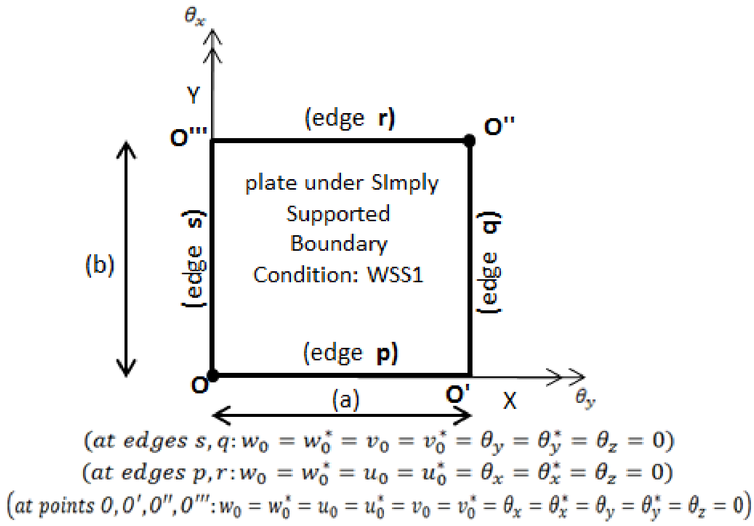

Figure 6.5: Plate under Simply supported boundary condition WSS1 for model-2

Boundary condition: simply supported on four side

For displacement model-1(Fig.6.4):

$W_0 = W_0^* = \theta_y = \theta_y^* = 0$ at X=0 and X=a

$W_0 = W_0^* = \theta_x = \theta_x^* = 0$ at Y=0 and Y=a

WSS-1 For displacement model-2(Fig.6.5):

$W_0 = W_0^* = V_0 = V_0^* = \theta_y = \theta_y^* = \theta_z = 0$ at X=0 and X=a

$W_0 = W_0^* = U_0 = U_0^* = \theta_x = \theta_x^* = \theta_z = 0$ at Y=0 and Y=a

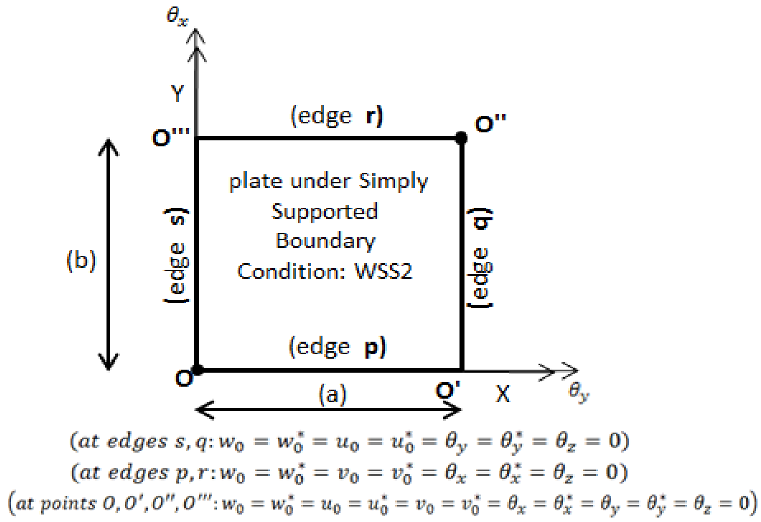

Figure 6.6: Plate under simply supported boundary condition WSS2 for model-2

WSS-2 For displacement model-2(Fig.6.6):

$W_0 = W_0^* = U_0 = U_0^* = \theta_y = \theta_y^* = \theta_z = 0$ at X=0 and X=a

$W_0 = W_0^* = V_0 = V_0^* = \theta_x = \theta_x^* = \theta_z = 0$ at Y=0 and Y=a

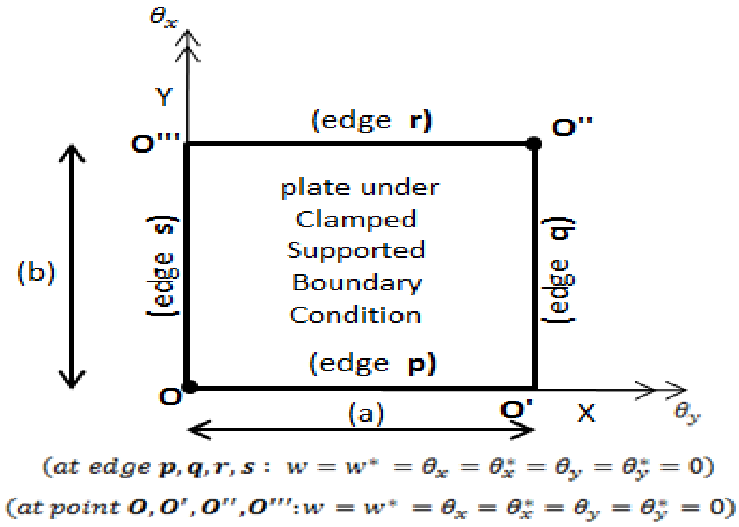

Figure 6.7: Plate under clamped supported boundary condition for model-1

Boundary condition: clamped supported on four side

For displacement model-1(Fig.6.7):

$W_0 = W_0^* = \theta_x = \theta_x^* = \theta_y = \theta_y^* = 0$ at X=0 and X=a

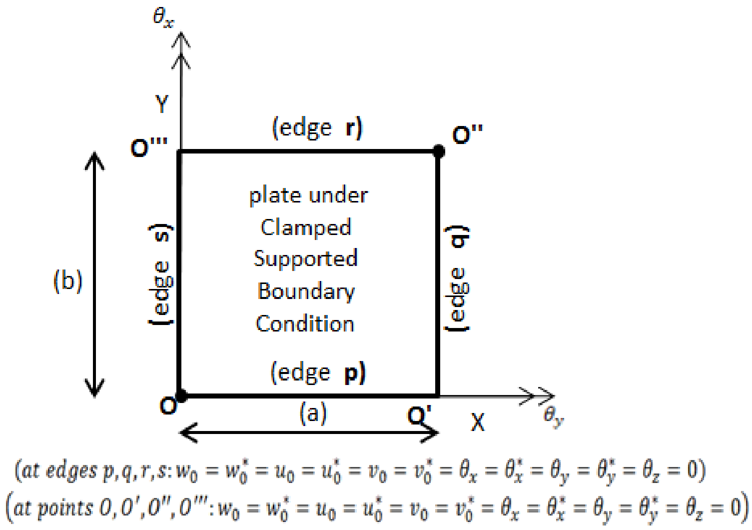

Figure 6.8: Plate under clamped supported boundary condition for model-2

$W_0 = W_0^* = \theta_x = \theta_x^* = \theta_y = \theta_y^* = 0$ at Y=0 and Y=a

For displacement model-2(Fig.6.8):

$W_0 = W_0^* = U_0 = U_0^* = V_0 = V_0^* = \theta_x = \theta_x^* = \theta_y = \theta_y^* = \theta_z = 0$ at X=0 and X=a

$W_0 = W_0^* = U_0 = U_0^* = V_0 = V_0^* = \theta_x = \theta_x^* = \theta_y = \theta_y^* = \theta_z = 0$ at Y=0 and Y=a

The numerical results of frequency are presented in nondimensional form. In solving of problems following material properties sets are considered,

Material Set-1;

$$\frac{E_1}{E_2} = open, E_2 = E_3, G_{12} = G_{13} = 0.6E_2, G_{23} = 0.5E_2, \nu_{12} = \nu_{23} = \nu_{13} = 0.25 \quad (6.1)$$

Material Set-2;

$$\frac{E_1}{E_2} = 40, E_2 = E_3, G_{12} = G_{13} = 0.6E_2, G_{23} = 0.5E_2, \nu_{12} = \nu_{23} = \nu_{13} = 0.25 \quad (6.2)$$

Material Set-3;

$$E = 1000, \nu = 0.3, \rho = 1, G = \frac{E}{2(1+\nu)} = 384.62, D = \frac{E * h^3}{12(1-\nu^2)} \tag{6.3}$$

Material Set-4;

$$E = 200000, \nu = 0.3, \rho = 0.08, G = \frac{E}{2(1+\nu)} = 76923, D = \frac{E * h^3}{12(1-\nu^2)} \tag{6.4}$$

Material Set-5;

$$FaceSheets: \quad E_1 = 131\times10^3 MPa, E_2 = 10.34\times10^3 MPa, E_2 = E_3, G_{12} = 6.895\times10^3 MPa,$$

$$G_{13} = 6.205\times10^3 MPa, G_{23} = 6.895\times10^3 MPa, \nu_{12} = \nu_{13} = 0.22, \nu_{23} = 0.49, \rho = 1627 kg/m^3$$

$$Core: \quad E_1 = E_2 = E_3 = 2G = 6.89 MPa, G_{12} = G_{13} = G_{23} = 3.45 MPa,$$

$$\nu_{12} = \nu_{13} = \nu_{23} = 0, \rho = 97 kg/m^3 \tag{6.5}$$

6.3 Comparison of Results

The developed finite element formulation is validated and assessed for its performance considering following cases of Laminated plate with different type of orientation scheme of lamina as shown in Fig.6.9 and 6.10,6.11.

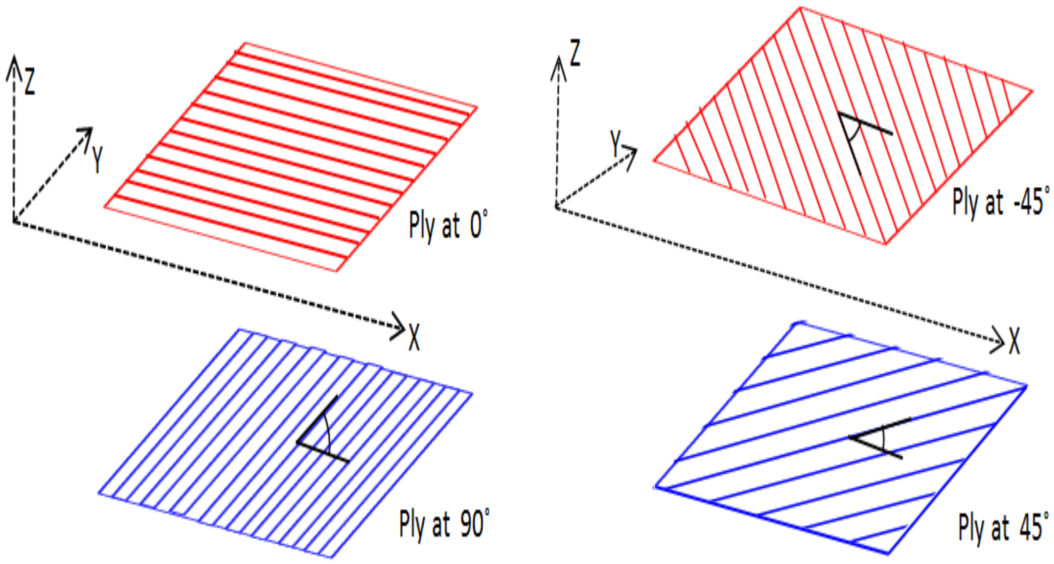

Figure 6.9: Orientation scheme of Lamina : (a) Cross Ply (b) Angle Ply

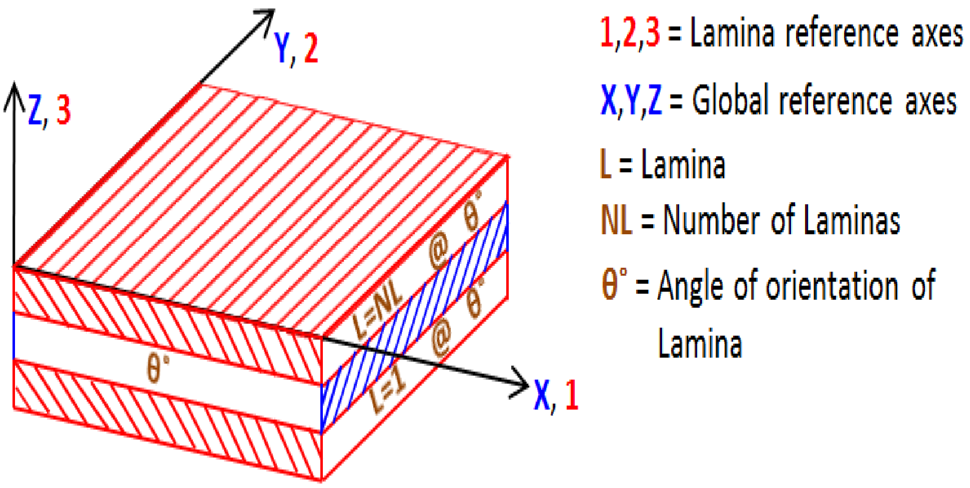

Figure 6.10: Cross Ply - Laminated Composite Plate

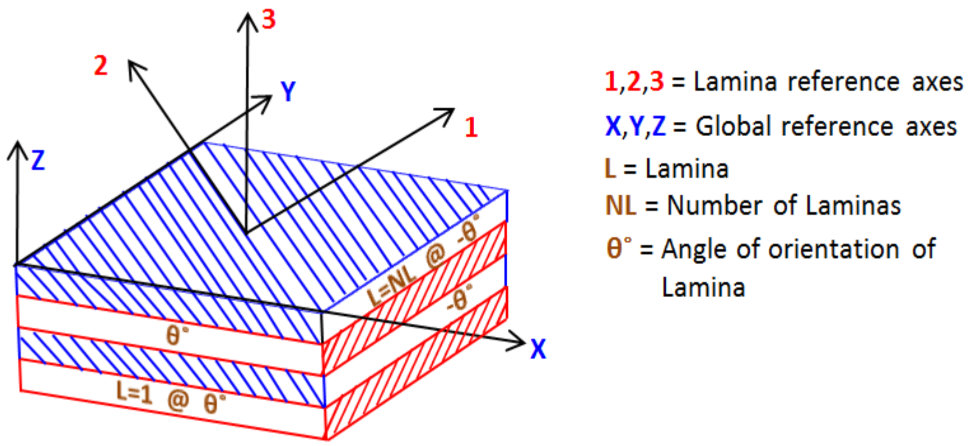

Figure 6.11: Angle Ply - Laminated Composite Plate

Case : 1

In Table 6.1 natural frequency is calculated for square simply supported isotropic plate and compared with available results in literature.

Table 6.1: Comparison of non-dimensionalized fundamental frequency $\bar{\omega} = \frac{\omega a^2}{\pi^2} \sqrt[2]{\frac{\rho h}{D}}$ for a symmetric simply supported isotropic square plate for $\frac{a}{h} = 10$ considering material set-3

Support Condition	*ModeNo.*	**Source**	ϖ
Simply Supported	1	Present Model 2	1.9370
		3-Order [25]	1.9281
	2	Present Model 2	4.7106
		3-Order [25]	4.5954
	3	Present Model 2	4.7106
		3-Order [25]	4.5954
Clamped Supported	1	Present Model 2	3.4797
		3-Order [25]	3.3047
	2	Present Model 2	6.8928
		3-Order [25]	6.3244
	3	Present Model 2	6.8928
		3-Order [25]	6.3244

It is observed that first three natural frequencies are very close to analytical results reported in literature by maximum error less than 2.5% for simply supported plate and 8.7% for clamped supported plate.

Case : 2

In this case the study on effect of coupling between bending and stretching in laminated plate is carried out by solving problem of cross ply and angle ply and the results are presented in Table 6.2 and 6.3.

Table 6.2: Effect of the coupling between bending and stretching on the non-dimensional fundamental frequencies $\bar{\omega} = \omega \sqrt[2]{\frac{\rho h^2}{E_2}}$, of a simply supported-WSS1 square plate with material set-2: CP- cross ply (0/90)

Lamination	**Source**	$\overline{\omega}$				
		$\frac{a}{h}$				
		5	**10**	**20**	**50**	**100**
$(0/90)_1$	Presented Model-1	0.471052	0.159505	0.044992	0.007495	0.001885
	Presented Model-2	0.348600	0.104418	0.027830	0.004593	0.001171
	PHOST11[22]	0.348106	0.104157	0.027651	0.004507	0.001129
	PHOST6[22]	0.469961	0.159299	0.044969	0.007495	0.001885
$(0/90)_2$	Presented Model-1	0.471052	0.159505	0.044992	0.007495	0.001885
	Presented Model-2	0.432900	0.146500	0.044240	0.007545	0.001925
	PHOST11[22]	0.432405	0.146309	0.041238	0.006868	0.001727
	PHOST6[22]	0.469961	0.159299	0.044969	0.007495	0.001885
$(0/90)_3$	Presented Model-1	0.471052	0.159505	0.044992	0.007495	0.001885
	Presented Model-2	0.45200	0.153600	0.043520	0.007312	0.001860
	PHOST11[22]	0.451414	0.153371	0.043329	0.007222	0.001817
	PHOST6[22]	0.469961	0.159299	0.044969	0.007495	0.001885
$(0/90)_{10}$	Presented Model-1	0.471052	0.159505	0.044992	0.007495	0.001885
	Presented Model-2	0.463500	0.157400	0.044520	0.007486	0.001906
	PHOST11[22]	0.462951	0.157158	0.044382	0.007397	0.001861
	PHOST6[22]	0.469961	0.159299	0.044969	0.007495	0.001885

Table 6.3: Effect of the coupling between bending and stretching on the non-dimensional fundamental frequencies $\bar{\omega} = \omega \sqrt[2]{\frac{\rho h^2}{E_2}}$, of a simply supported-WSS2 square plate with material set-2: AP- cross ply (45/-45)

Lamination	**Source**	$\overline{\omega}$				
		$\frac{a}{h}$				
		5	**10**	**20**	**50**	**100**
$(45/-45)_1$	Presented Model-1	0.524685	0.195808	0.059254	0.010177	0.002572
	Presented Model-2	0.400590	0.128770	0.035385	0.005873	0.001483
	PHOST11[22]	0.400602	0.128794	0.035329	0.005824	0.001463
	PHOST6[22]	0.523067	0.195608	0.059217	0.010174	0.002572
$(45/-45)_2$	Presented Model-1	0.524685	0.195808	0.059254	0.010177	0.002572
	Presented Model-2	0.477725	0.178605	0.054043	0.009323	0.002367
	PHOST11[22]	0.477902	0.178639	0.054020	0.009274	0.002344
	PHOST6[22]	0.523067	0.195608	0.059217	0.010174	0.002572
$(45/-45)_3$	Presented Model-1	0.524685	0.195808	0.059254	0.010177	0.002572
	Presented Model-2	0.499007	0.187586	0.056921	0.009840	0.002495
	PHOST11[22]	0.498825	0.187647	0.056912	0.009782	0.002473
	PHOST6[22]	0.523067	0.195608	0.059217	0.010174	0.002572
$(45/-45)_{10}$	Presented Model-1	0.524685	0.195808	0.059254	0.010177	0.002572
	Presented Model-2	0.513933	0.192646	0.058376	0.010072	0.002560
	PHOST11[22]	0.513729	0.192685	0.058388	0.010035	0.002537
	PHOST6[22]	0.523067	0.195608	0.059217	0.010174	0.002572

The effect of the coupling between bending and stretching on the fundamental frequencies of simply-supported cross-ply (0/90) and angle-ply (45/-45) laminates with material set - 2 for different a/h ratios is shown in Table 6.2 and 6.3. The six-degrees-of-freedom solution, which includes bending action only is obtained by suppressing the in-plane displacement degrees of freedom. As the a/h ratio increased the effect of the coupling between bending and stretching increased for two layers and four layers. The percentage errors are as high as 67 % for cross-ply and 75.8 % for angle-ply. The percentage error decreased with the increase in number of layers. It is thus seen that the coupling between bending and stretching has a significant effect on the behaviour of antisymmetric laminates with few lamina.

Case : 3

The nondimensionalized natural frequencies are computed using presented model-2 for two, four, six and ten layer antisymmetric cross-ply laminated plate with layers of equal thickness for open E1/E2 ratio with consideration of material set-1 and results are presented in Table 6.4.

Table 6.4: Non-dimensionalized fundamental frequency $\bar{\omega} = \frac{\omega a^2}{h}\sqrt{\frac{\rho}{E_2}}$ for a simply supported antisymmetric cross-ply square laminated plates with $\frac{a}{h} = 5$.

Lamination	**Source**	$\overline{\omega}$				
		$\frac{E_1}{E_2}$				
		3	**10**	**20**	**30**	**40**
$(0/90)_1$	Presented Model-2	6.2075	6.9552	7.6965	8.2624	8.7152
	3D-Elasticity[23]	6.2578	6.9845	7.6745	8.1763	8.5625
	Model -1[21]	6.2336	6.9741	7.7140	8.2775	8.7272
	Model-2[21]	6.1566	6.9363	7.6883	8.2570	8.7097
$(0/90)_2$	Presented Model-2	6.4882	8.1333	9.4630	10.2725	10.8213
	3D-Elasticity[23]	6.5455	8.1445	9.4055	10.1650	10.6798
	Model-1[21]	6.5146	8.1482	9.4675	10.2733	10.8221
	Model-2[21]	6.4319	8.1010	9.4338	10.2463	10.7993
$(0/90)_3$	Presented Model-2	6.5454	8.3690	9.8253	10.7053	11.2988
	3D-Elasticity[23]	6.6100	8.4143	9.8398	10.6958	11.2728
	Model -1[21]	6.5711	8.3852	9.8346	10.7113	11.3051
	Model-2[21]	6.4873	8.3372	9.8012	10.6853	11.2838
$(0/90)_5$	Presented Model-1	6.6199	8.5919	10.1696	11.1242	11.776
	Presented Model -2	6.5740	8.4955	10.0287	11.0133	12.6523
	3D-Elasticity[23]	6.5458	8.5625	10.0843	11.0027	11.6245
	Model -1[21]	6.6019	8.5163	10.0438	10.9699	11.5993

For comparison study three dimensional elasticity solutions and HSDT solutions are considered. For all laminated plate the error is decrease with the increase in value of E1/E2 ratio.For two, four and six layer lamina at higher value of E1/E2 ratio 20,30 and 40 the presented model-2 gives accurate result compare to other theories.

Case : 4

The variation of natural frequencies with respect to side to width thickness ratio a/h is presented in Table 6.5 by solving problem of simply supported-WSS1 cross-ply square laminated plate using material set-2.

Table 6.5: Variation of non-dimensionalized fundamental frequency $\bar{\omega} = \frac{\omega a^2}{h} \sqrt[2]{\frac{\rho}{E_2}}$ with a/h for a symmetric simply supported cross-ply square laminated plate with material set-2

Lamination	**Source**	$\overline{\omega}$					
		$\frac{a}{h}$					
		2	**4**	**10**	**20**	**50**	**100**
0/90	Presented Model-2	4.7295	7.8931	10.4419	11.1325	11.4823	11.7068
	Model -1[21]	5.0918	7.9081	10.4319	11.0663	11.2688	11.2988
	Model -2[21]	5.0746	7.8904	10.4156	11.0509	11.2537	11.2837
0/90/90/0	Presented Model-2	5.406	9.4159	15.2927	17.7341	18.6890	18.8472
	Model -1[21]	5.4033	9.2870	15.1048	17.6470	18.6720	18.8357
	Model -2[21]	5.3929	9.2710	15.0949	17.6434	18.6713	18.8355

The results show that for thick plates the results of Presented Model-2 are in good agreement as very less negligible error is present in comparison with Model-1[21] and Model-2[21].

Case : 5

To study the effect of side-thickness ratio on the non-dimensional fundamental frequencies , the results are obtained for the two and eight layer antisymmetric angle ply lamina corresponding to material set-2 as shown in Table 6.6.

Table 6.6: Comparison of non-dimensionalized fundamental frequency $\bar{\omega} = \frac{\omega a^2}{h} \sqrt[2]{\frac{\rho}{E_2}}$ for a symmetric simply supported cross-ply (45/-45) square laminated plates for different $\frac{a}{h}$ ratios.

$\frac{a}{h}$	$\overline{\omega}$					
	2 layer(45/-45)WSS2			**8 layer(45/-45)$_8$WSS2**		
	Present Model-2	PHOST11[22]	HOST[24]	Present Model-2	PHOST11[22]	HOST[24]
5	10.015	10.215	10.692	12.720	12.718	12.967
10	12.878	12.879	13.207	19.100	19.107	19.274
20	14.154	14.132	14.228	23.173	23.169	23.236
50	14.683	14.561	14.568	24.985	24.889	24.901
100	14.888	14.626	14.619	25.399	25.174	25.173

It is observed that for both 2 layer and 8 layer antisymmetric laminates the Present Model-2 give accurate result in excellent agreement with other higher order theories.

Case : 6

To facilitate extrapolation to aspect ratio (a/b), nondimensional frequency is presented as a function of a/b for various values of a/h and lamination angle in Table 6.7.

Table 6.7: Effects of plate aspect ratio (a/b), lamination angle and length-to-thickness ratio (a/h) on the dimensionless fundamental frequency, $\bar{\omega} = \omega \sqrt[2]{\frac{\rho h^2}{E_2}}$ of a simply supported rectangular plate with material set-2 of stacking sequence $(\theta/-\theta/\theta/-\theta)$

$\frac{a}{h}$	θ	**Source**	$\overline{\omega}$			
			$\frac{a}{b}$			
			0.5	1	2	4
5	30	Present Model 2	3.5924	4.3994	7.5260	14.788
		HOST [24]	3.7448	4.8554	7.5261	15.3144
	45	Present Model 2	3.3324	4.7789	8.0760	16.0920
		HOST [24]	3.4594	5.0178	8.5404	17.0529
	60	Present Model 2	2.8724	4.7300	8.5760	11.2160
		HOST [24]	2.9357	4.8554	8.9875	11.6581
10	30	Present Model 2	1.2580	1.6716	2.7320	6.284
		HOST [24]	1.2829	1.7513	2.9357	6.1819
	45	Present Model 2	1.1318	1.7860	3.3540	7.3920
		HOST [24]	1.1501	1.8326	3.4594	7.5371
	60	Present Model 2	0.9312	1.7323	3.6960	5.7920
		HOST [24]	0.9376	1.7513	3.7448	5.9289
20	30	Present Model 2	0.3631	0.5088	0.9185	2.1880
		HOST [24]	0.3646	0.5165	0.9376	2.1461
	45	Present Model 2	0.3203	0.5404	1.1450	2.9530
		HOST [24]	0.3213	0.5450	1.1501	2.8785
	60	Present Model 2	0.2563	0.5151	1.2890	2.9250
		HOST [24]	0.2563	0.5165	1.2829	2.9793
50	30	Present Model 2	0.0613	0.0879	0.1700	0.4468
		HOST [24]	0.0609	0.0877	0.1660	0.4121
	45	Present Model 2	0.0536	0.0931	0.2152	0.6524
		HOST [24]	0.0533	0.0928	0.2088	0.5962
	60	Present Model 2	0.0424	0.0881	0.2461	0.8256
		HOST [24]	0.0422	0.0877	0.2376	0.7621

It is observed from the table 6.7 that the fundamental frequencies decrease with the increase in lamination angle for a/b = 0.5, and for a/b = 2.0 frequencies increase with the increase in the lamination angle. As the a/h ratio increases, the fundamental frequency decreases.

Case : 7

In this case the nondimensionalized natural frequencies are computed considering presented model-2 for isotropic plate with square cutout at centre as shown in Fig.6.2. The numerical values are presented of first 4 mode considering material set-4 for h/a=0.01. The results are compared with available results in literatures as shown in Table 6.8.

Table 6.8: Non dimensionalized natural frequencies, $\bar{\omega} = \sqrt[4]{\frac{\rho h \omega^2 a^4}{D(1-\nu^2)}}$ of simply supported square plates with a square hole at centre considering material set-4 and h/a=0.01

Mode	$\overline{\omega}$		
	P	resent Model-2	RPIM[26]
	Without Cutout	With Cutout	With Cutout
1	4.6640	5.0120	4.9217
2	7.8671	7.1355	6.4810
3	7.9654	7.1355	6.4821
4	11.8302	9.4337	8.5509

It is observed from the table that results obtained by Present Model-2 overestimate natural frequencies by 8.01% while comparing them with results available in literatures. Also the rate of increase of natural frequency is more incase of plate without cutout compare to plate with square cut out at centre.

Case : 8

In this case variation of nondimensional natural frequency is studied with respect to the various parameters like the side-to-thickness ratio (a/h), thickness of core to thickness of flange (t_c/t_f) and the aspect ratio (a/b) of a five-layer sandwich plate with antisymmetric cross-ply face sheets as shown in Fig.6.12 using material set-1 under simply supported boundary condition.

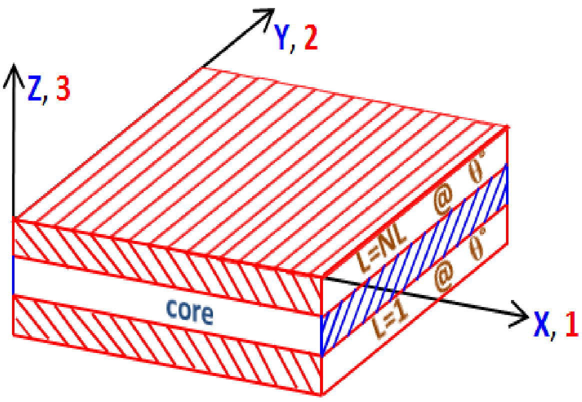

Figure 6.12: Sandwich laminated composite plate

Table 6.9: Non-dimensionalized fundamental frequency $\bar{\omega} = \frac{\omega b^2}{h}\sqrt[2]{\frac{\rho}{E_2}}$ of an antisymmetric (0/90/core/0/90)sandwich plate with $\frac{a}{b} = 1$ and $\frac{t_c}{t_f} = 10$.

$\frac{a}{h}$	$\overline{\omega}$		
	Present model-2	HSDT Model-1[21]	HSDT Model-2[21]
2	1.2185	1.1941	1.1734
4	2.1530	2.1036	2.0913
10	4.9686	4.8594	4.8519
20	8.7532	8.5955	8.5838
30	11.2594	11.0981	11.0788
40	12.8349	12.6821	12.6555
50	13.8360	13.6899	13.6577
60	14.4958	14.3497	14.3133
70	14.9536	14.7977	14.7583
80	15.2835	15.1119	15.0702
90	15.5231	15.3380	15.2946
100	15.7175	15.5093	15.4647

The results presented in Table 6.9 clearly show that natural frequency for sandwich laminate is increase with increase in a/h ratio. Also in comparison with Model-1[21] and Model-2[21], the Present Model-2 gives accurate result with maximum error less than 2.4%.

6.4 Summary

In this chapter Results of Dynamic Analysis(free vibration analysis) of laminated composite plate are discussed. Natural frequencies are calculated using developed computer program. In solving of problems 8x8 uniform mesh size is considered. To validate the finite element formulation comparison study of obtained numerical results is carried out with available results reported in literature. The computer program developed under consideration of the present two displacement models gives sufficiently accurate results for laminated composite plate with varying width-to-thickness ratio, material anisotropy, stacking sequence, orientation of fibres and support conditions.

Chapter 7

Study of Piezolaminated Composite Plate

7.1 Introduction

When a piezoelectric material is subjected to mechanical strain or stress, it develops electric polarization which generates electric charge. This occurrence is called as direct piezoelectric effect. Conversely when piezoelectric material is electrically polarized by applying electric field, it will experience strain. This action is called converse or reciprocal piezoelectric effect. Here elastic deformation can be an expansion or contraction in either direction according to the sign and magnitude of applied electric field. So as piezoelectric material exhibit both direct and converse effects, the same structural element can be used as an actuator or sensor, or both simultaneously. The converse effect enables actuation and the direct effect accelerates sensing of structural element vibrations [6].

7.2 Piezoelectric Constitutive relationship

Piezoelectric effect maintains a linear relationship between the mechanical strain and electric fields. The direct and converse piezoelectric property found a characteristic electromechanical coupling that is included in the constitutive relations of the structural analysis problem. Here constitutive equations for electromechanical coupling are derived from the relation of Electric enthalpy density with strain energy, electric displacement density and electric field [6].

For 2-D problems the constitutive law model for a piezoelectric material is:

Here first law equation is called actuation law and second is called sensing law.

$$\sigma = [C]\varepsilon - [e]E$$

$$D = [e]^T\varepsilon - [\mu]E \tag{7.1}$$

Where,

In equation 7.1 first part represents the stresses developed due to mechanical loading and second part represents the stresses developed due to voltage applied. From equation it can be concluded that even in absence of mechanical load the structure will be stressed due to application of electric field [5].

7.2.1 Actuation Problem

Here actuation action is demonstrated using Bimorph piezoelectric of dimensions L x W x t, where L and W are the length and width of the plate and t is the thickness. Thin piezoelectric electrodes are placed on the top and bottom surfaces of the plate, as shown in Fig.7.1. When a voltage is applied to the electrodes, the plate will experience the deformations in the length, width and thickness directions as shown in Fig.7.1. Deformations in the respective directions are given by:

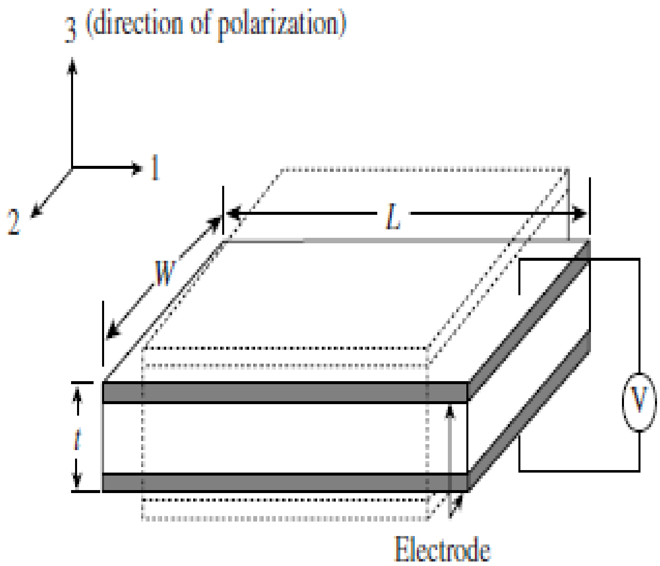

Figure 7.1: Actuation effect in a piezoelectric plate

$$\delta L = d_{31}E_1L = \frac{d_{31}VL}{t}, \delta W = d_{31}E_2W = \frac{d_{31}VW}{t}, \delta t = d_{33}V \tag{7.2}$$

Where, d_{31} and d_{33} are the electromechanical coupling coefficients in the directions 1 and 3, respectively. For converse effect if a force F is applied in any of the length, width or thickness directions, the voltage V will be developed across the electrodes in the thickness direction, Which is given by:

$$V = \frac{d_{31}F}{\mu L} or V = \frac{d_{31}F}{\mu W} or V = \frac{d_{33}F}{\mu LW} \tag{7.3}$$

Where, μ is the dielectric permittivity of the material.

7.3 Finite Element Modeling

From constitutive law relationship which represents the electromechanical coupling, finite element formulation is derived using 8-node isoparametric finite element based on considered displacement fields.

Constitutive law relationship is given by:

$$\begin{Bmatrix} \{\sigma\} \\ \{D\} \end{Bmatrix} = \begin{bmatrix} Q & -e \\ e^T & \mu \end{bmatrix} \begin{Bmatrix} \{\varepsilon\} \\ \{E\} \end{Bmatrix} \quad or \quad \bar{\sigma} = [\bar{Q}]\bar{\varepsilon} \tag{7.4}$$

Above equation is simplified as follows:

$$\begin{Bmatrix} \sigma_{11} \\ \sigma_{22} \\ \sigma_{33} \\ \sigma_{12} \\ \sigma_{23} \\ \sigma_{13} \\ D_1 \\ D_2 \\ D_3 \end{Bmatrix} = \begin{bmatrix} Q_{11} & Q_{12} & Q_{13} & 0 & 0 & 0 & 0 & 0 & -e_{31} \\ Q_{21} & Q_{22} & Q_{23} & 0 & 0 & 0 & 0 & 0 & -e_{32} \\ Q_{31} & Q_{32} & Q_{33} & 0 & 0 & 0 & 0 & 0 & -e_{33} \\ 0 & 0 & 0 & Q_{44} & 0 & 0 & 0 & -e_{24} & 0 \\ 0 & 0 & 0 & 0 & Q_{55} & 0 & -e_{15} & 0 & 0 \\ 0 & 0 & 0 & 0 & 0 & Q_{66} & 0 & 0 & 0 \\ 0 & 0 & 0 & 0 & e_{15} & 0 & \mu_{11} & 0 & 0 \\ 0 & 0 & 0 & e_{24} & 0 & 0 & 0 & \mu_{22} & 0 \\ e_{31} & e_{32} & e_{33} & 0 & 0 & 0 & 0 & 0 & \mu_{33} \end{bmatrix} \begin{Bmatrix} \varepsilon_{11} \\ \varepsilon_{22} \\ \varepsilon_{33} \\ \varepsilon_{12} \\ \varepsilon_{23} \\ \varepsilon_{13} \\ E_1 \\ E_2 \\ E_3 \end{Bmatrix} \tag{7.5}$$

The constitutive model is then transformed to the global axis using transformation

7.3.1 2-D Isoparametric smart composite finite element

For 2-D analysis the stresses $\sigma_{22} = \sigma_{12} = \sigma_{23} = D_1 = D_2 = 0$ in equation 7.5.

$$[T] = \begin{bmatrix} T_{11} & 0 \\ 0 & T_{22} \end{bmatrix} \tag{7.6}$$

where,

$$[T_{11}] = \begin{bmatrix} C^2 & S^2 & 0 & 0 & 0 & -2CS \\ S^2 & C^2 & 0 & 0 & 0 & 2CS \\ 0 & 0 & 1 & 0 & 0 & 0 \\ 0 & 0 & 0 & C & S & 0 \\ 0 & 0 & 0 & S & C & 0 \\ CS & -CS & 0 & 0 & 0 & C^2 - S^2 \end{bmatrix} \tag{7.7}$$

$$[T_{22}] = \begin{bmatrix} C^2 & S^2 & 0 \\ S^2 & C^2 & 0 \\ 0 & 0 & 1 \end{bmatrix} \quad C = cos(\theta), \quad S = sin(\theta) \tag{7.8}$$

Here θ is angle of fibre orientation.So constitutive model can be written in global x-y-z direction as follows:

$$\sigma = [T]^T \begin{bmatrix} Q & -e \\ e^T & \mu \end{bmatrix} [T]\varepsilon = \begin{bmatrix} \bar{Q} & -\bar{e} \\ \bar{e}^T & \bar{\mu} \end{bmatrix} \varepsilon \tag{7.9}$$

from above equation 7.9 the expanded form can be written as follow:

$$\begin{Bmatrix} \sigma_{xx} \\ \sigma_{yy} \\ \sigma_{zz} \\ \tau_{xy} \\ \tau_{yz} \\ \tau_{xz} \\ D_x \\ D_y \\ D_z \end{Bmatrix} = \begin{bmatrix} \bar{Q}_{11} & \bar{Q}_{12} & \bar{Q}_{13} & 0 & 0 & 0 & 0 & 0 & -\bar{e}_{31} \\ \bar{Q}_{21} & \bar{Q}_{22} & \bar{Q}_{23} & 0 & 0 & 0 & 0 & 0 & -\bar{e}_{32} \\ \bar{Q}_{31} & \bar{Q}_{32} & \bar{Q}_{33} & 0 & 0 & 0 & 0 & 0 & -\bar{e}_{33} \\ 0 & 0 & 0 & \bar{Q}_{44} & 0 & 0 & 0 & -\bar{e}_{24} & 0 \\ 0 & 0 & 0 & 0 & \bar{Q}_{55} & 0 & -\bar{e}_{15} & 0 & 0 \\ 0 & 0 & 0 & 0 & 0 & \bar{Q}_{66} & 0 & 0 & 0 \\ 0 & 0 & 0 & 0 & \bar{e}_{15} & 0 & \bar{\mu}_{11} & 0 & 0 \\ 0 & 0 & 0 & \bar{e}_{24} & 0 & 0 & 0 & \bar{\mu}_{22} & 0 \\ \bar{e}_{31} & \bar{e}_{32} & \bar{e}_{33} & 0 & 0 & 0 & 0 & 0 & \bar{\mu}_{33} \end{bmatrix} \begin{Bmatrix} \varepsilon_x \\ \varepsilon_y \\ \varepsilon_z \\ 2\varepsilon_{xy} \\ 2\varepsilon_{yz} \\ 2\varepsilon_{xz} \\ E_x \\ E_y \\ E_z \end{Bmatrix} \tag{7.10}$$

The coefficients of $[\bar{Q}]$ and $[-\bar{e}]$ are given by:

$\bar{Q}_{11} = Q_{11}C^4 + (2Q_{12} + 4Q_{44})\ S^2C^2 + Q_{22}S^4$

$\bar{Q}_{12} = (S^4 + C^4)\ Q_{12} + (Q_{11} + Q_{22}\text{ - }4Q_{44})\ S^2C^2$

$\bar{Q}_{13} = C^2Q_{13} + S^2Q_{23}$

$\bar{Q}_{14} = (Q_{11}\text{ - }Q_{12}\text{ - }2Q_{44})\ C^3S + (Q_{12}\text{ - }Q_{22} + 2Q_{44})S^3C$

$\bar{Q}_{22} = Q_{11}S^4 + Q_{22}C^4 + (2Q_{12} + 4Q_{44})S^2C^2$

$\bar{Q}_{23} = C^2Q_{23} + S^2Q_{13}$

$\bar{Q}_{24} = (Q_{11}\text{ - }Q_{12}\text{ - }2Q_{44})\ S^3C + (Q_{12}\text{ - }Q_{22} + 2Q_{44})C^3S$

$\bar{Q}_{33} = Q_{33}$

$\bar{Q}_{34} = (Q_{13}\text{ - }Q_{23})\text{SC}$

$\bar{Q}_{44} = (Q_{11} + Q_{22}\text{ - }2Q_{12}\text{ - }2Q_{44})S^2C^2 + (C^4 + S^4)Q_{44}$

$\bar{Q}_{55} = C^2Q_{55} + S^2Q_{66}$

$\bar{Q}_{56} = (Q_{66}\text{ - }Q_{55})\text{SC}$

$\bar{Q}_{66} = S^2Q_{55} + C^2Q_{66}$

$\bar{e}_{31} = (e_{31}C^2 + e_{32}S^2)$

$\bar{e}_{32} = (e_{31}S^2 + e_{32}C^2)$

$\bar{e}_{33} = e_{33}$

$\bar{e}_{14} = (e_{15}C^2S + e_{24}CS^2)$

$\bar{e}_{24} = (e_{24}C^3 + e_{15}S^3)$

$\bar{e}_{15} = (e_{15}C^3 + e_{24}S^3)$

$\bar{e}_{25} = (e_{24}C^2S + e_{15}CS^2)$

$\bar{\mu}_{12} = C^2S^2(\mu_{11} + \mu_{22})$

$\bar{\mu}_{22} = \mu_{22}C^4 + \mu_{11}S^4$

$\bar{\mu}_{33} = \mu_{33}$

In present work for finite element formulation the 8-node isoparametric element is shown in Fig.7.2.

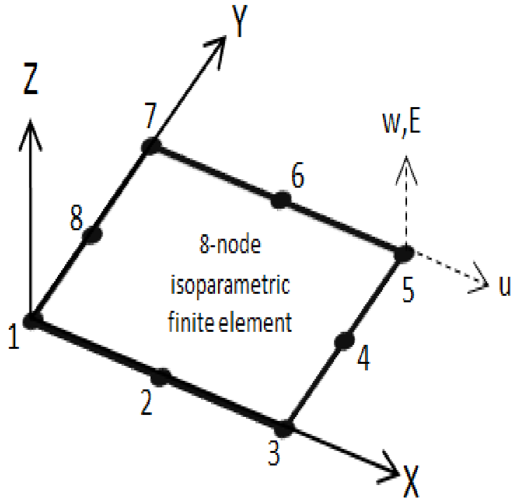

Figure 7.2: 8-node isoparametric element with displacement fields at each node

Displacement Model: The element will have two mechanical degrees of freedom U(x,y,t) and W(x,y,t) respectively in x and z direction and one electrical degree of freedom $E_z(x,y,z)$ in z - direction per node as shown in Fig.7.2. Therefore element will have 24 degrees of freedom.

The displacement related at any point within the element is:

$$u(x,y,t) = \sum_{i=1}^{8} N_i(\xi,\eta)u_i(t),\ w(x,y,t) = \sum_{i=1}^{8} N_i(\xi,\eta)w_i(t),\ E_z(x,y,t) = \sum_{i=1}^{8} N_i(\xi,\eta)E_{zi}(t) \tag{7.11}$$

Here ζ and η are the isoparametric coordinates and $u_i(t), w_i(t)$ are the mechanical nodal degrees of freedom, and $E_{zi}(t)$ is the electrical nodal degree of freedom.

Strain - Displacement Relationship is given by:

$$\left\{\begin{array}{c}\varepsilon_{xx}\\ \varepsilon_{zz}\\ 2\varepsilon xz\\ E_z\end{array}\right\}=\begin{bmatrix}\frac{\partial}{\partial x} & 0 & 0\\ 0 & \frac{\partial}{\partial z} & 0\\ \frac{\partial}{\partial z} & \frac{\partial}{\partial x} & 0\\ 0 & 0 & 1\end{bmatrix}\left\{\begin{array}{c}u\\ w\\ D_z\end{array}\right\} \tag{7.12}$$

By substituting equation 7.11 in above equation, will allow to express strain in terms of nodal displacement vector $\{q\}_e$ and electrical field vector $\{E_z\}_e$:

$$\{q\}_e=\{u_1\ \ w_1\ \ u_2\ \ w_2\ \ u_3\ \ w_3\ \ u_4\ \ w_4\ \ u_5\ \ w_5\ \ u_6\ \ w_6\ \ u_7\ \ w_7\ \ u_8\ \ w_8\}^T$$

$$\{E_z\}_e=\{E_1\ \ E_2\ \ E_3\ \ E_4\ \ E_5\ \ E_6\ \ E_7\ \ E_8\}^T$$

Now from above relation [B] matrix for mechanical field $[B]_u$ and electrical field $[B]_E$ can be written as:

$$[B]_u=\sum_{i=1}^{NN}\left|\begin{array}{cc}\frac{\partial N_i}{\partial x} & 0\\ 0 & \frac{\partial N_i}{\partial z}\\ \frac{\partial N_i}{\partial x} & \frac{\partial N_i}{\partial x}\end{array}\right|_{(3X16)}\left|\begin{array}{c}u_i\\ w_i\end{array}\right|_{(16X1)} \tag{7.13}$$

$$[B]_E=\sum_{i=1}^{NN}\left|\ N_i\ \right|_{(1X8)}\left|\ E_i\ \right|_{(8X1)} \tag{7.14}$$

Where NN = Number of node.

Concise matrix form obtained from the weak form governing equation for a composite laminate with piezoelectric smart patches using Hamilton's principle is shown by differential equation 7.15.

$$\begin{bmatrix} [M_{uu}] & [0] \\ [0] & [0] \end{bmatrix} \begin{Bmatrix} \{\ddot{u}\}_e \\ \{\ddot{E}_z\}_e \end{Bmatrix} + \begin{bmatrix} [K_{uu}] & [K_{uE}] \\ K_{uE}^T & [K_{EE}] \end{bmatrix} \begin{Bmatrix} \{u\}_e \\ \{E_z\}_e \end{Bmatrix} = \begin{Bmatrix} \{F\}_e \\ \{q\}_e \end{Bmatrix} \tag{7.15}$$

For static analysis here mass matrix form is not considered. Therefore concise form will be as given by:

$$\begin{bmatrix} [K_{uu}] & [K_{uE}] \\ K_{uE}^T & [K_{EE}] \end{bmatrix} \begin{Bmatrix} \{u\}_e \\ \{E_z\}_e \end{Bmatrix} = \begin{Bmatrix} \{F\}_e \\ \{q\}_e \end{Bmatrix} \tag{7.16}$$

Where the $[K_{uu}]$ is the stiffness matrix corresponding to the mechanical degrees of freedom. $[K_{uE}]$ is the stiffness matrix due to electromechanical coupling. $[K_{EE}]$ is the stiffness matrix due to electrical degrees of freedom. F_e is the element load vector and q_e is the element charge vector. These all matrices are given by:

$$[K_{uu}] = t \int_{-1}^{+1} \int_{-1}^{+1} [B_u]^T [\bar{Q}] [B_u] \ \ |J| \ d\xi \ d\eta$$

$$[K_{uE}] = -t \int_{-1}^{+1} \int_{-1}^{+1} [B_u]^T [\bar{e}] [B_E] \ \ |J| \ d\xi \ d\eta$$

$$[K_{EE}] = t \int_{-1}^{+1} \int_{-1}^{+1} [B_E]^T [\bar{\mu}_{33}] [B_E] \ \ |J| \ d\xi \ d\eta \tag{7.17}$$

Element Load and Charge vector are given by:

$$F_e = F_c \ + \ \int_{s1} [N]^T F_s \ \ dS_1$$

$$q_e = -\int_{s2} [N]^T D_s \ \ dS_2 \tag{7.18}$$

To solve Integration form 2x2 Gauss Integration scheme is used for both stiffness matrix due to mechanical and electromechanical coupling.

$$\begin{aligned}
[K_{uu}] &= \sum_{a=1}^{NG}\sum_{b=1}^{NG} t\ [B_u]^T\ [\bar{Q}]\ [B_u]\ |J|\ W_a\ W_b \\
[K_{uE}] &= \sum_{a=1}^{NG}\sum_{b=1}^{NG} -t\ [B_u]^T\ [\bar{e}]\ [B_E]\ |J|\ W_a\ W_b \\
[K_{EE}] &= \sum_{a=1}^{NG}\sum_{b=1}^{NG} t\ [B_E]^T\ [\bar{e}]\ [B_E]\ |J|\ W_a\ W_b \\
[F_e] &= \sum_{a=1}^{NG}\sum_{b=1}^{NG} F_s\ [N_i]^T\ [J] W_a W_b
\end{aligned} \tag{7.19}$$

After evaluating stiffness matrices and load vectors individually, they are assembled to obtain overall stiffness matrix and load vector. Subsequently incorporating boundary conditions they are solved for displacement and voltage.

In sensing problem for a given mechanical loading, developed voltage across the smart patch is determined. First mechanical displacement due to applied load is calculated. Then from obtained mechanical displacement the developed voltage across the patch is determined. This sensing problem is exhibits a direct effect of piezoelectric material.

In actuation problem for a given electric field, developed strain across the smart patch is determined. If an arbitrary value of E_z is specified, the problem comes under the category of open-loop control and if the value of E_z comes from sensor output that is fed back to the controller, then the control scheme is referred to as closed-loop control. This actuation problem exhibits a converse effect of piezoelectric material.

7.4 Computer Program Development

A computer program is developed in C++ environment for analysis of composite laminate embedded with patches of piezoelectric material. The first computer program performs a meshing of laminated plate and generates a input data file for further analysis of problem. The second program performs a static analysis of composite laminate using a finite element formulation with considered displacement fields.

7.4.1 Features of Computer Program

Features of computer program are as follows:

1. Automatic Mesh generation
2. Generation of element mechanical stiffness matrix
3. Generation of load vector
4. Generation of element electromechanical coupling stiffness matrix
5. Generation of overall mechanical stiffness matrix,load vector and electromechanical coupling stiffness matrix in banded form
6. Incorporating Boundary conditions
7. Static solution using counterpart of global assembled governing equations
8. Calculation of displacement
9. Solution for secondary unknowns

7.4.2 Flow of Computer Program

Automatic Mesh Generation with Input Data:

The meshing of composite laminate is performed automatically. The laminated plate is divided in number of elements by assigning the number of divisions in along length and width direction. Numbering to the elements is assigned automatically moving in the direction from left to right and bottom to top. Each element has 8 nodes, which are numbered sequentially from left to right and bottom to top as shown in Fig.7.3.

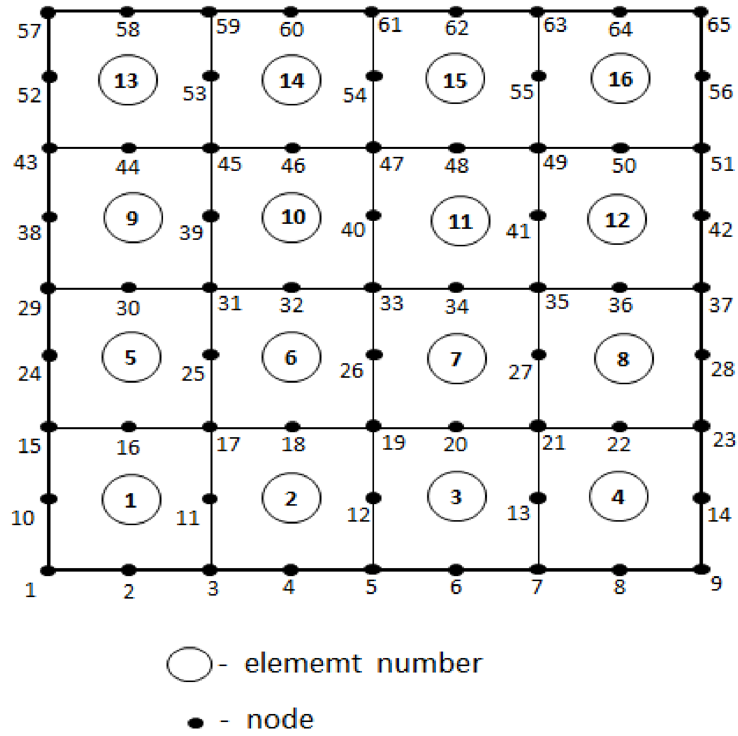

Figure 7.3: Meshing of composite laminate

After numbering the required input data for analysis are given. The required data for analysis are as follows:

a. Plate Dimension

b. Number of Materials with properties

c. Number of Laminate

d. Laminate id with angle of orientation and thickness

e. Assigning of Load

After material properties the element incidences and element coordinates are evaluated automatically. And based on support condition the boundary condition is assigned to the each node. Flow chart is shown in Fig.??.

Generation of Constitutive Law Matrix:

A formulation of constitutive law matrix is executed in computer program based on the finite element formulation discussed in previous section. Constitutive law matrix is formulated using the entered material properties, which exhibits the coupling of mechanical and electrical field.

Generation of [B] Matrix:

Matrix is formulated using shape functions and curvature - nodal displacement relationship. Here two [B] matrices are derived, one is for mechanical field $[B_u]$ and other one is for electrical field $[B_E]$ as shown in flow chart Fig.7.5.

Generation of Overall Stiffness Matrix and Load Vector:

The element stiffness matrix of mechanical field for the laminate is generated by laminate constitutive relation $[\bar{Q}]$ and $[B_u]$ matrix. Similarly stiffness matrix for electrical field is generated by piezoelectric coefficient matrix $[\bar{e}]$, $[B_u]$ and $[B_E]$ matrix. Then generated element stiffness matrices for the laminate are assembled in banded form. The integration for stiffness matrix is evaluated by 2x2 Gauss integration scheme.

Load Vector and Electrical Charge Vector:

For load vector each element load vector is generated by reading loading type and value from input data. Then element load vectors are assembled in banded form. For charge vector also at each node it is obtained from applied voltage and thickness of laminate. Then element charge vectors are assembled in banded form.

Incorporating Boundary conditions :

In input data file at each node based on displacement model and according to degrees of freedom 0 or 1 value is assigned to each degree of freedom. From this data file boundary condition is assigned to all overall stiffness matrices in core program.

Solution Using Governing Equation :

After assigning boundary condition to overall stiffness matrices from counterpart of global assembled governing equations 7.16, displacement is calculated using subroutine based on Gauss Elimination method. The procedure of solution is as follows:

$$\begin{aligned}
[K_{uu}] * u_e + [K_{uE}] * E_{ze} &= F \\
[K_{uu}] * u_e &= F - [K_{uE}] * E_{ze} \\
[K_{uu}] * u_e &= F^* \qquad (7.20)
\end{aligned}$$

Output :

Output data file is consist of following data and results:

1. Plate Dimension
2. Number of elements, nodes and materials
3. Material Properties
4. Laminate data: id, angle of orientation, thickness
5. Element incidences
6. Joint Coordinates
7. Boundary condition
8. Lamina thickness
9. Overall mechanical, electromechanical stiffness matrices
10. Overall load vector
11. Overall field intensity vector
12. Displacement vector
13. Stresses in various elements

Flow Chart for the program of Meshing of laminated composite plate with Input Data

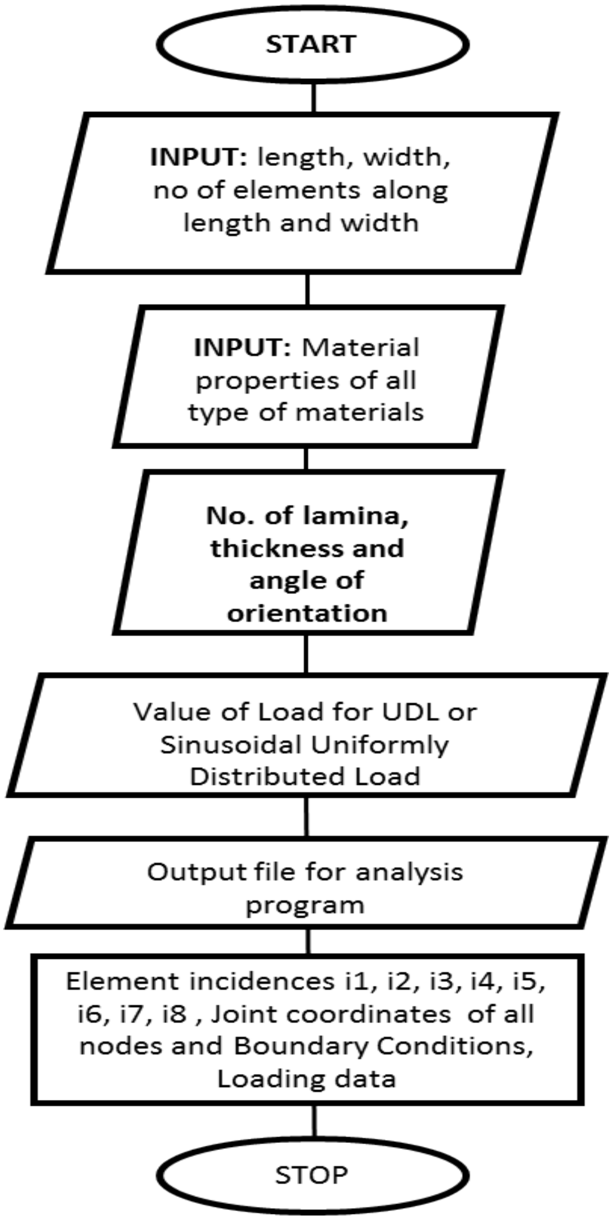

Figure 7.4: Input data with meshing of composite laminate

Flow Chart for the static analysis program

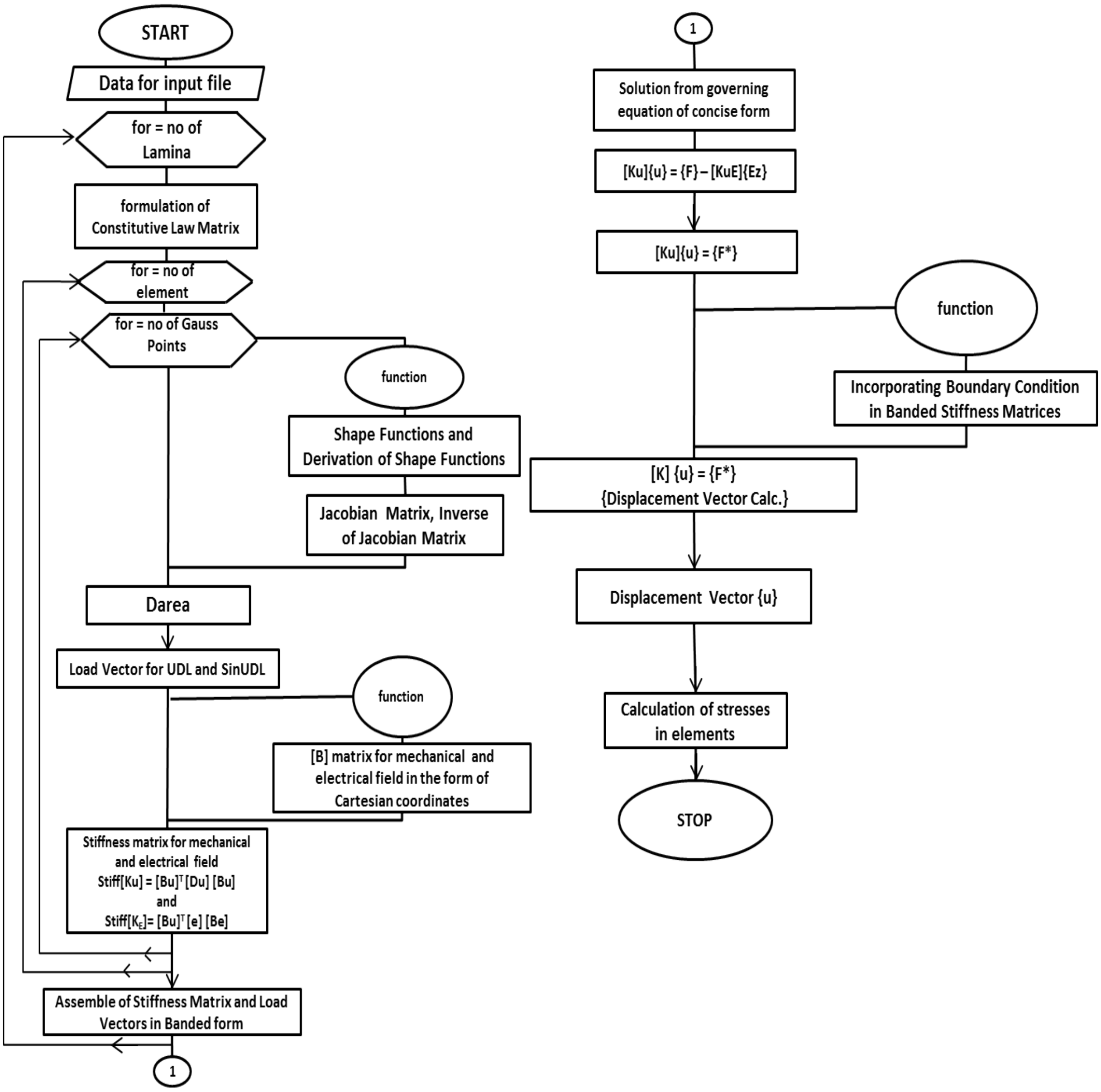

Figure 7.5: Analysis of composite laminate embedded with smart patches of piezo-electric material

7.5 Illustrative Example

The Finite Element Method is formulated based on considered displacement fields and employed for analysis of composite laminate embedded with smart patches of piezoelectric material. In order to establish the reliability and accuracy of the present finite element formulation an illustrative example is solved and results are compared with that available comparison is made with available in literature.

Material Properties:

$e_1 = 0.2 * 10^{10}$, $e_2 = 0.2 * 10^{10}$, $e3 = 0.2 * 10^{10}$, $g_{12} = 0.775 * 10^9$, $g_{23} = 0.775 * 10^9$, $g_{13} = 0.775 * 10^9$
$v_{12} = 0.29$, $v_{21} = 0.28$, $v_{13} = 0$, $v_{31} = 0$, $v_{23} = 0$, $v_{32} = 0$ $E_{31} = 0.046$, $e_{32} = 0.046$, $e_{33} = 0$, $u_{11} = 0.1062 * 10^{-9}$, $u_{22} = 0.1062 * 10^{-9}$, $u_{33} = 0.1062 * 10^{-9}$

A bimorph beam with dimensions of 100mm x 5.0mm x 0.5mm is considered. Theoretical solution is also obtained and compared with analytical. Theoretical equation: $w(x) = 0.375 \frac{e_{31}V}{E} \frac{x}{t}^2$ w(x) = 0.345 * 10^{-6} mm

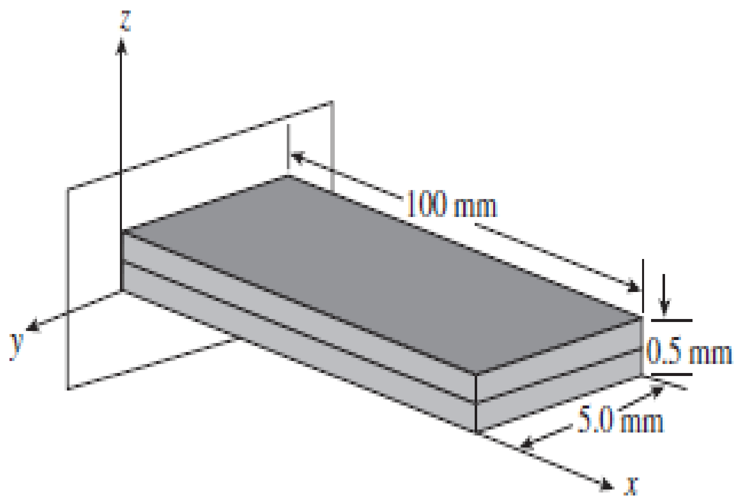

Figure 7.6: Schematic of the piezoelectric PVDF bimorph cantilever beam

7.5.1 Problem Discretization

Here modelling and analysis of a piezoelectric bimorph beam is done. The beam is discretized with 29 elements in the direction of length and 1 element in the direction of width (29x1 mesh size) as shown in Fig.7.7 Here deflection is calculated at various points on beam by applying voltage to each node. The bimorph beam consists of two identical PVDF beams laminated together with opposite polarities.

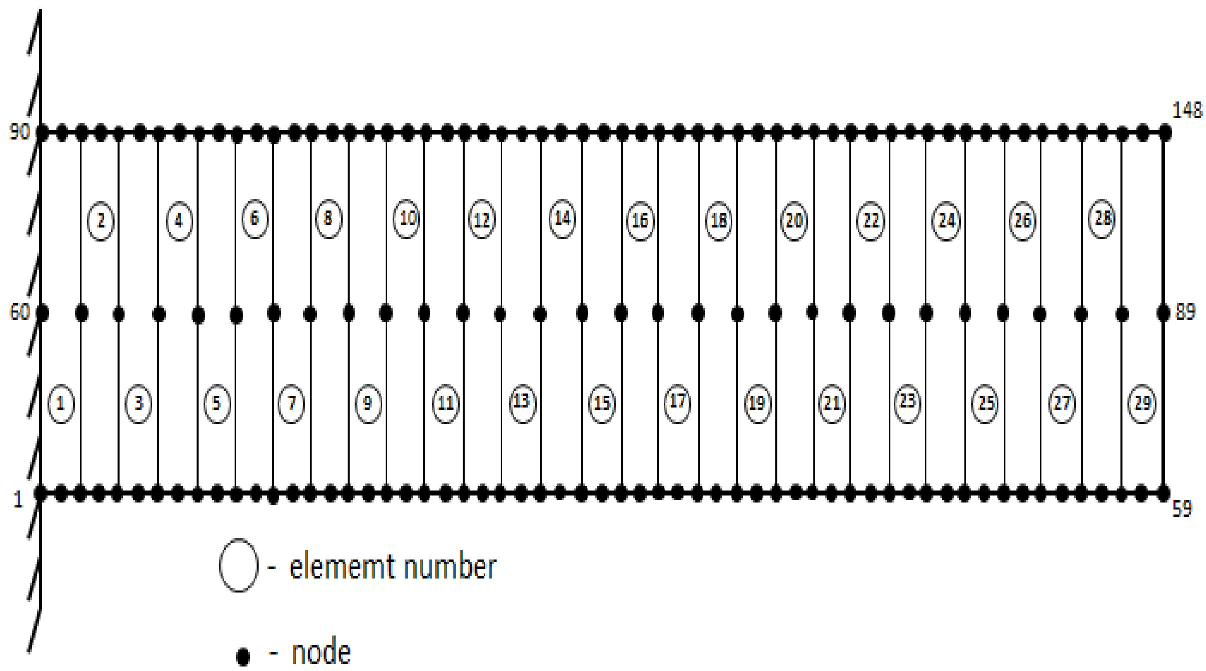

Figure 7.7: (29x1) Meshing of bimorph PVDF beam

A unit voltage is applied across the thickness and the deflections at the nodes are computed. The deflection of the beam along the central longitudinal axis obtained from the present formulation is compared with the value given by theoretical equation and reported in literature as shown in Table 7.1.

Table 7.1: comparison of deflection along the length of beam for a unit voltage applied across the thickness

Source	**Deflection(W)**
Present Model	$0.23\text{x}10^{-6}$
Theoretical	$0.345\text{x}10^{-6}$
Chen[33]	$0.35\text{x}10^{-6}$
Hwang[32]	$0.35\text{x}10^{-6}$

7.6 Summary

The behaviour of the composite laminates embedded with smart patches of piezoelectric materials is studied. The electromechanical coupling behaviour and constitutive relationship are studied from actuation and sensing action of embedded patches. Finite element formulation is derived using 8-node isoparametric quadrilateral element considering two-mechanical displacements and one-electrical fields at each node for 2 - dimensional problem. For validation of formulated model an example of bimorph beam constructed by two PVDF beam is analysed using developed computer program and analysis results are compared with that available in literature.

Chapter 8

Summary and Conclusion

8.1 Summary

This present study comprises the introduction of fibre reinforced composites, classification of composites especially focusing on laminated composites with introduction of piezoelectric laminated composite material with their applications in structural engineering.

Basic Mechanics of Laminated Composite is studied and presented. The finite element analysis of composite plate using Higher Order Shear Deformation Theory is discussed. Finite element formulation for static and dynamic analysis of laminated composite plate by considering two displacement models based on Higher Order Shear Deformation Theory is presented. First displacement model is having 6 - degrees of freedom (w, θ_x, θ_y, w^*, θ_x^*, θ_y^*) and second one is having 11 - degrees of freedom (u_0, v_0,w_0,θ_x,θ_y,θ_z,u_0^*, v_0^*, w_0^*, θ_x^*, θ_y^*). Using these two displacement models, properties of eight node isoparametric Quadrilateral element i.e. stiffness matrix, load vector and mass matrix are dirived.

To perform static analysis of laminated composite plate a computer program is developed. The program is capable for analysis of laminated composite plate with different loading condition like uniformly distributed load and sinusoidal load, support conditions, width to thickness ratio and material anisotropy. In static solution, nondimensional displacement and stresses are calculated for both the considered displacement models. To perform free vibration analysis of laminated composite plate another computer program is developed. The program is capable of obtaining natural frequencies and mode shapes of composite plates with different support conditions and material anisotropy through Eigen value analysis. The validity of program is checked by comparing the analysis results with that reported in literature. Further variety of problems are solved by considering different parameters like material properties, stacking sequence, fibre angle, support conditions etc.

This study is extended to include composite laminates embedded with smart patches of piezoelectric materials to understand the behaviour of composite smart structure. The electromechanical coupling behaviour and constitutive relationship are studied from actuation and sensing action of embedded patches. For analysis of piezoelectric laminated composite, a finite element formulation is derived using 8-node isoparametric quadrilateral element considering mechanical displacements and electrical fields at each node for 2 - dimensional problem. For validation of formulated model an example of bimorph beam constructed by two PVDF beam is analysed using developed computer program and analysis results are compared with that available in literature.

8.2 Conclusion

Generally in classical plate theory a transverse displacement is assumed constant through the thickness. Therefore to perform analysis of laminated composite plates a Higher Order Shear Deformation Theory is used. Based on static and dynamic finite element analysis of laminated composite plate using eight node isoparametric elements with 48 degrees of freedom and 88 degrees of freedom, following conclusions are derived:

Static Analysis:

1. In case of square plate, due to symmetry quarter part is discretized with 1x1, 2x2, 3x3, 4x4, 5x5 and 6x6 mesh size. It is observed that 4x4 mesh size give sufficiently accurate results.

2. In static analysis of square laminated composite plates concept of symmetry is exploited in solving problems, to reduce computational effort.

3. In analysis of rectangular plate using displacement model-1 the values of maximum deflection and stresses are differ by 8.78% for thick plate in comparison with 3D-elasticity solution. And using displacement model-2 values differ by 5.82%. Whereas for thin plate the values are differ by 0.27% in model-1 and 3.28% in model-2. So with higher a/h ratio i.e. for thinner laminated plate, displacement model-1 gives better results compared to model-2.

4. From comparison of analysis results of various problems in terms of nondimensional displacements, it is observed that displacement model-2 gives more accurate result than displacement model-1. As displacement model-2 is having additional inplane degrees of freedom and their higher order terms, it yields more accurate constant value of transverse displacement through thickness.

5. For two-equal layer cross ply laminate for all a/h ratios the displacement model-2 gives excellent results, whereas model-1 under estimate the displacement by 3.87%.

6. In static analysis of orthotropic plate model-2 gives results in good agreement with 3D-FEM solution, whereas by using model-1 over estimate the displacement by 6.01%, 11.85% and 9.19% in two layers, four layers and five layers laminated composite.

Dynamic Analysis:

1. In free vibration analysis of isotropic plate displacement Present Model-2 predicts natural frequencies in good agreement with literature values, as results are

differ by less than 2.5% for simply supported boundary condition and 8.7% for clamped supported boundary condition.

2. In the case of solution with displacement model-1, which includes bending action only, as the a/h ratio increase the effect of the coupling between bending and stretching increases for two layers and four layers.The percentage errors in natural frequency of laminated composite plate are as high as 67% for cross-ply and 75.8% for angle-ply. The percentage error decreases with the increase in number of layers. Therefore it is concluded that the coupling between bending and stretching has a significant effect on the behaviour of antisymmetric laminates with few lamina. So displacement model - 1 can be considered for vibration analysis of laminated composite plate having symmetrical lamina orientation but can not be used for unsymmetrical orientation. For antisymmetric orientation of lamina displacement model - 2 should be used, for obtaining natural frequencies and modeshapes.

3. For all laminated plate displacement model-2 gives less error in solution at lower value of E1/E2 ratio i.e. 3 and 10, compared to other theories. Whereas for two, four and six layer lamina with higher value of E1/E2 ratio of 20,30 and 40 the displacement model-2 gives accurate result with negligible error compared to other theories.

4. It can be also concluded that the fundamental frequencies decrease with the increase in lamination angle for a/b = 0.5, and increases for a/b = 2.0 with the increase in the lamination angle. As the a/h ratio increases, the fundamental frequency decreases.

5. It is observed that for laminated plate with square cutout of $a_0 = 0.5 * a$ size at centre, results of natural frequencies are overestimated by 8.01% while comparing those with literature. Also the rate of increase of natural frequency is more incase of plate without cutout compare to plate with square cut out at centre.

6. The developed computer program is capable to carry out static and dynamic analysis of laminated composite plates with any geometry, support conditions, loading conditions and with varying width-to-thickness ratio, material anisotropy, and number of layers and orientation of layers.

In present project analysis of laminated composite embedded with piezoelectric material is also studied. From study of analysis results and behaviour of plate under electromechanical coupling following conclusions are made:

- Finite element formulation derived using 8-node isoparametric finite element gives accurate results.
- To make structure smart and multifunctional, piezoelectric material can be introduced. By taking advantage of direct piezoelectric effect, electrical field can be generated and could be employed for energy harvesting. By converse piezoelectric effect, mechanical displacement and vibration can be controlled.

8.3 Future Scope of Work

The present work can be extended in future to include following aspects:

- Static and dynamic analysis of laminated composite plate having different shapes and geometry.
- Static and dynamic analysis of laminated composite plate with cut outs.
- Analysis of piezolaminated composite plate of closed - loop control system domain.
- Study of vibration control of structure by using piezoelectric material.
- Finite element analysis of laminated composite plate constructed from Functionally Graded Material(FGM) to explore the applications and to make structure multifunctional.

References

[1] Mukhopadhyay M., “Mechanics of composite materials and structures”, Universities Press Private Limited, Hyderabad, India, 2004.

[2] Reddy J.N. and Ochoa O.O., “Finite Element Analysis of Composite Laminates”, Kluwer Academic Publishers, London, 1992.

[3] Logan D. L., “A First Course in the Finite Element Method”, Thomson Canada Limited, 2007.

[4] Chndrupatla T.R. and Belegundu A.D., “Introduction to finite elements in engineering”, New Delhi, India, 1997.

[5] Daniel I.M. and Ishai O., “Engineering Mechanics of Composite Materials”, Oxford University Press, New York, 2007.

[6] Varadan V.K., Vinoy K.J. and Gopalakrishnan S.,“Smart Material Systems and MEMS:Design and Development Methodologies”, John Wiley and Sons Ltd, England, 2006.

[7] Sivkumaran K.S., Chowhury S.H. and Vajarasathira K., “Some studies on finite elements for laminated composite plates”, Computers and Structures 1994, Vol. 52, pp. 729-741.

[8] Pandya B.N. and Kant T., “Flexural analysis of laminated composites using Refined higher-order C^0 plate bending elements”, Elsevier Science Publishers, October 1986.

[9] Pandya B.N. and Kant T., “Finite Element Analysis of Laminated Composite Plates using a Higher-Order Displacement Model”, Composites Science and Technology 1988, Vol. 32, pp. 137-155.

[10] Kant T. and Swaminathan K., “Analytical solutions for the static analysis of laminated composite and sandwich plates based on a higher order refined theory”, Composite Structures 2002, Vol. 56, pp. 329-344.

[11] Reddy J.N. and Chao W.C., “A comparison of closed-form and finite element solutions of thick laminated anisotropic rectangular plates”, Nuclear Engineering and Design 1981, Vol. 64, pp. 153-167.

[12] Xiao J.R., Gilhooley D.F., Batra R.C., Gillespie Jr.J.W. and McCarthy M.A., “Analysis of thick composite laminates using a higher-order shear and normal deformable plate theory (HOSNDPT) and a meshless method”, Composites: Part B 2007, Vol. 39, pp. 414-427.

[13] Pagano N.J., “Exact solutions for rectangular bidirectional composites and sandwich plates”, J. Composite Materials 1970, Vol. 4, pp. 20-34.

[14] Sundara Raja Iyengar K.T. and Pndya S.K., “Analysis of orthotropic rectangular thick plates”, Fibre science and technology 1983, Vol. 18, pp. 19-36.

[15] Shimpi R.P. and Patel H.G., “A two variable refined plate theory for orthotropic plate analysis”, Elsevier Science Publishers 1988.

[16] Ghugal Y.M. and Sayyad A.S., “A Static Flexure of Thick Isotropic Plates Using Trigonometric Shear Deformation Theory”, Journal of Solid Mechanics 2010, Vol.2, No. 1, pp.79-90.

[17] Park T., Kim K. and Han S., “Linear static and dynamic analysis of laminated composite plates and shells using a 4-node quasi-conforming shell element”, Composites: Part B 2006, Vol. 37, pp. 237-248.

[18] Kant T. and Mallikarjuna, “Free vibration of isotropic, orthotropic and multilayer plates based on higher order refined theories”, International Journal of Non-Linear Mechanics 1991, Vol. 26, pp. 335-343.

[19] Khante S.N., Rode V. and Kant T., “Nonlinear transient dynamic response of damped plates using a higher order shear deformation theory”, Nonlinear Dynamic 2007, Vol. 47, pp. 389-403.

[20] Jameel A.N. and Abed S.A., “Free vibration analysis of composite laminated plates using host 12”, Journal of Engineering 2012, Vol. 18, pp. 267-278.

[21] Kant T. and Swaminathan K., “Analytical Solutions for Free Vibration of LAminated Composite and Sandwich plates based on a higher-order refined theory”, Composite Structures 2001, Vol. 53, pp. 73-85.

[22] Kant T. and Mallikarjuna, “Vibrations of Unsymmetrically Laminated Plates Analyzed by Using A Higher Order Theory with A C^0 Finite Element Formulation”, Jornal of Sound and Vibration 1989, Vol. 134, No. 01, pp. 1-16.

[23] Noor A.K., “Free Vibration of multilayered composite plates”, AIAA Journal 1973, Vol. 11, pp. 1038-1039.

[24] Kant T. and Mallikarjuna, “A Higher-Order Theory for Free Vibration Of Unsymmetically Laminated Composite And Sandwich Plates - Finite Element Evaluations”, Journal of Computers and Structures 1989, Vol. 32, No. 05, pp. 1125-1132.

[25] Kulkarni S.D. and Khandagale N.G., “Finite Element Analysis of Thick Isotropic Plates for Free Vibration Response”, International Journal of Earth Sciences and Engineering 2011, Vol. 04, No. 06, pp. 490-493.

[26] Liu G.R., Zhao X., Dai K.Y., Zhong Z.H., Li G.Y., and Han X., “Static and Free Vibration Analysis of Lamianted Composite Plates using the Conforming Radial Point Interpolation Method”, Composites Science and Technology 2008, Vol. 68, pp. 354-366.

[27] Shiyekar S.M. and Kant T., "Higher order shear deformation effects on analysis of laminates with piezoelectric fibre reinforced composite actuators", Composite Structures 2011, Vol. 93, pp. 3252-3261.

[28] Neto M.A., Leal R.P. and Yu W., "A triangular finite element with drilling degrees of freedom for static and dynamic analysis of smart laminated structures", Computers and Structures 2012.

[29] Gl M.K. and Bucalem M.L., "Analysis of smart laminates using piezoelectric MITC plate and shell elements", Computers and Structures 2005, Vol. 83, pp. 1153-1163.

[30] Fukunaga H., Hu N. and Ren G.X., "FEM modelling of adaptive composite structures using a reduced higher-order plate theory via penalty functions", International Journal of Solids and Structures 2001, Vol. 38, pp. 8735-8752.

[31] Huang J.H. and Liu Y.-C., "Electro Elastic Response of a Laminated Composite Plate with Piezoelectric Sensors and Actuators", Journal Of Engineering Mechanics ASCE 2006. Vol. 132, pp. 889-897.

[32] Hwang W.S. and Park H.C., "Finite Element Modeling of Piezoelectric Sensors and Actuators", AIAA Journal 1993, Vol. 31, No. 05, pp. 930-937.

[33] Chen S.H., Wang Z.D. and Liu X.H., "Active Vibration Contro; And Suppression For Intelligent Structures", Journal of Sound and Vibration 1997, Vol. 200, No. 02, pp. 167-177.

[34] Alieldin S.S., Alshorbagy A.E. and Shaat M., "A first-order shear deformation finite element model for elastostatic analysis of laminated composite plates and the equivalent functionally graded plates", Ain Shams Engineering Journal 2011, Vol. 02, pp. 53-62.

[35] Pendhari S.S., Kant T., Desai Y.M. and Subbaiah C.V., "Static solutions for functionally graded simply supported plates", International Journal of Mechanical Mater 2012, Vol. 08, pp. 51-69.

[36] Shiyekar S.M. and Kant T., "An electromechanical higher order model for piezoelectric functionally graded plates", International Journal of Mechanical Mater 2010, Vol. 06, pp. 163-174.

[37] Bandyopadhyay J.N., "Application of Fiber-Reinforced composites in civil engineering and other engineering structures", Procedia Structural Engineering Convention IIT Bombay 2000, pp. 5-8.

[38] ANSI/IEEE Standard 176, "IEEE standard on piezoelectricity", 1987.

[39] Bevan J.S.,"Analysis and Testing of Plates With Piezoelectric Sensors and Actuators", Research Study, National Aeronautics and Space Administration and Old Dominion University, Norfolk, Virginia and .

[40] http://www.abdn.ac.uk/engineering/research/project-1-156.php

Appendix A

List of Paper Published / Communicated

List of Paper Published

- Patel Dhrudat M., "Static Finite Element Analysis of Laminated Composite Plate", 5^{th} National Civil Engineering Student's Symposium - AAKAAR, Department of Civil Engineering, IIT Bombay, 9 March 2013.

List of Communicated

- Patel Dhrudat M., Patel Paresh V. and Purohit Sharad P., "Static and Dynamic Finite Element Analysis of Laminated Composite Plates", 4^{th} International Conference (NUiCONE), Nirma University, Ahmedabad, India, 28-30 November 2013. (Abstract Communicated)